Stability analyses of multi–component convection–diffusion problems

by

John Tracey

A thesis submitted to the Faculty of Science, University of Glasgow, for the degree of Doctor of Philosophy

Department of Mathematics,
University of Glasgow
July 1997

ProQuest LLC.
789 East Eisenhower Parkway
P.O. Box 1346
Ann Arbor, MI 48106 – 1346

For my mother

Contents

Preface

This thesis is submitted to the University of Glasgow in accordance with the requirements for the degree of Doctor of Philosophy.

I would like to express my gratitude to my supervisor Professor Brian Straughan for his help and encouragement during my period of study.

I would also like to thank Professor Ray Ogden for his assistance during all my years at Glasgow University.

This work was supported by the Engineering and Physical Sciences Research Council through studentship number 94004400

Summary

This thesis employs analytical and numerical techniques to investigate the stability of multi–component convection–diffusion problems.

In chapter 1 the physical importance of these problems is discussed and a brief review of the relevant literature is given. The ideas of linear and nonlinear stability are introduced here via a simple one–dimensional example.

The second chapter presents linear and classical energy stability analyses for a system consisting of an infinite layer of a fluid–saturated porous medium with two salt fields present, using the Darcy–Oberbeck–Boussinesq scheme of equations. The linear stability analysis produces highly unusual neutral curves and it is the investigation of these curves that motivates the rest of this thesis. The nonlinear stability analysis in chapter 2 produces a nonlinear boundary that may be far from the linear boundary, highlighting a weakness of the energy method when the onset of linear instability is by an oscillatory mode. However, this problem is somewhat ameliorated in the third chapter by a generalised energy analysis which produces far more satisfactory results.

In the fourth chapter a non–Boussinesq buoyancy law is employed in this multi–component porous problem, introducing the phenomenon of penetrative convection. A numerical investigation of the linear stability of the problem is given, using a Chebyshev tau method, and the effect of the non–Boussinesq buoyancy law on the neutral curves is shown. A weighted energy method is used to obtain an unconditional nonlinear stability boundary

In the fifth chapter rather than the fluid–saturated porous medium of previous chapters attention is turned to an infinite layer of viscous fluid. An internal heat source is introduced as an alternative model of penetrative convection. The

linearised version of this problem is shown to be the adjoint of previous work by Straughan and Walker (1997). The linear stability of the problem is again investigated numerically.

Finally an appendix gives details of the Chebyshev tau method employed in chapters 4 and 5.

Chapter 1

Introduction

In this thesis linear and nonlinear energy stability analyses are presented for a variety of multi–component convection–diffusion problems in fluid dynamics. The phrase "multi–component" refers to the presence of one or more salt fields dissolved in the fluid. Alternatively, the problems will be referred to as "double diffusive" (fluid plus one salt concentration), "triple diffusive" (fluid plus two salt fields), etc. The introduction of these salt fields produces a variety of interesting convective phenomena not found in the single component (i.e. fluid only) problem. We will investigate multi–component convection–diffusion in both viscous fluid and fluid–saturated porous media.

The subject of double diffusive convection has been actively researched for the last 40 years, particularly in the viscous fluid case. Comprehensive reviews of the viscous flow problem can be found in Turner (1979) and Huppert and Turner (1981). Research has been mainly driven by oceanographers but other engineering fields have found use for the double diffusive phenomenon, for instance in sewage disposal (Fischer (1971)) or, in a particularly interesting example, the storage of solar energy (Tabor (1979)). Tabor (1979) describes the collection of solar radiation in a shallow (about 1m deep) black–bottomed pond. Normally the increased temperature at the bottom will eventually lead to the onset of convection. In order to increase the temperature difference between the top and bottom of the pond a stabilising salt field is imposed This inhibits the onset of convection and consequently greater amounts of solar energy are able to be stored. The hot brine is then piped out from

the pond and the thermal energy extracted. Tabor (1979) predicts a pond of area 1 km^2 as producing annual energy output equivalent to 43 000 tonnes of fuel oil.

Workers in porous media fluid mechanics have been attracted to the double diffusive problem by the many geophysical applications such as the geothermal reservoirs found in the Imperial Valley in California (Cheng (1978)), near Lake Kinnert in Israel (Rubin (1973)) and the Wairakei geothermal system in New Zealand (Griffiths (1981)). Reviews of the theoretical treatment of the porous problem can be found in Cheng (1978) and Nield and Bejan (1992).

There has been comparatively little work on the effect of a third diffusing agent, i.e. a second salt field. There are many physical situations where a second salt field is present, for instance the oceans contain many salts other than sodium chloride. Other applications may be found in the growth of crystals (Coriell *et al.* (1987)), in cloud physics (Kaye and Rood (1989)) or in the area of contaminant transport (Celia *et al.* (1989), Allen and Curran (1993), Allen and Khosravani (1992)). Another possible motivation for investigating triply diffusive convection occurs in experiments on double diffusive convection where the effect of dyes or small temperature gradients should be considered. It is the intention of this thesis to investigate further the influence of a second salt field.

In this introductory chapter the concepts of stability and the energy method are introduced through a simple one–dimensional example. The energy method yields sufficient conditions for the nonlinear stability of a chosen steady state, usually through a critical Rayleigh number. For values of the Rayleigh number less than this critical value the basic state will be nonlinearly stable, i.e. all perturbations to this basic state will decay to zero in time.

In the second chapter the physical relevance of multi–component convection–diffusion problems is further discussed, as are the previous analytical investigations. Linear and classical energy stability analyses are presented to investigate the stability of a system consisting of a fluid–saturated porous layer with two salt concentrations present, using the Darcy–Oberbeck–Boussinesq scheme of equations. The analytical linear stability analysis presented there produces highly unusual neutral curves.

The application of the energy method in chapter 2 produces a nonlinear stability boundary that may be far away from the linear stability boundary. In order to improve upon these results a generalised energy method is presented in the third chapter for the triple diffusive porous problem.

In chapters 2 and 3 the density is assumed to be linear in temperature (i.e. the Boussinesq approximation). In chapter 4 penetrative convection is introduced to the triple diffusive porous problem by employing a non–Boussinesq buoyancy law, namely one where the temperature appears as a quadratic term. A numerical investigation of the linear stability is given by making use of the Chebyshev tau method. Particular emphasis is given to the effect that the change in buoyancy law has on the unusual neutral curves found in chapter 2. A weighted energy method is then used to investigate the nonlinear stability of the problem.

An alternative model of penetrative convection is the introduction of an internal heat source. In chapter 5 this model is used for the multi–component viscous flow problem. The Chebyshev tau method is again used here to look at the linear stability of this problem. The influence of adiabatic sidewalls is also investigated here.

Finally, an appendix describes one of the numerical methods employed in this thesis, namely the Chebyshev tau method.

Standard notation is employed throughout this thesis. Partial derivatives are denoted in the usual way, e.g. $\dfrac{\partial u}{\partial t}$ or by subscripts e.g.,

$$u_t = \frac{\partial u}{\partial t}, u_{xx} = \frac{\partial^2 u}{\partial x^2}.$$

Standard vectorial and indicial notation is also used in conjunction with the Einstein summation convention, e.g.,

$$u_{i,i} = \sum_{i=1}^{i=3} \frac{\partial u_i}{\partial x_i}.$$

In order to introduce the stability analyses used in this thesis a simple application is now given.

Consider the following one–dimensional equation,

$$u_t + uu_x = \frac{1}{R} u_{xx} + u, \tag{1.1}$$

for $x \in (0,1)$ with boundary conditions $u(0,t) = u(1,t) = 0, \forall t > 0$.

The zero solution $u \equiv 0$ is a solution to (1.1). In order to show that the zero solution is stable, it must be shown that the solution is stable against any perturbation to which it is subjected. This can be accomplished by showing that all disturbances decay to zero as time advances. The energy method can give a stronger criterion than this as it usually ensures exponential decay of the perturbations.

On the other hand, to show instability of the zero solution one need only find a single disturbance that grows in amplitude in time. A linear *instability* analysis for (1.1) is given first. Equation (1.1) becomes, upon linearising,

$$u_t = \frac{1}{R}u_{xx} + u. \tag{1.2}$$

A perturbation to the zero solution of the form

$$u(x,t) = e^{\sigma t}\sin kx \tag{1.3}$$

is considered. Although this appears to be a special choice of perturbation it allows the instability of the zero solution against any x–periodic disturbance to be studied. The reason behind this is an assumption that u is periodic in x, but allowing any periodic behaviour. This allows u to be written as the following Fourier series:

$$u(x,t) = \sum_{n=0}^{\infty} A_n e^{\sigma_n t} e^{ik_n x}.$$

The cosine terms of this Fourier series do not individually satisfy the boundary conditions and consequently the perturbation reduces to

$$u(x,t) = \sum_{n=0}^{\infty} A_n e^{\sigma_n t}\sin k_n x. \tag{1.4}$$

As only one destabilising perturbation is sufficient to cause instability only equation (1.3) need be considered, since by varying k over all admissible values the most destabilizing mode will be picked up. Note that the boundary conditions restrict k to

$$k = n\pi, \qquad\qquad n = 1, 2, \ldots$$

For a disturbance of form (1.3) equation (1.2) gives

$$\sigma = -\frac{k^2}{R} + 1.$$

Linear stability is ensured if $\sigma < 0$ since this guarantees that the perturbations will decay in time. This requires $R < k^2$. However $k^2_{\min} = \pi^2$. The linear instability boundary is then given by

$$R = \pi^2.$$

i.e., the zero solution is linearly unstable for $R > \pi^2$.

An energy argument is now used to study the *stability* of the zero solution to (1.1). The first step is to multiply equation (1.1) by u and integrate over (0,1), resulting in

$$\int_0^1 uu_t\,dx + \int_0^1 u^2u_x\,dx = \frac{1}{R}\int_0^1 uu_{xx}\,dx + \int_0^1 u^2\,dx. \tag{1.5}$$

Write $\|u\|^2 = \int_0^1 u^2dx$ and set $E(t) = \frac{1}{2}\|u\|^2$. After using integration by parts, equation (1.5) becomes

$$\frac{dE}{dt} = -\frac{1}{R}\|u_x\|^2 + \|u\|^2, \tag{1.6}$$

since

$$\int_0^1 uu_t\,dx = \int_0^1 \frac{1}{2}(u^2)_t\,dx = \frac{d}{dt}\frac{1}{2}\int_0^1 u^2\,dx = \frac{d}{dt}\frac{1}{2}\|u\|^2 = \frac{dE}{dt},$$

$$\int_0^1 u^2u_x\,dx = \int_0^1 \frac{1}{3}(u^3)_x\,dx = \frac{1}{3}[u^3(1) - u^3(0)] = 0,$$

$$\int_0^1 uu_{xx}\,dx = uu_x|_0^1 - \int_0^1 u_xu_x\,dx = -\|u_x\|^2.$$

Equation (1.6) may be rewritten as

$$\begin{aligned}
\frac{dE}{dt} &= -\frac{1}{R}\|u_x\|^2 + \|u\|^2, \\
&= -\|u_x\|^2\left(\frac{1}{R} - \frac{\|u\|^2}{\|u_x\|^2}\right), \qquad (\|u_x\|^2 \neq 0), \\
&\leq -\|u_x\|^2\left(\frac{1}{R} - \max_{\mathcal{H}}\frac{\|u\|^2}{\|u_x\|^2}\right),
\end{aligned} \tag{1.7}$$

where $\mathcal{H}$ is the space of admissible functions over which a maximum is sought and is here selected as

$$\mathcal{H} = \left\{u \in C^2(0,1) \mid u = 0 \text{ when } x = 0, 1\right\}.$$

By defining

$$\frac{1}{R_E} = \max_{\mathcal{H}}\frac{\|u\|^2}{\|u_x\|^2},$$

the energy inequality (1.7) may be written

$$\frac{dE}{dt} \leq -\|u_x\|^2\left(\frac{1}{R} - \frac{1}{R_E}\right).$$

Clearly, if $R < R_E$ then $\dfrac{1}{R} - \dfrac{1}{R_E} = a > 0$ and so

$$\frac{dE}{dt} \leq -a\|u_x\|^2. \tag{1.8}$$

The Poincaré inequality is $\|u_x\|^2 \geq \pi^2\|u\|^2$ for u satisfying $u = 0$ at $x = 0, 1$. Using this in equation (1.8) gives

$$\frac{dE}{dt} \leq -a\pi^2\|u\|^2 = -2a\pi^2 E,$$

which can be integrated to yield

$$E(t) \leq E(0)e^{-2a\pi^2 t}. \tag{1.9}$$

Hence, if $R < R_E$, then

$$E(t) = \frac{1}{2}\|u\|^2 \to 0 \quad \text{as} \quad t \to 0.$$

Equation (1.9) shows that the decay is at least exponential in time. The zero solution to (1.1) is therefore nonlinearly stable for $R < R_E$.

The problem now is to find R_E, which was defined as

$$\frac{1}{R_E} = \max_{\mathcal{H}} \frac{\|u\|^2}{\|u_x\|^2}, \tag{1.10}$$

Define $I_1 = \|u\|^2, I_2 = \|u_x\|^2$. The Euler–Lagrange equations for this maximum are derived from

$$\begin{aligned} \frac{d}{d\epsilon}\left.\frac{I_1(u+\epsilon\eta)}{I_2(u_x+\epsilon\eta_x)}\right|_{\epsilon=0} = \delta\left(\frac{I_1}{I_2}\right) &= \frac{I_2\delta I_1 - I_2\delta I_2}{I_2^2} \\ &= \frac{1}{I_2}\left(\delta I_1 - \left.\frac{I_1}{I_2}\right|_{\max}\delta I_2\right) \\ &= \frac{1}{I_2}\left(\delta I_1 - \frac{1}{R_E}\delta I_2\right) = 0. \end{aligned}$$

Clearly then

$$\delta I_1 - \frac{1}{R_E}\delta I_2 = 0. \tag{1.11}$$

Here

$$\begin{aligned} \delta I_1 &= \left.\frac{d}{d\epsilon}\int_0^1 (u+\epsilon\eta)^2\,dx\right|_{\epsilon=0}, \\ \delta I_2 &= \left.\frac{d}{d\epsilon}\int_0^1 (u_x+\epsilon\eta_x)^2\,dx\right|_{\epsilon=0}, \end{aligned}$$

where η is an arbitrary $C^2(0,1)$ function that vanishes at the endpoints.

Equation (1.11) here results in

$$\int_0^1 (u\eta - \frac{1}{R_E}\eta_x u_x)\, dx = 0,$$

which can be integrated by parts to show that

$$\int_0^1 \eta(u_{xx} + R_E u)\, dx = 0.$$

However, η is an arbitrary function and consequently

$$u_{xx} + R_E u = 0, \qquad u(0) = u(1) = 0. \tag{1.12}$$

Equation (1.12) is the Euler equation and constitutes an eigenvalue problem for R_E. Its general solution is

$$u = A \sin \sqrt{R_E}x + B \cos \sqrt{R_E}x,$$

where A and B are constants yet to be determined. The boundary condition $u(0) = 0$ forces B to be zero and the boundary condition $u(1) = 0$ yields

$$\sqrt{R_E} = n\pi, \qquad n = \pm 1, \pm 2, \ldots.$$

This is an infinite sequence of values for R_E. The stability criterion is $R < R_E(\min)$ and $R_E(\min) = \pi^2$. The nonlinear stability boundary is then

$$R = \pi^2.$$

Notice that this boundary, found by employing an energy technique, is the same as the linear instability boundary.

Chapter 2

Multi–component convection–diffusion in a porous medium

2.1 Introduction

The subject of double diffusive convection of a viscous fluid, or of a fluid–saturated porous layer, has been an active area of research for many years. In the viscous fluid case in particular there is a considerable body of work. Reviews of this subject can be found in Turner (1979) and Huppert and Turner (1981). In the area of porous media fluid mechanics there are many physical problems that can be modelled as fluid–saturated porous layers stratified by heat and salt concentration, such as the geothermal reservoirs found in the Imperial Valley in California (Cheng (1978)), near Lake Kinnert in Israel (Rubin (1973)) and the Wairakei geothermal system in New Zealand (Griffiths (1981)).

Reviews of the theoretical treatment of the double diffusive porous problem can be found in Cheng (1978) and Nield and Bejan (1992). The linear stability of a fluid–saturated porous layer stratified by heat and salt concentration was first studied by Nield (1968) and Taunton *et al.* (1972) who considered the onset of salt fingers. The formulation of Nield (1968) has been extended by Rubin (1973) to introduce a nonlinear salinity profile, by Patil and Rudraiah (1980) who included the effect of

thermal diffusion (the Soret effect) and by Murray and Chen (1989) to account for the effects of temperature dependent viscosity and volumetric expansion coefficients and a nonlinear basic state salinity profile. There has been very little experimental work in double diffusive convection in porous media. Griffiths (1981) obtained values of heat and salt flux through a thin "diffusive" interface between two layers of fluid with different temperatures and salt concentrations while Murray and Chen (1989) incorporate a nonlinear time–dependent basic–state salinity profile in considering the onset of double diffusive convection in a finite box of porous medium.

In comparison there has been very little study of the effect of a third diffusing component on the onset of convection. Given the number of double diffusive problems there must be many examples where more than one salt concentration is present. There are many fluid system containing more than two components. For example, Degens at al (1973) have described the waters of Lake Kivu in East Africa as having a salinity which is the sum of many salts and the oceans contain many salts with concentrations much less than the sodium chloride concentration. One particular application of triple diffusive convection can be found in experiments on double diffusive porous convection in which the effect of dyes or small temperature gradients should be considered.

Further applications may be found in the area of contaminant transport. Celia *et al.* (1989) present a new numerical procedure, an optimal test function method, for the problem of reactive transport in porous media while Allen and Curran (1993) employ a finite–element method to model transport of a single contaminant in porous media. Chen *et al.* (1994) use a finite difference method to investigate biofilm growth in tortuous porous media and solute transport has been studied by Curran and Allen (1990) and Allen and Khosravani (1992) using finite–element collocation methods.

The linear stability of triple diffusive *porous* convection has been studied by Rudraiah and Vortmeyer (1982) and Poulikakos (1985). They adapt the method of Griffiths (1979) who considered the effect of a third component in the viscous fluid case. Since then the triple diffusive viscous flow problem has been studied by Pearlstein *et al.* (1989). They found that the results of Griffiths (1979) were not always true. In particular the conclusion of Griffiths (1979) that "marginal stability

of oscillatory modes occurs on a hyperboloid in Rayleigh number space but the surface is very closely approximated by its planar asymptotes for any diffusivity ratios" is shown to be incorrect. Pearlstein *et al.* (1989) show that for some fixed values of the diffusivity ratios, Prandtl number and two of the three Rayleigh numbers, three values of the third Rayleigh number may be required in order to specify the linear stability criteria. The effect of this is that the fluid is linearly unstable in two sections of the Rayleigh number domain and stable in the intermediate section. These novel results can be attributed to the existence of disconnected oscillatory neutral curves lying below the stationary neutral curve. In addition Pearlstein *et al.* (1989) find that the oscillatory neutral curve can be heart–shaped which those authors claim offers the possibility of simultaneous onset of instability at two different horizontal wavenumbers but the same Rayleigh number.

The results of Rudraiah and Vortmeyer (1982) and Poulikakos (1985) are similar to those of Griffiths (1979). Rudraiah and Vortmeyer (1982) also claim that the stability boundary for oscillatory convection is a hyperboloid in Rayleigh number space that is closely approximated by its planar asymptotes. Motivated by the fact that Pearlstein *et al.* (1989) have shown the results of Griffiths (1979) to be incomplete, a systematic investigation of the topology of the neutral curves of the porous problem is presented here and the results of Rudraiah and Vortmeyer (1982) and Poulikakos (1985) are reconsidered.

The linear stability analysis given here clearly does not yield any information on the effect of nonlinear terms. In section 2.6 the possible effects that nonlinear terms may have on the experimental realisation of the unusual results predicted by the heart–shaped oscillatory curves are discussed. Of particular relevance is the work of Proctor (1981) and Hansen and Yuen (1989). Both consider subcritical instabilities in the double diffusive fluid problem and show that subcritical instability can occur at values of the thermal Rayleigh number much less than that predicted by the linear theory. Rudraiah, Srimani and Friedrich (1982) consider the nonlinear stability of finite–amplitude convection of a two–component fluid–saturated porous layer using truncations of Fourier series. These authors also find that finite–amplitude instability is possible at subcritical values of the thermal Rayleigh number. Rudraiah,

Shivakumara and Friedrich (1986) use a similar method to investigate the effect of rotation on the double diffusive problem. Kaloni and his co–workers (Qin *et al.* (1995), Guo and Kaloni (1995a), Guo and Kaloni (1995b), Kaloni and Guo (1996), Kaloni and Qiao (1997)) have recently produced several papers applying the energy method to the double diffusive problem.

There has been no work on the triple diffusive problem, however, and hence the need for the present analysis. One very important advantage of the application of the energy method given in the present work is that it provides unconditional results, i.e. nonlinear stability is guaranteed for initial perturbations of arbitrary sized amplitude.

The layout of this chapter is as follows. In section 2.3 a linear stability analysis of the triple diffusive problem in a porous medium is presented in the vein of Pearlstein *et al.* (1989). The problem is formulated for heat and two salt concentrations as the three stratifying agencies. In section 2.4 the energy method is applied to this problem for two distinct cases. Firstly, when all three stratifying agencies are destabilizing and secondly the case corresponding to heating from below with one salt field destabilizing and the other stabilizing. In section 2.5 numerical results for both the linear and nonlinear analyses are presented and in the final section the difficulties of reproducing these results experimentally are discussed.

This chapter has essentially appeared as Tracey (1996).

2.2 Governing equations

Consider a fluid–saturated porous layer lying in the infinite three–dimensional region $0 < z < d$. The boundaries $z = 0$ and $z = d$ are maintained at temperatures T_l and T_u respectively. Suppose further that the fluid has dissolved in it two different chemical components or "salts". Denote the concentration of component α by C^α $(\alpha = 1, 2)$. The concentration of component α at the lower and upper boundaries is held constant at C_l^α and C_u^α respectively.

The equation of state is given by

$$\rho = \rho_0 \left(1 - A\left(T - T_0\right) + A_1 \left(C^1 - C_0^1\right) + A_2 \left(C^2 - C_0^2\right)\right),$$

where ρ_0, T_0 and C_0^α $(\alpha = 1, 2)$ are reference values of density, temperature and salt concentration respectively. The constants A and A_α $(\alpha = 1, 2)$ represent the thermal and solute expansion coefficients respectively.

The equations of motion which govern flow in a porous medium are largely based on a relation which is a generalisation of empirical observations (c.f. Joseph (1976). This relation is known as Darcy's Law and can be written

$$\nabla p = -\frac{\mu}{k}\mathbf{v} + \rho\mathbf{g},$$

where the variables $p, \mu, k, \mathbf{v}$ and $\mathbf{g}$ represent pressure, dynamic viscosity, permeability, velocity and gravity. In addition to Darcy's Law the governing equations consist of the incompressibility condition and the equations of conservation of temperature and solute. Combining these equations with the Darcy law and the equation of state the following system of governing equations is obtained:

$$\begin{aligned} p_{,i} &= -\frac{\mu}{k}v_i - g\rho_0(1 - A(T - T_0) \\ &\quad + A_1(C^1 - C_0^1) + A_2(C^2 - C_0^2))k_i, && (2.1) \\ v_{i,i} &= 0, && (2.2) \\ T_{,t} + v_i T_{,i} &= \kappa\Delta T, && (2.3) \\ C^\alpha_{,t} + v_i C^\alpha_{,i} &= \kappa_\alpha \Delta C^\alpha, \ (\alpha = 1, 2), && (2.4) \end{aligned}$$

where indicial notation and the Einstein summation convention have been employed. The vector $\mathbf{k}$ is the unit vector in the z–direction. The variables κ and κ_α $(\alpha = 1, 2)$ represent thermal and solute diffusivities respectively.

The boundary conditions considered are

$$\begin{aligned} &T(0) = T_l, \ T(d) = T_u, \\ &C^\alpha(0) = C_l^\alpha, \ C^\alpha(d) = C_u^\alpha, \ (\alpha = 1, 2), \\ &v_3 = 0 \ \text{at} \ z = 0, d. \end{aligned} \qquad (2.5)$$

The experimental realisation of prescribing these boundary conditions, especially those on the concentration fields, is discussed in section 2.6.

Consider a steady solution $(\bar{v}_i, \bar{p}, \bar{T}, \bar{C}^\alpha)$ of (2.1)–(2.5) where $\bar{v}_i = 0$ and $\bar{T}$ and $\bar{C}^\alpha$ are functions of z. Equations (2.3) and (2.4) show that, utilising (2.5),

$$\begin{aligned}\bar{T} &= T_l - \beta z, \ (\beta = \frac{T_l - T_u}{d}),\\ \bar{C^\alpha} &= C_l^\alpha - \frac{\triangle C^\alpha}{d} z, \ (\triangle C^\alpha = C_l^\alpha - C_u^\alpha).\end{aligned}$$

The steady state pressure $\bar{p}$ can be obtained from (2.1) which shows that

$$\frac{d\bar{p}}{dz} = -g\rho_0 \left[1 - A(T_l - \beta z - T_0) + A_1 \left(C_l^1 - \frac{\triangle C^1}{d} z - C_0^1\right) + A_2 \left(C_l^2 - \frac{\triangle C^2}{d} z - C_0^2\right)\right],$$

and so,

$$\begin{aligned}\bar{p} &= \rho_0 g z^2 \left[-\frac{A\beta}{2} + A_1 \frac{\triangle C^1}{2d} + A_2 \frac{\triangle C^2}{2d}\right]\\ &\quad -\rho_0 g z \left[1 - A(T_l - T_0) + A_1(C_l^1 - \hat{C^1}) + A_2(C_l^2 - \hat{C^2})\right] + p_0,\end{aligned}$$

where p_0 is constant.

In order to investigate the stability of this basic solution perturbations $(u_i, \pi, \theta, \phi^\alpha)$ are introduced to the steady solution $(\bar{v_i}, \bar{p}, \bar{T}, \bar{C^\alpha})$ via

$$v_i = \bar{v_i} + u_i, \ p = \bar{p} + \pi, \ T = \bar{T} + \theta, \ C^\alpha = \bar{C^\alpha} + \phi^\alpha.$$

The resultant perturbation equations are non–dimensionalised using the following scalings:

$$t = t^* \frac{d^2}{\kappa}, \ \mathbf{u} = \mathbf{u}^* \frac{\kappa}{d}, \ \pi = \pi^* \frac{\mu\kappa}{k}, \ \mathbf{x} = \mathbf{x}^* d,$$

$$\theta = \theta^* T^\#, \ \phi^\alpha = (\phi^\alpha)^* \Phi^\alpha,$$

$$T^\# = \left(\frac{\mu\kappa|\delta T|}{A\rho_o g k d}\right)^{1/2}, \ \Phi^\alpha = \left(\frac{\mu\kappa P_\alpha |\triangle C^\alpha|}{A_\alpha \rho_o g k d}\right)^{1/2},$$

$$R = \left(\frac{A\rho_o g k d|\delta T|}{\mu\kappa}\right)^{1/2}, \ R_\alpha = \left(\frac{A_\alpha \rho_o g k d P_\alpha |\triangle C^\alpha|}{\mu\kappa}\right)^{1/2},$$

$$\delta T = T_l - T_u, H = \mathrm{sgn}(\delta T), \ H_\alpha = \mathrm{sgn}(\triangle C^\alpha), \ P_\alpha = \frac{\kappa}{\kappa_\alpha}.$$

Here R and R_α are the thermal and salt Rayleigh numbers and P_α are salt Prandtl numbers.

The nonlinear perturbation equations are then, in non–dimensional form (dropping the asterisks),

$$\pi_{,i} = -u_i + \left[R\theta - R_1\phi^1 - R_2\phi^2\right] k_i, \tag{2.6}$$

$$u_{i,i} = 0, \tag{2.7}$$

$$\theta_{,t} + u_i\theta_{,i} = HRw + \Delta\theta, \tag{2.8}$$

$$P_1(\phi^1_{,t} + u_i\phi^1_{,i}) = H_1R_1w + \Delta\phi^1, \tag{2.9}$$

$$P_2(\phi^2_{,t} + u_i\phi^2_{,i}) = H_2R_2w + \Delta\phi^2. \tag{2.10}$$

where $w = u_3$. The boundary conditions which follow from (2.5) for the perturbed quantities are

$$w = \theta = \phi^1 = \phi^2 = 0 \text{ on } z = 0, 1. \tag{2.11}$$

2.3 Linear stability analysis

A linearised stability analysis on (2.6)–(2.11) in the vein of Pearlstein *et al.* (1989) is now given. Firstly, equations (2.6)–(2.10) are linearised by neglecting terms containing products of the perturbed quantities. A time dependence of $e^{\sigma t}$ is introduced by substituting

$$\begin{aligned}
\mathbf{u}(\mathbf{x}, t) &= \mathbf{u}(\mathbf{x})e^{\sigma t}, \\
\theta(\mathbf{x}, t) &= \theta(\mathbf{x})e^{\sigma t}, \\
\phi^\alpha(\mathbf{x}, t) &= \phi^\alpha(\mathbf{x})e^{\sigma t} \quad (\alpha = 1, 2).
\end{aligned}$$

The pressure term is eliminated by taking curlcurl of equations (2.6) and then choosing the third component. This gives

$$\Delta w = R\Delta^*\theta - R_1\Delta^*\phi^1 - R_2\Delta^*\phi^2, \tag{2.12}$$

$$\sigma\theta = HRw + \Delta\theta, \tag{2.13}$$

$$P_1\sigma\phi^1 = H_1R_1w + \Delta\phi^1, \tag{2.14}$$

$$P_2\sigma\phi^2 = H_2R_2w + \Delta\phi^2, \tag{2.15}$$

where $\Delta^* = \dfrac{\partial^2}{\partial x^2} + \dfrac{\partial^2}{\partial y^2}$ is the horizontal Laplacian.

In order to obtain an equation in w alone eliminate θ, ϕ^1 and ϕ^2 from equation (2.12) by operating on (2.12) with $(\sigma - \Delta)(P_1\sigma - \Delta)(P_2\sigma - \Delta)$ and then using equations (2.13) – (2.15). The resultant equation for w is found to be

$$\begin{aligned}(\sigma - \Delta)(P_1\sigma - \Delta)(P_2\sigma - \Delta)\Delta w &= \Delta^* w \left\{ HR^2(P_1\sigma - \Delta)(P_2\sigma - \Delta) \right. \\ &\quad -H_1R_1^2(\sigma - \Delta)(P_2\sigma - \Delta) \\ &\quad \left. -H_2R_2^2(\sigma - \Delta)(P_1\sigma - \Delta) \right\} \qquad (2.16)\end{aligned}$$

A normal mode representation is assumed, i.e.

$$w = W(z)e^{i(mx+ny)}.$$

In order to put equation (2.16) into a similar form to equation (2.3) of Pearlstein *et al.* (1989) the following transformations are introduced:

$$HR^2 \to R,\ H_\alpha R_\alpha^2 \to -R_\alpha,\ (\alpha = 1, 2).$$

Equation (2.16) becomes

$$\begin{aligned}(\sigma - (D^2 - k^2))(P_1\sigma - (D^2 - k^2))(P_2\sigma - (D^2 - k^2))(D^2 - k^2)W \\ = -k^2 \{ R(P_1\sigma - (D^2 - k^2))(P_2\sigma - (D^2 - k^2)) \\ +R_1(\sigma - (D^2 - k^2))(P_2\sigma - (D^2 - k^2)) \\ +R_2(\sigma - (D^2 - k^2))(P_1\sigma - (D^2 - k^2)) \} W,\end{aligned}$$

where $k^2 = m^2 + n^2$ is a wavenumber and $D = \dfrac{d}{dz}$.

The boundary conditions on w imply that $W(z) = \sin n\pi z$. Putting $y_n = n^2\pi^2 + k^2$ yields

$$\begin{aligned}(\sigma + y_n)(P_1\sigma + y_n)(P_2\sigma + y_n)y_n = k^2 \{ & R(P_1\sigma + y_n)(P_2\sigma + y_n) \\ & +R_1(\sigma + y_n)(P_2\sigma + y_n) \\ & +R_2(\sigma + y_n)(P_1\sigma + y_n) \}. \end{aligned} \qquad (2.17)$$

In order to use this equation to obtain information about the stability of the basic solution one can consider y_n, P_1, P_2, R_1 and R_2 to be known while R can be varied until a neutral solution (i.e. $Re(\sigma) = 0$) is obtained. Rewrite (2.17) as

$$R = \left(\frac{\sigma + y_n}{k^2}\right) y_n - R_1 \frac{\sigma + y_n}{P_1\sigma + y_n} - R_2 \frac{\sigma + y_n}{P_2\sigma + y_n}. \tag{2.18}$$

In order to find neutral solutions set the real part of σ equal to zero, i.e. let $\sigma = 0 + i\omega$. Then (2.18) becomes, upon removing complex quantities from the denominators,

$$\begin{aligned} R &= \frac{y_n^2}{k^2} - R_1 \frac{P_1\omega^2 + y_n^2}{P_1^2\omega^2 + y_n^2} - R_2 \frac{P_2\omega^2 + y_n^2}{P_2^2\omega^2 + y_n^2} \\ &\quad + i\omega y_n \left[\frac{1}{k^2} - R_1 \frac{1 - P_1}{P_1^2\omega^2 + y_n^2} - R_2 \frac{1 - P_2}{P_2^2\omega^2 + y_n^2}\right], \end{aligned} \tag{2.19}$$

which is rewritten as

$$R = f_1(k, \omega, R_1, R_2, P_1, P_2) + i\omega y_n f_2(k, \omega, R_1, R_2, P_1, P_2).$$

The quantity R is real so equation (2.19) implies that either $\omega = 0$ or $f_2 = 0$.

The case $\omega = 0$ corresponds to stationary onset of convection. Setting $\omega = 0$ in (2.19) yields

$$R = R^{\mathrm{s}} = \frac{y_n^2}{k^2} - R_1 - R_2. \tag{2.20}$$

So, for stationary neutral solutions R is a single–valued function of the wavenumber. The critical value of k which gives the minimum value of R^{s} can be found by setting the derivative of (2.20) with respect to k equal to zero, to find $k = n\pi$. So the critical Rayleigh number for steady onset is

$$R^{\mathrm{s,crit}} = 4\pi^2 - R_1 - R_2, \tag{2.21}$$

since $n = 1$ clearly gives the minimum value.

For oscillatory onset $\omega \neq 0$, so equation (2.19) requires that $f_2 = 0$, i.e.

$$\frac{1}{k^2} - R_1 \frac{1 - P_1}{P_1^2\omega^2 + y_n^2} - R_2 \frac{1 - P_2}{P_2^2\omega^2 + y_n^2} = 0.$$

Rewrite this as a quadratic dispersion relation in ω^2,

$$\begin{aligned} \omega^4 P_1^2 P_2^2 + \omega^2 \left[y_n^2(P_1^2 + P_2^2) + k^2(R_1(P_1 - 1)P_2^2 + R_2(P_2 - 1)P_1^2)\right] \\ + y_n^2 \left[y_n^2 + k^2(R_1(P_1 - 1) + R_2(P_2 - 1))\right] = 0, \end{aligned}$$

or as

$$\alpha(P_1, P_2)\omega^4 + \beta(k, R_1, R_2, P_1, P_2)\omega^2 + \gamma(k, R_1, R_2, P_1, P_2) = 0. \tag{2.22}$$

where

$$\begin{aligned} \alpha &= P_1^2 P_2^2 > 0, \\ \beta &= y_n^2(P_1^2 + P_2^2) + k^2(R_1(P_1 - 1)P_2^2 + R_2(P_2 - 1)P_1^2), \\ \gamma &= y_n^2\left[y_n^2 + k^2(R_1(P_1 - 1) + R_2(P_2 - 1))\right]. \end{aligned} \tag{2.23}$$

The fact that this is a quadratic in ω^2 means that it may give rise to solutions with more than one positive value of ω^2 for fixed P_1, P_2, R_1, R_2, k. This has important consequences for the linear stability of the basic solution and attention is now concentrated on finding such solutions.

Firstly, necessary conditions for the existence of multiple oscillatory neutral solutions are obtained.

If two real positive roots of (2.22) exist then $\beta < 0$ and $\gamma > 0$, i.e.,

$$y_n^2(P_1^2 + P_2^2) + k^2(R_1(P_1 - 1)P_2^2 + R_2(P_2 - 1)P_1^2) < 0, \tag{2.24}$$

and

$$y_n^2 + k^2(R_1(P_1 - 1) + R_2(P_2 - 1)) > 0. \tag{2.25}$$

Multiplying (2.25) by P_1^2 and adding to $-1\times$(2.24) gives

$$y_n^2(P_1^2 - P_1^2 - P_2^2) + k^2\left[R_1(P_1 - 1)(P_1^2 - P_2^2) + R_2(P_2 - 1)(P_1^2 - P_1^2)\right] > 0,$$

i.e.

$$R_1(P_1 - 1)(P_1 - P_2) > \frac{y_n^2 P_2^2}{k^2(P_1 + P_2)} > 0.$$

Similarly, multiplying (2.25) by P_2^2 and adding to $-1\times$(2.24) yields

$$R_2(P_2 - 1)(P_2 - P_1) > \frac{y_n^2 P_1^2}{k^2(P_1 + P_2)} > 0.$$

So, necessary conditions for the existence of two frequencies on the oscillatory curve are

$$R_1(P_1 - 1)(P_1 - P_2) > 0, \tag{2.26}$$

$$R_2(P_2 - 1)(P_2 - P_1) > 0. \tag{2.27}$$

For fixed P_1, P_2 satisfying $(P_1-1)(P_2-1)(P_1-P_2) \neq 0$, i.e. the three diffusivities being distinct from each other, (2.26) and (2.27) are satisfied in exactly one quadrant of the (R_1, R_2)–plane. For the case of $R_1 < 0$ and $R_2 < 0$ (i.e. both salt fields

stabilizing) then (2.26) and (2.27) imply that one cannot have two onset frequencies at one wavenumber, so in order to have two onset frequencies at one wavenumber one of these stratifying agencies must be destabilizing. This is in apparent contrast with Pearlstein *et al.* (1989) who claim that two destabilizing effects cannot give rise to two onset frequencies at one wavenumber. However, examination of the sign convention used by Griffiths (1979) and subsequently by Pearlstein *et al.* (1989) shows that the effects that Pearlstein *et al.* (1989) claim are destabilizing are actually stabilizing.

Now look for values of R, R^o, on the oscillatory (R, k) neutral curve corresponding to two different onset frequencies at one wavenumber. To do this, rewrite the real and imaginary parts of (2.17) as

$$-\omega^2\left[y_n^2 f_1 - k^2(R^o f_2 + f_3)\right] + y_n^2\left[y_n^2 - k^2(R^o + f_4)\right] = 0, \tag{2.28}$$

$$-\omega^3 f_2 + \omega\left[y_n^2 f_5 - k^2(R^o f_6 + f_7)\right] = 0, \tag{2.29}$$

where

$$f_1 = P_1 + P_2 + P_1P_2, f_2 = P_1P_2, f_3 = R_1P_2 + R_2P_1, f_4 = R_1 + R_2,$$

$$f_5 = 1 + P_1 + P_3, f_6 = P_1 + P_2, f_7 = R_1(1 + P_2) + R_2(1 + P_1).$$

On the oscillatory (R, k) neutral curve $\omega = 0$ only at the bifurcation points with the stationary (R, k) neutral curve. Here a bifurcation point is one at which the oscillatory and stationary neutral curves intersect *and* the frequency ω tends to zero as the bifurcation point is approached. So, away from the bifurcation points equation (2.29) can be divided by ω, yielding

$$\omega^2 = \frac{y_n^2 f_5 - k^2(R^o f_6 + f_7)}{f_2}. \tag{2.30}$$

Substitute (2.30) into (2.28) to get

$$\frac{y_n^4}{k^4} f_8 + \frac{y_n^2}{k^2}(R^o f_9 + f_{10}) - (R^o f_6 + f_7)(R^o f_2 + f_3) = 0, \tag{2.31}$$

where

$$f_8 = -f_1 f_5 + f_2,\ f_9 = f_1 f_6 + f_2 f_5 - f_2,\ f_{10} = f_1 f_7 + f_3 f_5 - f_2 f_4.$$

Equation (2.31) is satisfied on the oscillatory neutral curve. It can be used to locate extremal points on the oscillatory curve (i.e. points on the neutral curve where the gradient is zero) in the (R, k)–plane. To find these points differentiate (2.31) with respect to k and set $\dfrac{\partial R^{\circ}}{\partial k} = 0$ to get

$$2y_n(2k^2 - y_n)(2y_n^2 f_8 + k^2(R^{\circ} f_9 + f_{10})) = 0.$$

So the extremal values of R° occur at either

$$2k^2 - y_n = 0, \tag{2.32}$$

or

$$2y_n^2 f_8 + k^2(R^{\circ} f_9 + f_{10}) = 0. \tag{2.33}$$

Equation (2.32) corresponds to the case $k = n\pi$. From (2.32), $\dfrac{y_n^2}{k^2} = 4n^2\pi^2$ which is substituted into (2.31) to obtain

$$(R^{\circ})^2 f_2 f_6 + R^{\circ}(f_2 f_7 + f_3 f_6 - 4n^2\pi^2 f_9) + (f_3 f_7 - 16n^4\pi^4 f_8 - 4n^2\pi^2 f_{10}) = 0. \tag{2.34}$$

For fixed P_1, P_2, R_1, R_2 this is a quadratic in R° which has zero, one or two real solutions. For each solution the sign of ω^2 in (2.30) must be checked (ω is real, consequently its square must be positive). So there may be zero, one or two physically meaningful extremal values of R° on the oscillatory neutral curve corresponding to $k = n\pi$.

In the other case ($k \neq n\pi$) substitution of (2.33) into (2.31) yields

$$(R^{\circ})^2(f_9^2 + 4f_2 f_6 f_8) + R^{\circ}(2f_9 f_{10} + 4f_2 f_7 f_8 + 4f_3 f_6 f_8) + (f_{10}^2 + 4f_3 f_7 f_8) = 0. \tag{2.35}$$

Again this is a quadratic in R° which may have zero, one or two physically meaningful ($\omega^2 \geq 0$) solutions at wavenumbers other than $k = n\pi$. In this case some more information can be deduced. Define

$$f_{11} = -\frac{R^{\circ} f_9 + f_{10}}{2f_8},$$

then (2.33) may be rewritten as

$$(n^2\pi^2 + k^2)^2 - f_{11}k^2 = 0,$$

i.e.

$$k^4 + (2n^2\pi^2 - f_{11})k^2 + n^4\pi^4 = 0.$$

This has zero or two positive real roots. So, for each physically meaningful value of R^o satisfying (2.33) there are two extrema on the oscillatory neutral curve with $k \neq n\pi$. So there may be two extrema at one R^o (from (2.33)) and two extrema at $k = n\pi$ (from (2.32)) in which case the oscillatory neutral curve is heart-shaped.

2.3.1 Locating the oscillatory neutral curves

The existence of closed oscillatory curves can be decided by locating any bifurcation points and points of infinite slope on the oscillatory neutral curves. The advantage of this approach is that it eliminates the need to search for the oscillatory curves in the (R, k)–plane.

Bifurcation points are the only points on the oscillatory curve at which $\omega = 0$. They can be located by setting $\omega = 0$ in (2.22). This yields $\gamma = 0$, i.e.,

$$y_n^2 + k^2(R_1(P_1 - 1) + R_2(P_2 - 1)) = 0.$$

Set $\delta = R_1(P_1 - 1) + R_2(P_2 - 1)$ and rewrite this as a quadratic in k^2,

$$k^4 + k^2(2n^2\pi^2 + \delta) + n^4\pi^4 = 0.$$

This has zero or two real positive solutions, corresponding to zero or two bifurcation points. The value of R^o corresponding to k can be found by setting $\omega = 0$ in (2.28). This gives

$$R^o = \frac{y_n^2}{k^2} - f_4.$$

At points of infinite slope the number of branches on the oscillatory curve changes from zero to two or vice–versa. Consequently, at these points the number of positive roots of (2.22) changes from zero to two, so points of infinite slope may be determined by solving

$$\beta^2 - 4\alpha\gamma = 0$$

from (2.22). Rearranging this yields a quartic in k^2

$$Ak^8 + k^6(4n^2\pi^2A + B) + k^4(6n^4\pi^4A + 2n^2\pi^2B + C) + k^2(4n^6\pi^6A + n^4\pi^4B) + An^8\pi^8 = 0,$$

where

$$A = \left(P_1^2 - P_2^2\right)^2 \geq 0,$$

$$B = -2(P_1 + P_2)\left[P_2^2 R_1(P_1 - 1)(P_1 - P_2) + P_1^2 R_2(P_2 - 1)(P_2 - P_1)\right],$$

$$C = \left[R_1(P_1 - 1)P_2^2 + R_2(P_2 - 1)P_1^2\right]^2 \geq 0.$$

This has four possible sign changes and so, by Descartes' rule of signs, four possible positive real roots. However, it can be shown that there are at most two physically meaningful positive roots and consequently at most two points of infinite slope.

The value of R on the oscillatory curve at the point of infinite slope can be found by differentiating (2.31) and setting $\dfrac{\partial k}{\partial R^o} = 0$. This yields

$$R^o = -\frac{(f_2 f_7 + f_3 f_6)k^2 - y_n^2 f_9}{2k^2 f_2 f_6}.$$

Again for each pair (R^o, k) the sign of ω^2 in (2.30) must be checked.

2.3.2 Topology of the neutral curves

The possible combinations of bifurcation points and points of infinite slope allow us to determine the shape of the neutral curves. If there are no bifurcation points and no points of infinite slope then there is no oscillatory curve, since the oscillatory curve must be either connected to the the stationary curve (and so there are two bifurcation points), or disconnected from the stationary curve and closed (and so there are two points of infinite slope).

If there are two bifurcation points and no points of infinite slope then the neutral curves look like fig 2.1(i). The oscillatory curve is single–valued between k_{b1} and k_{b2} and does not exist for any other values of k.

If there are two points of infinite slope and two bifurcation points then the neutral curves look like fig 2.1(ii). The oscillatory curve is double–valued between k_{s1} and k_{b1} and between k_{b2} and k_{s2} and single–valued between k_{b1} and k_{b2}. This has no bearing on stability as the single critical Rayleigh number still occurs at the minimum of the oscillatory curve.

If there are two points of infinite slope and no bifurcation points then the neutral curves will look like fig 2.1(iii) or fig 2.1(iv). In fig 2.1(iii) the oscillatory neutral

curve does not lie entirely below the stationary curve and so still only one critical Rayleigh number is required to describe linear instability. The points where the stationary and oscillatory curves meet are not true bifurcation points. As the point of intersection is approached along the oscillatory curve the frequency, ω, does not tend to zero. In fig 2.1(iv) the oscillatory curve lies wholly below the stationary curve and now three values of R are required to specify the linear instability criteria. The fluid is linearly unstable for $R^1 < R < R^2$ and for $R > R^3$ and stable for $R^2 < R < R^3$.

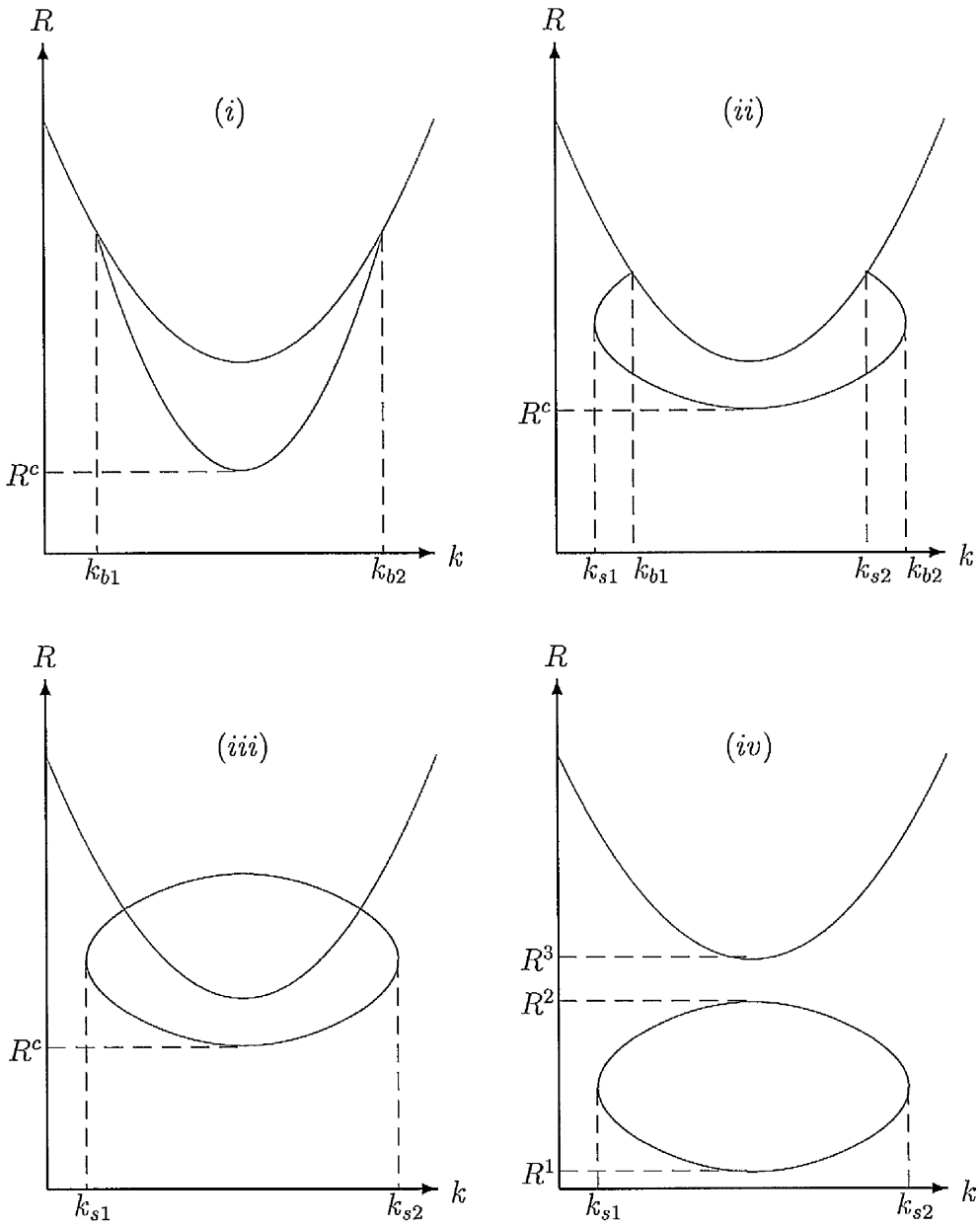

Figure 2.1: Topology of the neutral curves. (i) Two bifurcation points, no points of infinite slope. (ii) Two bifurcation points, two points of infinite slope. (iii) No bifurcation points, two points of infinite slope. (iv) No bifurcation points, two points of infinite slope.

2.4 Nonlinear stability analysis

In this section we present an analysis of the nonlinear stability of the basic solution by use of the energy method. The nonlinear perturbation equations are, from (2.6)–(2.10),

$$\pi_{,i} = -u_i + [R\theta - R_1\phi - R_2\psi]\, k_i, \tag{2.36}$$

$$u_{i,i} = 0, \tag{2.37}$$

$$\theta_{,t} + u_i\theta_{,i} = HRw + \Delta\theta, \tag{2.38}$$

$$P_1\left(\phi_{,t} + u_i\phi_{,i}\right) = H_1R_1w + \Delta\phi, \tag{2.39}$$

$$P_2\left(\psi_{,t} + u_i\psi_{,i}\right) = H_2R_2w + \Delta\psi, \tag{2.40}$$

where, for later convenience, the following transformations have been used

$$\phi^1 \to \phi, \quad \phi^2 \to \psi,$$

Let V denote a period cell for the solution. The boundary conditions we consider are

$$w = \theta = \phi = \psi = 0 \quad \text{on } z = 0, 1,$$

and further that u_i, θ, ϕ, ψ and π are periodic on the lateral boundaries of V.

To commence multiply (2.36) by u_i, (2.38) by θ, (2.39) by ϕ and (2.40) by ψ and integrate over V. Integration by parts and use of the boundary conditions yields

$$0 = -\|\mathbf{u}\|^2 + R(\theta, w) - R_1(\phi, w) - R_2(\psi, w), \tag{2.41}$$

$$\frac{d}{dt}\frac{1}{2}\|\theta\|^2 = HR(w, \theta) - \|\nabla\theta\|^2, \tag{2.42}$$

$$\frac{d}{dt}\frac{P_1}{2}\|\phi\|^2 = H_1R_1(w, \phi) - \|\nabla\phi\|^2, \tag{2.43}$$

$$\frac{d}{dt}\frac{P_2}{2}\|\psi\|^2 = H_2R_2(w, \psi) - \|\nabla\psi\|^2, \tag{2.44}$$

where $\|\cdot\|$ denotes the $L^2(V)$ norm and $(f, g) = \int_V fg\, dV$.

Now form (2.41) + λ (2.42) + ξ (2.43) + μ (2.44), where λ, ξ and μ are positive coupling parameters to be selected at our discretion, then

$$\begin{aligned} & \frac{d}{dt}\left(\frac{\lambda}{2}\|\theta\|^2+\frac{\xi P_1}{2}\|\phi\|^2+\frac{\mu P_2}{2}\|\psi\|^2\right) \\ = \; & (\lambda H+1)R(w,\theta)+(\xi H_1-1)R_1(w,\phi)+(\mu H_2-1)R_2(w,\psi) \\ & -\left(\|\mathbf{u}\|^2+\lambda\|\nabla\theta\|^2+\xi\|\nabla\phi\|^2+\mu\|\nabla\psi\|^2\right). \end{aligned} \tag{2.45}$$

Define an energy

$$E(t)=\frac{\lambda}{2}\|\theta\|^2+\frac{\xi P_1}{2}\|\phi\|^2+\frac{\mu P_2}{2}\|\psi\|^2,$$

then (2.45) shows that

$$\frac{dE}{dt}=\mathcal{I}-\mathcal{D},$$

where

$$\mathcal{I}=(\lambda H+1)R(w,\theta)+(\xi H_1-1)R_1(w,\phi)+(\mu H_2-1)R_2(w,\psi),$$

$$\mathcal{D}=\|\mathbf{u}\|^2+\lambda\|\nabla\theta\|^2+\xi\|\nabla\phi\|^2+\mu\|\nabla\psi\|^2.$$

By rearrangement,

$$\frac{dE}{dt}=\mathcal{I}-\mathcal{D}=-\mathcal{D}\left(1-\frac{\mathcal{I}}{\mathcal{D}}\right).$$

Now define

$$\frac{1}{\Lambda}=\max_{\mathcal{H}}\frac{\mathcal{I}}{\mathcal{D}}, \tag{2.46}$$

where $\mathcal{H}$ is the space of admissible functions. In this case

$$\mathcal{H}=\left\{u_i,\theta,\phi,\psi \mid u_i\in L^2(V),\theta,\phi,\psi\in H^1(V),u_{i,i}=0\right\}.$$

Then

$$\frac{dE}{dt}\leq-\mathcal{D}(1-\frac{1}{\Lambda}).$$

If now

$$\Lambda>1, \tag{2.47}$$

then

$$1-\frac{1}{\Lambda}=a>0,$$

and so

$$\frac{dE}{dt}\leq-a\mathcal{D}.$$

The Poincaré inequality is (see e.g. Straughan (1992)

$$\|\nabla\theta\|^2 \geq \lambda_*\|\theta\|^2,$$

where $\lambda_* > 0$, with similar results for ϕ and ψ. Application of this gives that $\exists c > 0$ such that

$$\mathcal{D} \geq cE.$$

Therefore,

$$\frac{dE}{dt} \leq -acE, \tag{2.48}$$

which can be integrated to yield

$$E(t) \leq E(0)e^{-act}.$$

So, if $\Lambda > 1$ then $E(t) \to 0$ as $t \to \infty$ at least exponentially fast and so the steady solution is stable.

The problem remains to find the maximum in (2.46).

In order to clear the denominator of the maximisation problem of coupling parameters we make the following transformations

$$\sqrt{\lambda}\theta \to \theta,\ \sqrt{\xi}\phi \to \phi,\ \sqrt{\mu}\psi \to \psi.$$

The resultant maximisation problem to be considered is

$$\frac{1}{\Lambda} = \max_{\mathcal{H}} \frac{\left(\frac{\lambda H + 1}{\sqrt{\lambda}}\right)R(w,\theta) + \left(\frac{\xi H_1 - 1}{\sqrt{\xi}}\right)R_1(w,\phi) + \left(\frac{\mu H_2 - 1}{\sqrt{\mu}}\right)R_2(w,\psi)}{\|\mathbf{u}\|^2 + |\nabla\theta\|^2 + \|\nabla\phi\|^2 + \|\nabla\psi\|^2}.$$

The Euler–Lagrange equations for this maximum are derived as follows

$$\begin{aligned}
\delta\left(\frac{\mathcal{I}}{\mathcal{D}}\right) &= \frac{\delta\mathcal{I}}{\mathcal{D}} - \mathcal{I}\frac{1}{\mathcal{D}^2}\delta\mathcal{D} \\
&= \frac{1}{\mathcal{D}}\left(\delta\mathcal{I} - \frac{\mathcal{I}}{\mathcal{D}}\Big|_{\max}\delta\mathcal{D}\right) \\
&= \frac{1}{\mathcal{D}}\left(\delta\mathcal{I} - \frac{1}{\Lambda}\delta\mathcal{D}\right) = 0,
\end{aligned}$$

where

$$\delta\mathcal{F} = \frac{\partial\mathcal{F}}{\partial w_i} - \frac{\partial}{\partial x_j}\left(\frac{\partial\mathcal{F}}{\partial w_{i,j}}\right) = 0,$$

with w_i standing for u_i, θ, ϕ or ψ. Therefore,

$$\delta\mathcal{I} - \frac{1}{\Lambda}\delta\mathcal{D} = 0. \tag{2.49}$$

Since $\mathcal{H}$ is restricted to those functions that are divergence free, the solenoidal condition $u_{i,i} = 0$ must be added into the maximisation problem by means of a Lagrange multiplier. This is done by adding a term

$$\int_V \pi(\mathbf{x}) u_{i,i}\, dV = 0$$

in the maximisation. With the above condition included, the Euler–Lagrange equations are

$$\Lambda\left[\left(\frac{\lambda H+1}{2\sqrt{\lambda}}\right)R\theta - \left(\frac{1-H_1\xi}{2\sqrt{\xi}}\right)R_1\phi - \left(\frac{1-H_2\mu}{2\sqrt{\mu}}\right)R_2\psi\right]k_i - u_i = \pi_{,i} \tag{2.50}$$

$$\Lambda\left(\frac{\lambda H+1}{2\sqrt{\lambda}}\right)Rw + \Delta\theta = 0, \tag{2.51}$$

$$-\Lambda\left(\frac{1-H_1\xi}{2\sqrt{\xi}}\right)R_1 w + \Delta\phi = 0, \tag{2.52}$$

$$-\Lambda\left(\frac{1-H_2\mu}{2\sqrt{\mu}}\right)R_2 w + \Delta\psi = 0. \tag{2.53}$$

At the stability limit $\Lambda \to 1$. Setting $\Lambda = 1$ in the Euler–Lagrange equations (2.50)–(2.53) will then yield the optimum results. The equations to be solved are now

$$\left[\left(\frac{\lambda H+1}{2\sqrt{\lambda}}\right)R\theta - \left(\frac{1-H_1\xi}{2\sqrt{\xi}}\right)R_1\phi - \left(\frac{1-H_2\mu}{2\sqrt{\mu}}\right)R_2\psi\right]k_i - u_i = \pi_{,i} \tag{2.54}$$

$$\left(\frac{\lambda H+1}{2\sqrt{\lambda}}\right)Rw + \Delta\theta = 0, \tag{2.55}$$

$$-\left(\frac{1-H_1\xi}{2\sqrt{\xi}}\right)R_1 w + \Delta\phi = 0, \tag{2.56}$$

$$-\left(\frac{1-H_2\mu}{2\sqrt{\mu}}\right)R_2 w + \Delta\psi = 0. \tag{2.57}$$

At this point R_1 and R_2 are considered to be fixed and the variation of R is investigated, where now

$$R = R(\lambda,\, \xi,\, \mu,\, a^2),$$

where a is a wavenumber.

Two special cases are considered, Firstly,

$$H = 1, H_1 = H_2 = -1.$$

This corresponds to heating from below and salting from above with both salt fields. In this case all three effects are destabilizing. Equations (2.54)–(2.57) become

$$\left[\left(\frac{\lambda+1}{2\sqrt{\lambda}}\right) R\theta - \left(\frac{\xi+1}{2\sqrt{\xi}}\right) R_1\phi - \left(\frac{\mu+1}{2\sqrt{\mu}}\right) R_2\psi\right] k_i - u_i = \pi_{,i} \tag{2.58}$$

$$\left(\frac{\lambda+1}{2\sqrt{\lambda}}\right) Rw + \Delta\theta = 0, \tag{2.59}$$

$$-\left(\frac{\xi+1}{2\sqrt{\xi}}\right) R_1 w + \Delta\phi = 0, \tag{2.60}$$

$$-\left(\frac{\mu+1}{2\sqrt{\mu}}\right) R_2 w + \Delta\psi = 0. \tag{2.61}$$

Now vary each of λ, ξ and μ in turn and find the optimum values of these coupling parameters. Firstly, consider ξ, μ, R_1 and R_2 to be fixed and investigate the optimum value of λ by using parametric differentiation. Let now superscripts 1 and 2 refer to a solution of (2.58)–(2.61) corresponding to parameters λ^1 and λ^2 respectively. The inner products $((2.58)^1, \mathbf{u}^2), ((2.58)^2, \mathbf{u}^1), ((2.59)^1, \theta^2), ((2.59)^2, \theta^1), ((2.60)^1, \phi^2)$, $((2.60)^2, \phi^1), ((2.61)^1, \psi^2)$ and $((2.61)^2, \psi^1)$ are formed. Putting

$$f = \frac{\lambda+1}{2\sqrt{\lambda}}, g = \frac{\xi+1}{2\sqrt{\xi}}, h = \frac{\mu+1}{2\sqrt{\mu}}, \tag{2.62}$$

gives rise to the following equations

$$R^1 f^1(\theta^1, w^2) - R_1 g(\phi^1, w^2) - R_2 h(\psi^1, w^2) = (\mathbf{u}^1, \mathbf{u}^2), \tag{2.63}$$

$$R^2 f^2(\theta^2, w^1) - R_1 g(\phi^2, w^1) - R_2 h(\psi^2, w^1) = (\mathbf{u}^2, \mathbf{u}^1), \tag{2.64}$$

$$f^1 R^1(w^1, \theta^2) = D(\theta^1, \theta^2), \tag{2.65}$$

$$f^2 R^2(w^2, \theta^1) = D(\theta^2, \theta^1), \tag{2.66}$$

$$-R_1 g(w^1, \phi^2) = D(\phi^1, \phi^2), \tag{2.67}$$

$$-R_1 g(w^2, \phi^1) = D(\phi^2, \phi^1), \tag{2.68}$$

$$-R_2 h(w^1, \psi^2) = D(\psi^1, \psi^2), \tag{2.69}$$

$$-R_2 h(w^2, \psi^1) = D(\psi^2, \psi^1), \tag{2.70}$$

where $D(\alpha, \beta) = (\nabla\alpha, \nabla\beta)$.

To proceed, form (2.63)+(2.65)−(2.64)−(2.66)+(2.67)−(2.68)+(2.69)−(2.70) to find

$$\left(R^2 f^2 - R^1 f^1\right)\left[(\theta^2, w^1) + (\theta^1, w^2)\right] = 0.$$

Divide this by $\lambda^2 - \lambda^1$ and rearrange to find

$$\left[R^2 \frac{f^2 - f^1}{\lambda^2 - \lambda^1} + f^1 \frac{R^2 - R^1}{\lambda^2 - \lambda^1}\right]\left[(\theta^2, w^1) + (\theta^1, w^2)\right] = 0.$$

Letting $\lambda^2 \to \lambda^1$ then produces

$$\left(R\frac{\partial f}{\partial \lambda} + f\frac{\partial R}{\partial \lambda}\right)(\theta, w) = 0. \tag{2.71}$$

However, from (2.55)

$$Rf(\theta, w) = D(\theta, \theta) = \|\nabla\theta\|^2. \tag{2.72}$$

At the optimum value of λ, $\dfrac{\partial R}{\partial \lambda} = 0$ and so, from (2.71) and (2.72),

$$R\frac{\partial f}{\partial \lambda}\frac{\|\nabla\theta\|^2}{Rf} = 0,$$

and since $f > 0$, clearly $\dfrac{\partial f}{\partial \lambda} = 0$. From (2.62),

$$\frac{\partial f}{\partial \lambda} = \frac{\lambda - 1}{4\lambda^{\frac{3}{2}}}.$$

So,

$$\frac{\partial R}{\partial \lambda} = 0 \Rightarrow \lambda = 1. \tag{2.73}$$

By fixing λ and μ and varying ξ a similar argument to the above will show that

$$\frac{\partial R}{\partial \xi} = 0 \Rightarrow \xi = 1,$$

and similarly, for fixed λ and ξ the optimum value of μ is 1.

With $\lambda = \xi = \mu = 1$ the equations (2.58)–(2.61) are identical to the linearised versions of (2.36)–(2.40) with a time dependence $e^{\sigma t}$ assumed and σ set equal to zero. So, if σ can be shown to be real, the linear instability and nonlinear stability boundaries will coincide.

The linearised perturbation equations are, from (2.36)–(2.39) with a time dependence $e^{\sigma t}$ assumed,

$$\pi_{,i} = -u_i + [R\theta - R_1\phi - R_2\psi]\, k_i, \tag{2.74}$$

$$\sigma\theta = Rw + \Delta\theta, \tag{2.75}$$

$$P_1\sigma\phi = -R_1 w + \Delta\phi, \tag{2.76}$$

$$P_2\sigma\psi = -R_2 w + \Delta\psi. \tag{2.77}$$

Multiplying (2.74) by u_i^* (the complex conjugate of u_i), (2.75) by θ^*, (2.76) by ϕ^*, (2.77) by ψ^*, integrating each over V and making use of the boundary conditions yields

$$0 = -\|\mathbf{u}\|^2 + R(\theta, w^*) - R_1(\phi, w^*) - R_2(\psi, w^*), \tag{2.78}$$

$$\sigma\|\theta\|^2 = R(w, \theta^*) - (\theta_{,j}, \theta^*_{,j}), \tag{2.79}$$

$$P_1\sigma\|\phi\|^2 = -R_1(w, \phi^*) - (\phi_{,j}, \phi^*_{,j}), \tag{2.80}$$

$$P_2\sigma\|\psi\|^2 = -R_2(w, \psi^*) - (\psi_{,j}, \psi^*_{,j}), \tag{2.81}$$

where now $\|a\|^2 = (a, a^*)$. Adding (2.78) + (2.79) + (2.80) + (2.81) yields

$$\begin{aligned} &\sigma\left(\|\theta\|^2 + P_1\|\phi\|^2 + P_2\|\psi\|^2\right) \\ &= R\left[(\theta, w^*) + (\theta^*, w)\right] - R_1\left[(\phi, w^*) + (\phi^*, w)\right] \\ &-R_2\left[(\psi, w^*) + (\psi^*, w)\right] \\ &-\left(\|\mathbf{u}\|^2 + \|\nabla\theta\|^2 + \|\nabla\phi\|^2 + \|\nabla\psi\|^2\right), \end{aligned} \tag{2.82}$$

The right hand side of (2.82) is real and so letting $\sigma = \sigma_r + i\sigma_i$, then taking the imaginary part of (2.82) yields

$$\sigma_i\left(\|\theta\|^2 + P_1\|\phi\|^2 + P_2\|\psi\|^2\right) = 0.$$

Hence,

$$\sigma_i = 0.$$

Therefore the growth rate is real and so the linear instability and nonlinear stability boundaries coincide in this case. This is an important result and demonstrates that when $H = 1, H_1 = H_2 = -1$ there can be no subcritical instabilities.

The next case considered is

$$H = H_1 = 1, H_2 = -1.$$

This corresponds to the situation studied in section 2.3 where the layer is heated from below, salted from below in component 1 but salted from above in component 2. This means that heat and component 2 are destabilizing but component 1 is in competition and acts as a stabilizing agent. Since the differential equations (2.6)–(2.10) do not form a symmetric system one does not expect agreement between the linear and nonlinear stability results. In this case the Euler–Lagrange equations (2.54)–(2.57) become

$$\left[\left(\frac{\lambda+1}{2\sqrt{\lambda}}\right)R\theta - \left(\frac{1-\xi}{2\sqrt{\xi}}\right)R_1\phi - \left(\frac{\mu+1}{2\sqrt{\mu}}\right)R_2\psi\right]k_i - u_i = \pi_{,i} \tag{2.83}$$

$$\left(\frac{\lambda+1}{2\sqrt{\lambda}}\right)Rw + \Delta\theta = 0, \tag{2.84}$$

$$-\left(\frac{1-\xi}{2\sqrt{\xi}}\right)R_1 w + \Delta\phi = 0, \tag{2.85}$$

$$-\left(\frac{\mu+1}{2\sqrt{\mu}}\right)R_2 w + \Delta\psi = 0. \tag{2.86}$$

Now set

$$f = \frac{\lambda+1}{2\sqrt{\lambda}}, g = \frac{1-\xi}{2\sqrt{\xi}}, h = \frac{\mu+1}{2\sqrt{\mu}}. \tag{2.87}$$

Again, if one uses parametric differentiation to find the optimum values of λ, ξ and μ, then a similar argument to that leading to (2.73) will show that

$$\frac{\partial R}{\partial \lambda} = 0 \Rightarrow \lambda = 1, \quad \frac{\partial R}{\partial \mu} = 0 \Rightarrow \mu = 1.$$

However, applying this argument for λ and μ fixed and considering the variation in ξ produces, with $\lambda = \mu = 1$,

$$\frac{\partial R}{\partial \xi}(\theta, w) - R_1\frac{\partial g}{\partial \xi}(\phi, w) = 0,$$

which can be written as, using equations (2.84), (2.85) and (2.87),

$$\frac{\|\nabla\theta\|^2}{R}\frac{\partial R}{\partial \xi} = -R_1\frac{\partial g}{\partial \xi}\frac{\|\nabla\phi\|^2}{gR_1} = \frac{\xi+1}{2\xi(1-\xi)}\|\nabla\phi\|^2,$$

where $\|\cdot\|$ once again denotes the $L^2(V)$ norm. So the system is singular at $\xi = 1$. While one cannot find a solution for $\dfrac{\partial R}{\partial \xi} = 0$ note that

$$\xi < 1 \Rightarrow \frac{\partial R}{\partial \xi} > 0, \quad \xi > 1 \Rightarrow \frac{\partial R}{\partial \xi} < 0.$$

This suggests that the best value of ξ is one. With this value of ξ, equations (2.83)–(2.86) become (the ϕ equation dropping out),

$$R\theta k_i - R_2 \psi k_i - u_i = \pi_{,i}, \tag{2.88}$$

$$Rw + \Delta\theta = 0, \tag{2.89}$$

$$-R_2 w + \Delta\psi = 0. \tag{2.90}$$

These equations are now solved for R_2 fixed. The $\pi_{,i}$ term is eliminated by taking curlcurl of equations (2.88) and selecting the third component to leave

$$\begin{aligned} R\Delta^*\theta - R_2\Delta^*\psi - \Delta w &= 0, \\ \Delta\theta &= -Rw, \\ \Delta\psi &= R_2 w, \end{aligned}$$

where Δ^* is once again the horizontal Laplacian. Eliminate θ and ψ to obtain a single equation in w,

$$R^2\Delta^* w + R_2^2\Delta^* w + \Delta^2 w = 0.$$

Now assume $w = \sin n\pi z \, e^{i(m_1 x + m_2 y)}$ to find

$$R^2 + R_2^2 = \frac{(n^2\pi^2 + a^2)^2}{a^2},$$

where $a^2 = m_1^2 + m_2^2$ is a wavenumber. The right–hand side is now minimised over n and a to find the least value is $4\pi^2$. So, the nonlinear energy boundary is

$$\left(R^2 + R_2^2\right)_{\min} = 4\pi^2. \tag{2.91}$$

2.5 Results

2.5.1 Linear instability

All results are for the case $n = 1$. Although there is no proof that $n = 1$ yields the minimum critical Rayleigh number, both the present work and the results of Pearlstein *et al.* (1989) suggest this to be so.

The case where $P_1 = 4.545454$ and $P_2 = 4.761904$ yields similar results to those of Pearlstein *et al.* (1989). These values for P_1 and P_2 correspond to the values for κ, κ_1 and κ_2 chosen by Pearlstein *et al.* (1989). Figure 2.2 shows the stability boundary R^{crit} as a function of R_1 for fixed $R_2 = 261.0$. There are three regions of interest. To the left of the cusp ($R_1 < -285.28$) there is a region of oscillatory onset. Here oscillatory instability first occurs at a smaller value of R than does stationary instability and there is a single critical value of R. To the right of the point of infinite slope ($R_1 > -284.92$) instability occurs with real growth rate. Here oscillatory instability does not occur and again there is one critical value of R. The intervening region is the most interesting and is shown in the right–hand graph of figure 2.2. Here three values of R^{crit} are required to fully specify the linear instability criteria. Oscillatory instability sets in first at the lowest critical Rayleigh number. Then there is a region of oscillatory instability until the middle critical Rayleigh number is reached. At this point the system becomes linearly stable again until the third critical Rayleigh number is reached. Here stationary instability sets in and the system remains linearly unstable for all higher values of R. These stability boundaries are identical to those of Pearlstein *et al.* (1989) in that each of R^{crit} and R_1 can be a multi–valued function of the other for fixed R_2, P_1 and P_2.

Figure 2.3 shows the (R^{crit}, R_2) stability boundary for the same values of P_1 and P_2 with $R_1 = -284.0$. Clearly R^{crit} and R_2 can be multi–valued functions of each other. Again three values of R^{crit} may be required to fully describe the linear stability criteria.

Figures 2.4 and 2.5 show the (R, k) neutral curves for $R_2 = 261.0$, $P_1 = 4.545454$, $P_2 = 4.761904$ and various R_1. For $R_1 = -320.0$ the oscillatory curve is connected to the stationary curve at two bifurcation points and the single critical Rayleigh number occurs at the minimum on the oscillatory curve. As R_2 is increased to -310.0, -305.0 and -300.0 the bifurcation points move closer together. At $R_1 = -288.5$ the curve has lost its single–valued nature and there are two points of infinite slope. However, still only one critical Rayleigh number occurs. At a value of R_1 lying between -288.5 and -287.0 the bifurcation points move together and coalesce and a closed oscillatory neutral curve is formed. At $R_1 = -287.0$ the oscillatory curve has become

detached from the stationary curve. The graphs of $R_1 = -286.0$ show the heart–shaped curve more clearly. As R_1 is increased the oscillatory curve moves entirely below the stationary curve and now three critical values of R are required. For the larger values of R_1 shown the oscillatory curve becomes increasingly smaller until at a value of R_1 between -285.1 and -284.9 the oscillatory curve collapses to a point and disappears. At $R_1 = -284.9$ the oscillatory curve is no longer found and the single critical Rayleigh number occurs at the minimum on the stationary curve.

The case where $P_1 = 0.5$, $P_2 = 1.5$ and $R_1 = 115.0$ is of interest as the results correspond to heating the fluid from above while the two salts are gravitationally unstable. Similar results to the case where $R_2 = 261.0$, $P_1 = 4.545454$, $P_2 = 4.761904$ are found. The stability boundary is shown in figure 2.6. As before there is a multivalued region where three critical Rayleigh numbers occur. The neutral curves in figures 2.7 and 2.8 show similar behaviour to the previous numerical example. At $R_2 = 10.0$ the oscillatory curve is single–valued and connected to the stationary curve at two bifurcation points. The single critical Rayleigh number occurs at the minimum on the oscillatory curve. As R_2 is increased to 20.0 the bifurcation points move closer together and the oscillatory curve loses its single–valued nature. As R_2 is increased further the bifurcation points move closer together until at a value of R_2 between 35.0 and 41.0 they coalesce and a closed oscillatory curve is formed. This closed curve then moves below the stationary curve and three critical Rayleigh numbers are required. The closed curve is heart–shaped over a small range of values (approximately $R_2 = 41.0 - 43.0$). At $R_2 = 44.0$ the curve has lost its heart shape and is now a convex curve. For increasing values of R_2 this convex curve decreases in size until it eventually collapses to a point and disappears. At $R_2 = 50.0$ only the stationary neutral curve is found and the single critical Rayleigh number occurs at the minimum of this curve.

2.5.2 Nonlinear stability

Figure 2.9 shows the nonlinear stability boundary for the case $H = H_1 = 1, H_2 = -1$ from equation (2.91) plotted with the linear instability boundary for fixed values of $R_1 = -284.0, P_1 = 4.545454, P_2 = 4.761904$. In addition, the linear instability

boundaries for $R_1 = -184.0$ and $R_1 = -130.5$ are shown. For larger values of R_1 than -130.5 one does not find closed oscillatory neutral curves. Since these curves are the main interest of this thesis no larger values of R_1 are considered. As can be seen from the figure, the larger the value of R_1 the closer the nonlinear energy boundary is to the linear instability boundary and the smaller the region of possible subcritical instabilities. This is not surprising as the equation corresponding to R_1 (the ϕ equation) drops out of the analysis in section 2.4 and so does not provide any information. However, these results do have the important advantage that they are unconditional, i.e. nonlinear stability is guaranteed for initial perturbations of arbitrary sized amplitude.

2.6 Conclusions and discussion

In the case where $P_1 = 4.545454, P_2 = 4.761904$ it has been shown that the important results of Pearlstein *et al.* (1989) have carried over to the porous case. In particular the existence of stability boundaries in the (R, R_2) (or (R, R_1))–plane that are multi–valued functions of both R and R_2 (or both R and R_1) shows that the conclusion of Rudraiah and Vortmeyer (1982) that "marginal stability of oscillatory modes occurs on a hyperboloid in Rayleigh number space but the surface is very closely approximated by its planar asymptotes for any diffusivity ratios" is incorrect. In addition the existence of heart–shaped oscillatory neutral curves resulting in the onset of oscillatory instability at a given value of R for two different horizontal wavenumbers is a feature not seen before in multi–component porous convection.

In the case where $P_1 = 1.5, P_2 = 0.5$ one can find positive values of R_1 and R_2 that give rise to heart–shaped oscillatory curves. These values correspond to the case of having both salt fields destabilizing. In the work of Pearlstein *et al.* (1989) they claim (erroneously) that when the stratifying agencies corresponding to R_1 and R_2 are destabilizing then it is impossible to have two onset frequencies at the same wavenumber. As explained in section 2.3 the necessary conditions (2.26) and (2.27) derived here show that having both salt fields stabilizing rules out the possibility of having a multi–valued oscillatory curve.

In equations (2.5) both the temperature and normal component of velocity were regarded as being prescribed at the boundaries. These boundary conditions are discussed by Joseph (1976). In a porous medium the fluid will stick to a solid wall but this effect is confined to a boundary layer whose size is measured in pore diameters. As the wall friction does not overtly affect the motion in the interior it is reasonable to replace the true wall with a frictionless wall in this analysis.

Pearlstein *et al.* (1989) discuss the experimental problems of prescribing constant concentration at the boundaries. They suggest the use of semi–permeable membranes as boundaries through which solute can pass into the working fluid volume. If the fluid outside the membrane is maintained at a constant concentration then the solute boundary condition could be realised to within a good approximation.

There is some doubt as to whether the onset of instability at two wavenumbers and the same Rayleigh number would be seen experimentally. In a situation where a heart–shaped oscillatory neutral curve arises, the initial onset of instability occurs at the minimum on the oscillatory curve. The value of R corresponding to onset at two different frequencies is, however, not a minimum and this instability lies in the range where nonlinear effects are likely to be important. Work by Proctor (1981) and Hansen and Yuen (1989) on finite amplitude double diffusive convection and by Rudraiah, Srimani and Friedrich (1982) on the equivalent problem in a porous medium have shown that subcritical convection could occur at values of the thermal Rayleigh number much less than that predicted by the linear stability theory and hence the need for the nonlinear analysis presented here. As explained in section 2.4, the fact that the stabilizing salt field terms drop out of the analysis leads to energy results that may be far away from the linear results. To overcome this a generalised energy method is presented in the next chapter that yields superior results.

In addition there is the physical relevance of the equation of state. McKay and Straughan (1992) argue that the density of a fluid is never a linear function of temperature. In chapter 4 a nonlinear buoyancy law is adopted. The effect of this is that the closed oscillatory neutral curves are no longer perfectly heart–shaped but instead are slightly skewed. The phenomenon of onset of instability at two different

wavenumbers and the same Rayleigh number is no longer seen.

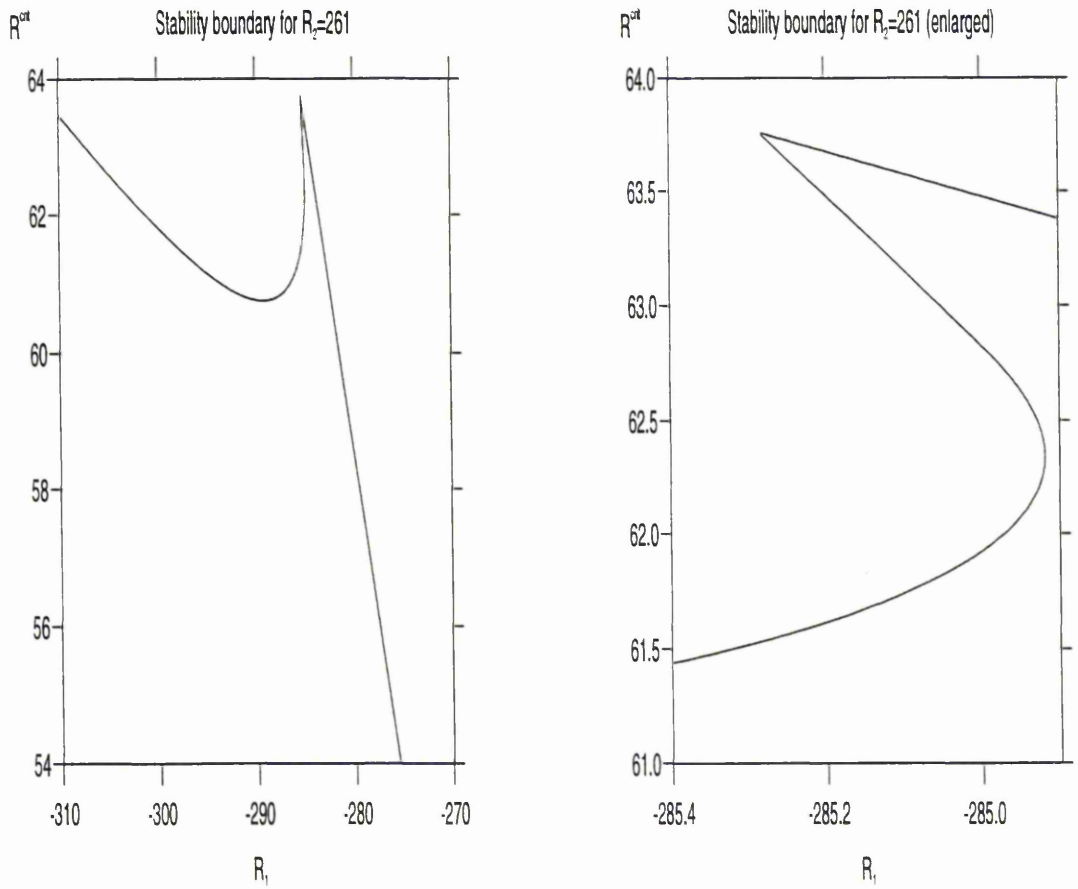

Figure 2.2: (R^{crit}, R_1) stability boundary for $R_2 = 261.0$, $P_1 = 4.545454$, $P_2 = 4.761904$. The right–hand graph shows the multi–valued region in more detail.

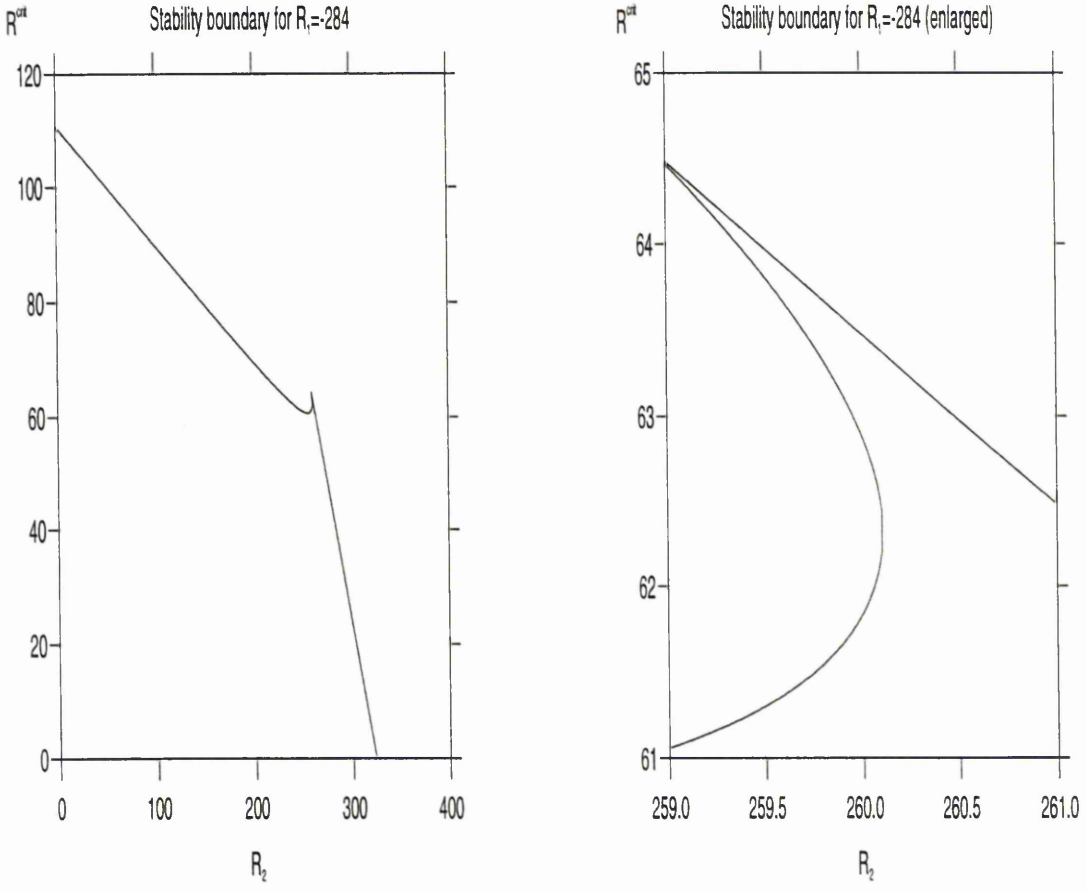

Figure 2.3: (R^{crit}, R_2) stability boundary for $R_1 = -284.0$, $P_1 = 4.545454$, $P_2 = 4.761904$. The right–hand graph shows the multi–valued region in more detail.

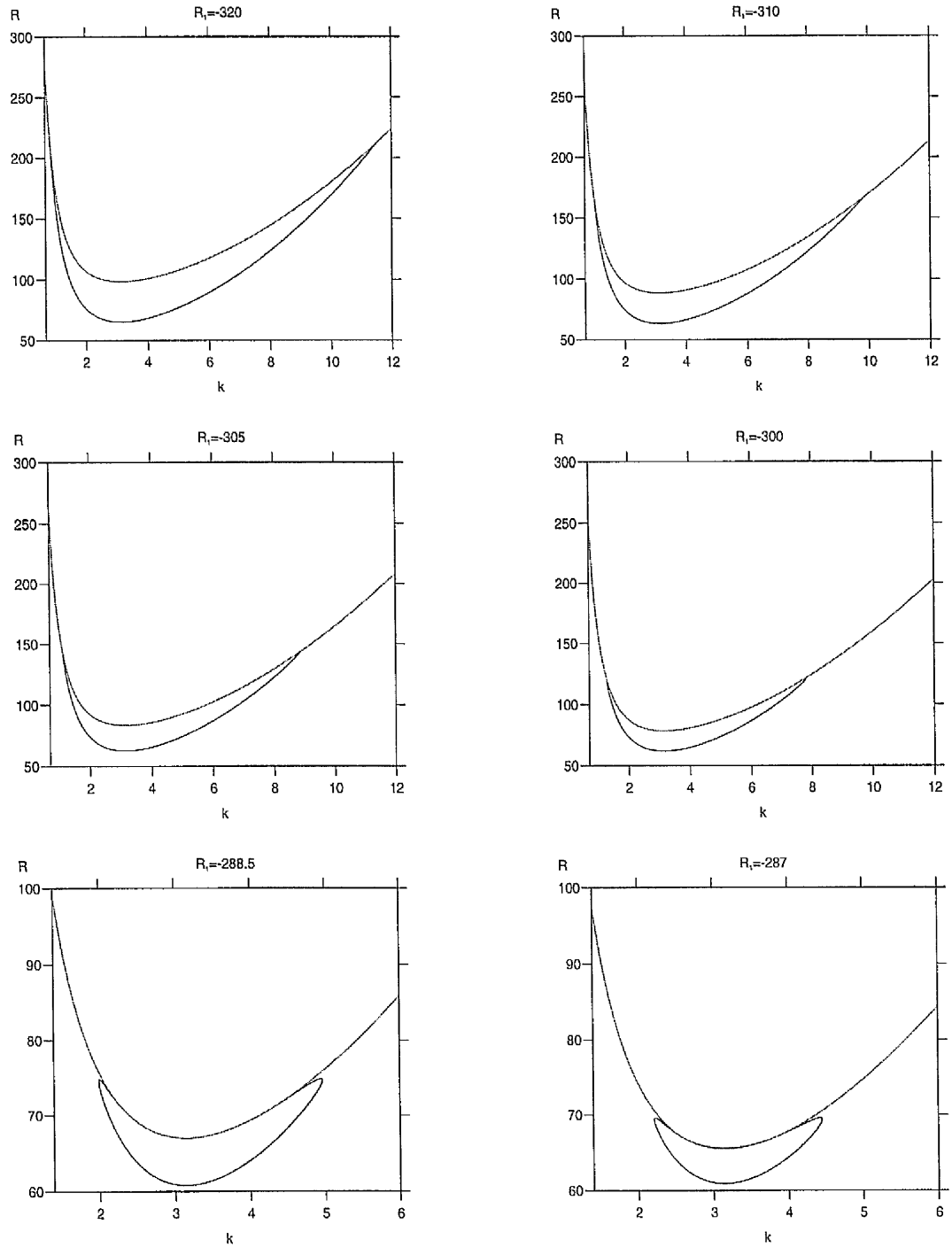

Figure 2.4: Neutral curves for $R_2 = 261.0$, $P_1 = 4.545454$, $P_2 = 4.761904$

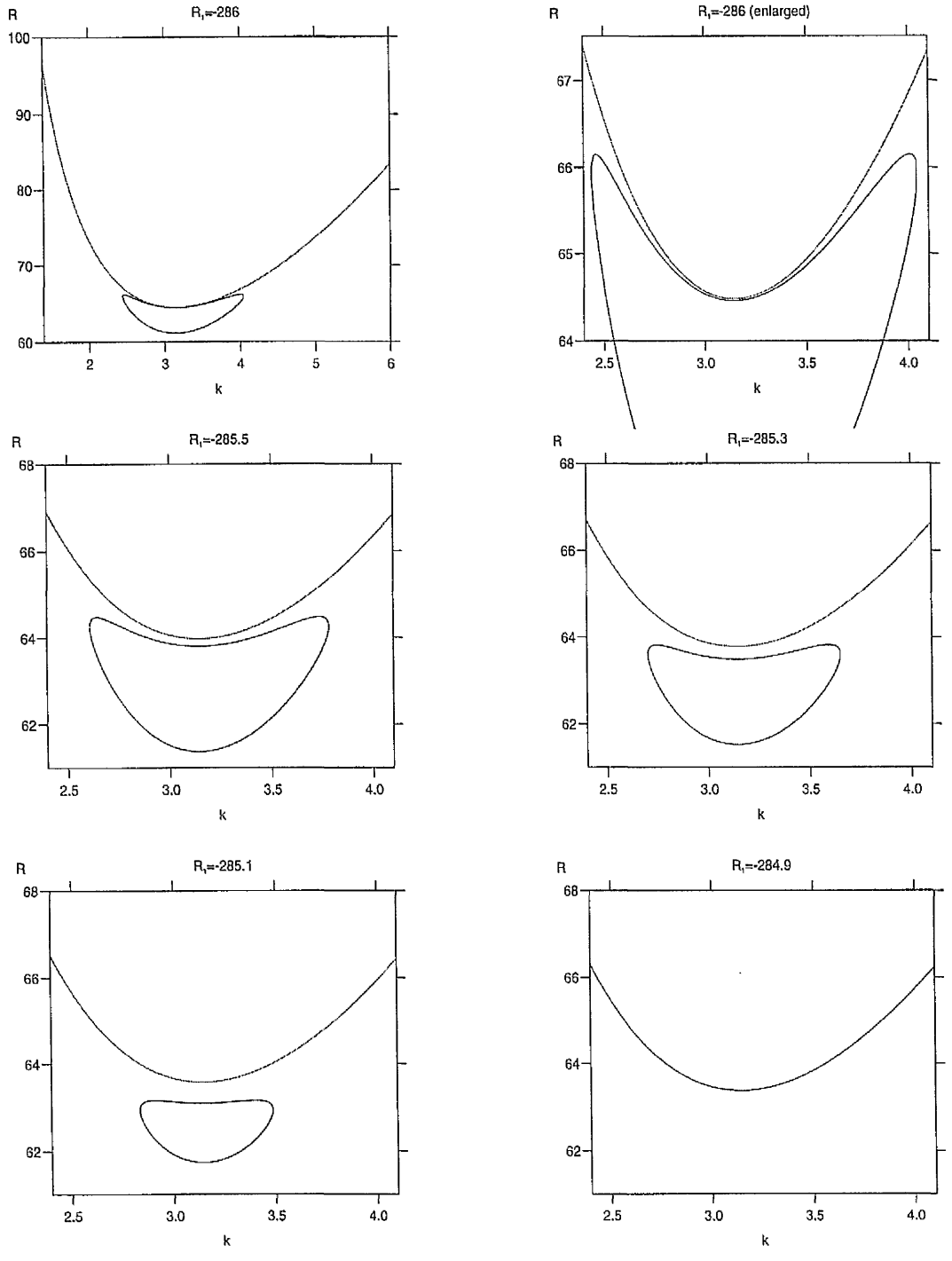

Figure 2.5: Further neutral curves for $R_2 = 261.0$, $P_1 = 4.545454$, $P_2 = 4.761904$

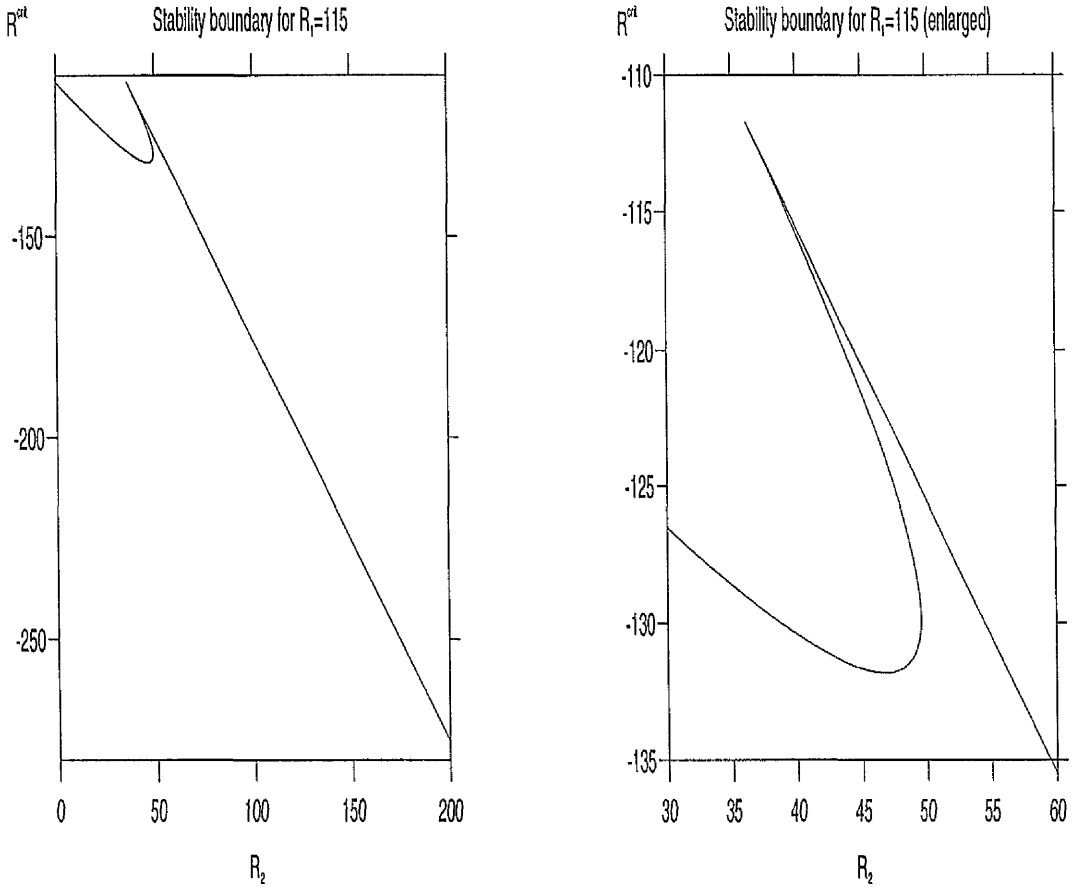

Figure 2.6: (R^{crit}, R_2) stability boundary for $R_1 = 115.0$, $P_1 = 0.5$, $P_2 = 1.5$. The right–hand graph shows the multi–valued region in more detail.

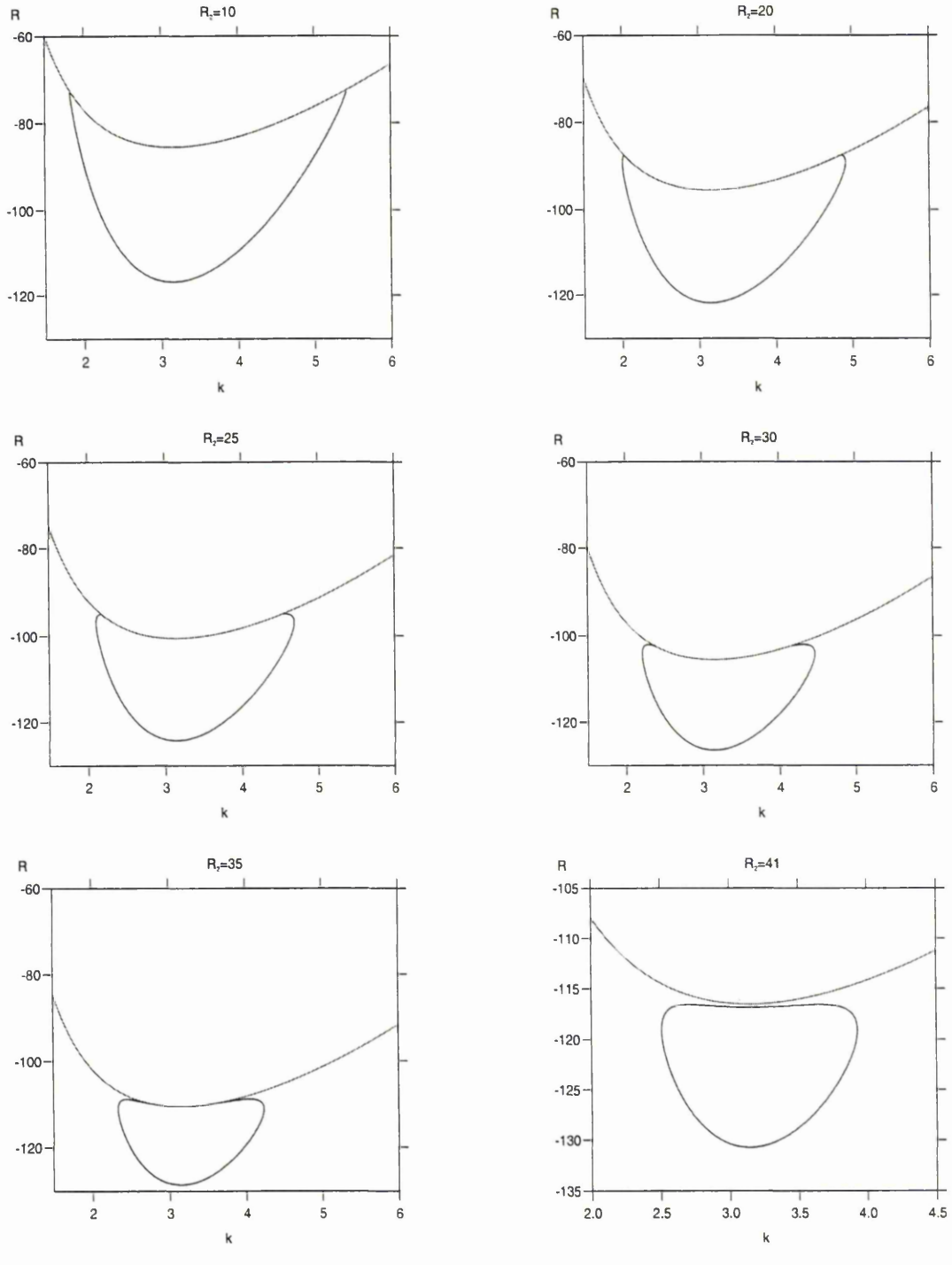

Figure 2.7: Neutral curves for $R_1 = 115.0$, $P_1 = 0.5$, $P_2 = 1.5$

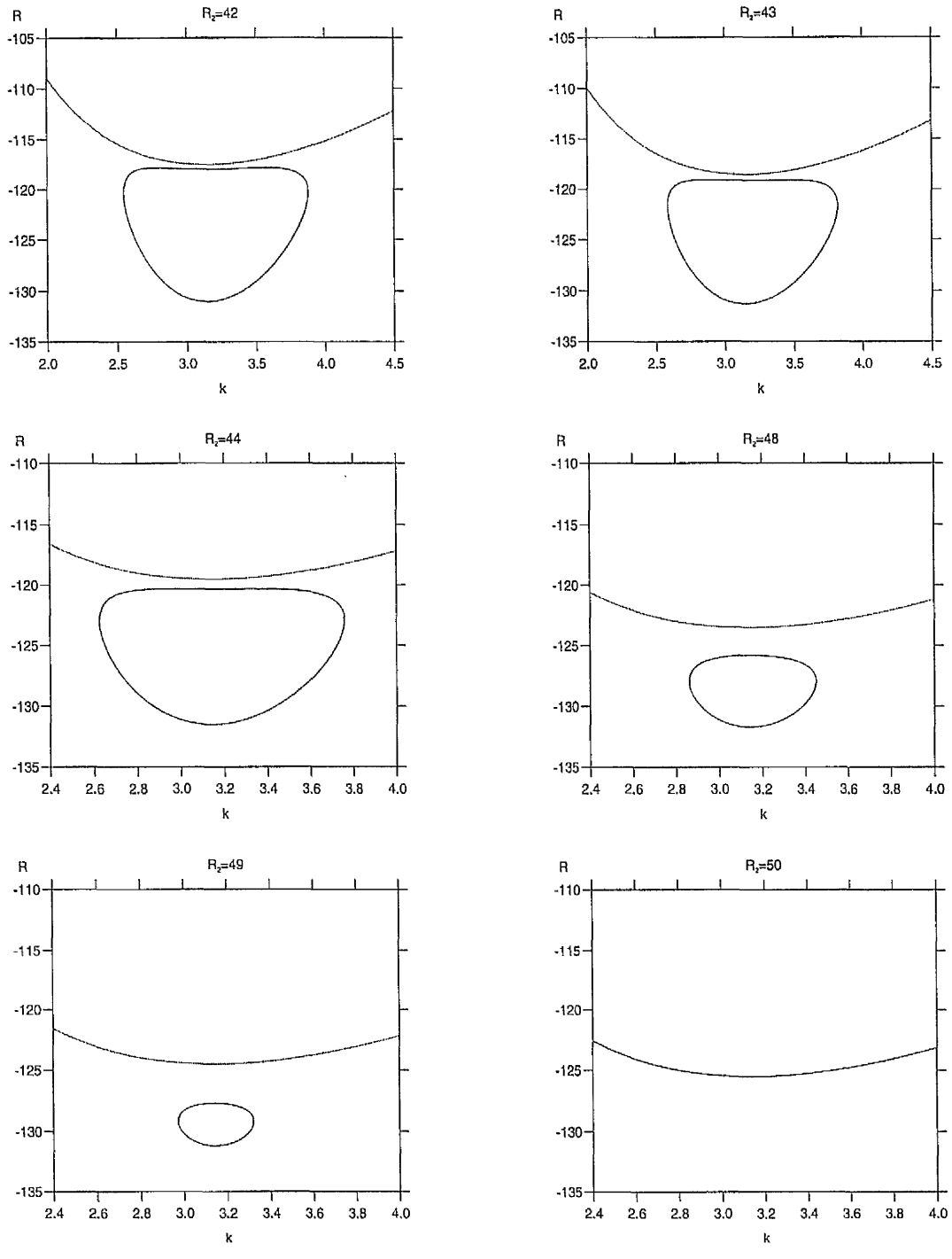

Figure 2.8: Further neutral curves for $R_1 = 115.0$, $P_1 = 0.5$, $P_2 = 1.5$

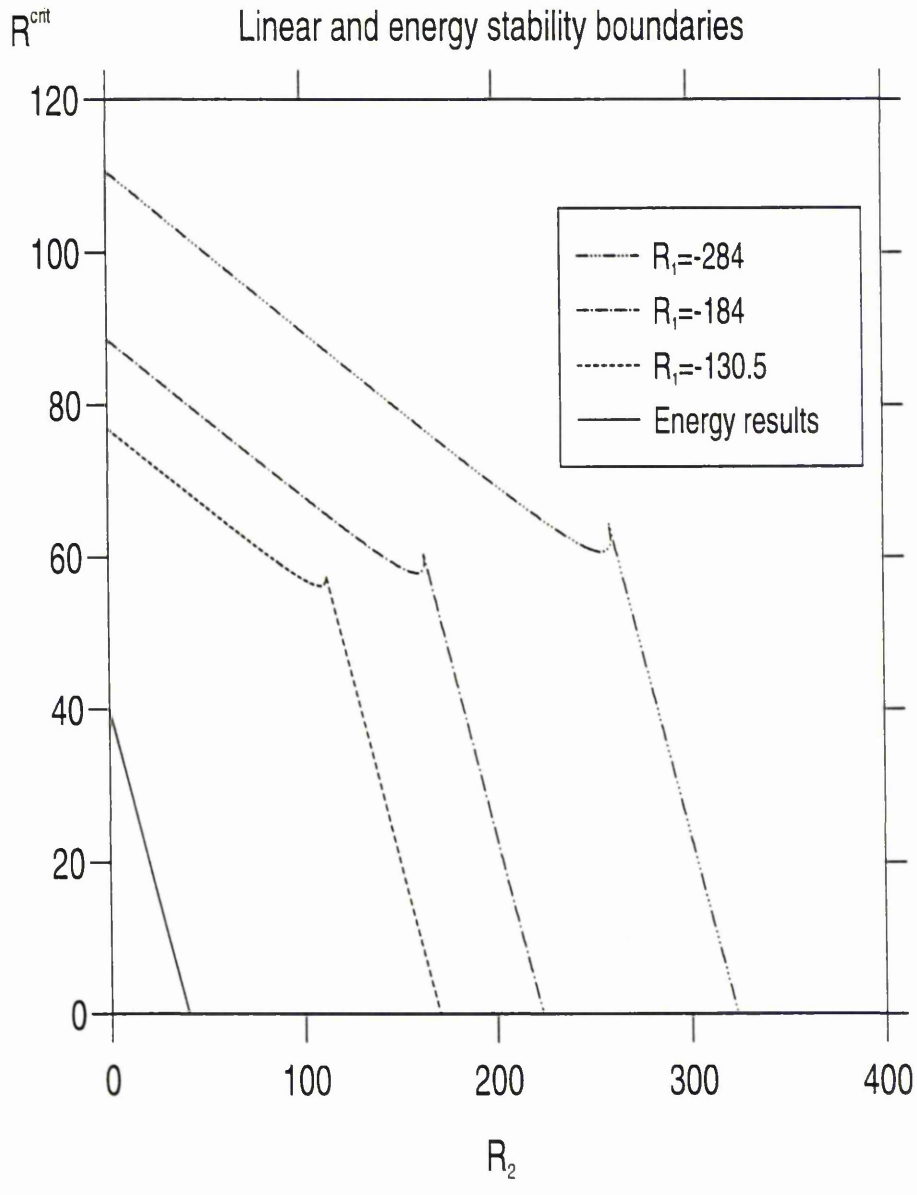

Figure 2.9: Linear instability and nonlinear stability boundaries. The linear instability boundaries are shown for three values of R_1.

Chapter 3

Nonlinear stability of multi–component convection–diffusion in a porous medium

3.1 Introduction

In chapter 2 interesting original results were found in considering the linear stability of a fluid–saturated porous layer with two salt fields dissolved in it. In particular it was shown that the earlier work of Rudraiah and Vortmeyer (1982) and Poulikakos (1985) was incomplete. Specifically, it was shown that for some fixed values of the diffusivity ratios, Prandtl number and two of the three Rayleigh numbers, three values of the third Rayleigh number may be required to fully describe the linear stability criteria. The reason for this is an unusual, symmetric, heart–shaped oscillatory neutral curve lying entirely below the stationary neutral curve (see figures 2.5 and 2.8). One interesting effect predicted by this heart–shaped curve is the onset of linear instability at the same thermal Rayleigh number but different wavenumbers. However, the Rayleigh number at which this occurs is not a minimum but instead lies in a region where nonlinear effects are likely to be of importance. Work by Proctor (1981) and Hansen and Yuen (1989) on the double–diffusive fluid prob-

lem shows that subcritical instability can occur at values of the thermal Rayleigh number much less than that predicted by linear theory. Rudraiah, Shivakumara and Friedrich (1986) find a similar result in considering the effect of rotation on the double–diffusive porous problem. Consequently an investigation of the nonlinear stability of the triple–diffusive porous problem was needed. In section 2.4 an application of the classical energy method is presented which yields unconditional exponential nonlinear stability. However, the results are somewhat unsatisfactory. When the optimum values of the coupling parameters are found one of the equations drops out of the analysis and so does not provide any information and as a consequence the results are rather disappointing, in the sense that the nonlinear stability boundary may be far from the equivalent linear one.

Mulone (1994) presents a generalised energy method for the problem of a fluid layer heated and salted from below. Rather than work with the salt concentration perturbation he introduces a new variable formed from a linear combination of the temperature and solute perturbations. He obtains a globally nonlinear exponential stability theorem and for certain values of the Schmidt and Prandtl numbers shows coincidence of the linear and nonlinear stability boundaries.

In the present chapter we study the situation concentrated on in chapter 2, i.e. where the layer is heated from below, salted from below in the component with larger salt diffusivity and salted from above in the other salt field. From a mathematical point of view the competition between the heat and salt fields means that the operator associated with the linear stability is not symmetric. Indeed, in chapter 2 oscillatory convection is found. When the operator is not symmetric it is usually hard to develop a nonlinear stability analysis to give a sharp nonlinear threshold. Here we have been able to construct a suitable generalised energy (Lyapunov functional) which does yield a useful stability threshold. This is a great improvement on results found by employing a standard "kinetic energy".

This chapter has essentially appeared as Tracey (1997a).

3.2 Governing equations

Consider a fluid saturated porous layer lying in the infinite three–dimensional region $0 < z < d$. The boundaries $z = 0$ and $z = d$ are maintained at temperatures T_l and T_u respectively. Suppose further that the fluid has dissolved in it two different chemical components. Denote the concentration of component α by C^α $(\alpha = 1, 2)$. The concentration of component α at the lower and upper boundaries is held at C_l^α and C_u^α respectively.

An equation of state which is linear in both the temperature field and the salt concentration is assumed, i.e.

$$\rho = \rho_0 \left(1 - A\left(T - T_0\right) + A_1 \left(C^1 - C_0^1\right) + A_2 \left(C^2 - C_0^2\right)\right),$$

where ρ_0, T_0 and C_0^α $(\alpha = 1, 2)$ are reference values of density, temperature and salt concentration respectively. The constants A and A_α $(\alpha = 1, 2)$ represent the thermal and solute expansion coefficients respectively.

The equations of motion which govern flow in a porous medium are largely based on a relation which is a generalisation of empirical observations (c.f. Nield and Bejan (1992)). This relation is known as Darcy's Law and can be written

$$\nabla p = -\frac{\mu}{k}\mathrm{v} + \rho \mathrm{g},$$

where the variables p, μ, k, v and g represent pressure, dynamic viscosity, permeability, velocity and gravitational acceleration respectively. In addition to Darcy's Law we have the incompressibility condition and the equations of conservation of temperature and solute. Combining these equations with the Darcy law and the equation of state we obtain the following system of governing equations

$$\begin{aligned}
p_{,i} &= -\frac{\mu}{k} v_i - g\rho_0(1 - A(T - T_0) \\
&\quad + A_1(C^1 - C_0^1) + A_2(C^2 - C_0^2))k_i, && (3.1)\\
v_{i,i} &= 0, && (3.2)\\
T_{,t} + v_i T_{,i} &= \kappa \Delta T, && (3.3)\\
C_{,t}^\alpha + v_i C_{,i}^\alpha &= \kappa_\alpha \Delta C^\alpha \ (\alpha = 1, 2), && (3.4)
\end{aligned}$$

where indicial notation and the Einstein summation convention have been employed. The vector $\mathbf{k}$ is the unit vector in the z–direction. The variables κ and κ_α represent thermal and solute diffusivities respectively.

The boundary conditions we consider are

$$\begin{aligned} &T(0) = T_l,\ T(d) = T_u, \\ &C^\alpha(0) = C_l^\alpha,\ C^\alpha(d) = C_u^\alpha\ (\alpha = 1, 2), \\ &v_3 = 0 \text{ at } z = 0, d. \end{aligned} \tag{3.5}$$

The experimental realisation of prescribing these boundary conditions for the salt concentrations has been investigated by Krishnamurti and Howard (1983).

Consider a steady solution $(\bar{v}_i, \bar{p}, \bar{T}, \bar{C}^\alpha)$ of (3.1)–(3.5) where $\bar{v}_i = 0$ and $\bar{T}$ and $\bar{C}^\alpha$ are functions of z. Equations (3.3) and (3.4) show that, utilising (3.5),

$$\begin{aligned} \bar{T} &= T_l - \beta z,\ (\beta = \frac{T_l - T_u}{d}), \\ \bar{C}^\alpha &= C_l^\alpha - \frac{\triangle C^\alpha}{d} z,\ (\triangle C^\alpha = C_l^\alpha - C_u^\alpha). \end{aligned}$$

and the steady state pressure $\bar{p}$ can be obtained from (3.1).

In order to investigate the nonlinear stability of this basic solution we introduce perturbations $(u_i, \pi, \theta, \phi^\alpha)$ to $(\bar{v}_i, \bar{p}, \bar{T}, \bar{C}^\alpha)$ via

$$v_i = \bar{v}_i + u_i,\ p = \bar{p} + \pi,\ T = \bar{T} + \theta,\ C^\alpha = \bar{C}^\alpha + \phi^\alpha.$$

The resultant perturbation equations are non–dimensionalised using the following scalings:

$$t = t^* \frac{d^2}{\kappa},\ \mathbf{u} = \mathbf{u}^* \frac{\kappa}{d},\ \pi = \pi^* \frac{\mu\kappa}{k},\ \mathbf{x} = \mathbf{x}^* d,$$

$$\theta = \theta^* T^\#,\ \phi^\alpha = (\phi^\alpha)^* \Phi^\alpha,$$

$$T^\# = \left(\frac{\mu\kappa|\delta T|}{A\rho_o g k d}\right)^{1/2},\ \Phi^\alpha = \left(\frac{\mu\kappa P_\alpha |\triangle C^\alpha|}{A_\alpha \rho_o g k d}\right)^{1/2},$$

$$R = \left(\frac{A\rho_o g k d|\delta T|}{\mu\kappa}\right)^{1/2},\ R_\alpha = \left(\frac{A_\alpha \rho_o g k d P_\alpha |\triangle C^\alpha|}{\mu\kappa}\right)^{1/2},$$

$$\delta T = T_l - T_u,\ H = \text{sgn}(\delta T),\ H_\alpha = \text{sgn}(\triangle C^\alpha),\ P_\alpha = \frac{\kappa}{\kappa_\alpha}.$$

Here R and R_α are the thermal and salt Rayleigh numbers and P_α are salt Prandtl numbers.

The nonlinear perturbation equations are then, in non–dimensional form (dropping the asterisks),

$$\begin{aligned}
\pi_{,i} &= -u_i + \left[R\theta - R_1\phi^1 - R_2\phi^2\right] k_i, && (3.6)\\
u_{i,i} &= 0, && (3.7)\\
\theta_{,t} + u_i\theta_{,i} &= HRw + \Delta\theta, && (3.8)\\
P_1(\phi^1_{,t} + u_i\phi^1_{,i}) &= H_1R_1w + \Delta\phi^1, && (3.9)\\
P_2(\phi^2_{,t} + u_i\phi^2_{,i}) &= H_2R_2w + \Delta\phi^2. && (3.10)
\end{aligned}$$

The boundary conditions which follow from (3.5) for the perturbed quantities are

$$u_3 = w = 0,\ \theta = \phi^1 = \phi^2 = 0, \quad \text{on } z = 0, 1. \tag{3.11}$$

For the nonlinear analysis which follows we further assume that $u_i, \theta, \phi^1, \phi^2$ and π are periodic on the lateral boundaries of a period cell V.

3.3 Nonlinear stability analysis

The classical energy method leads to results which may be far from the linear stability boundary, as can be seen from curves (a) and (c) in figures (3.1)–(3.3). To take account of the fact that there is competition between the heat and salt effects we must modify the basic functions in which we seek nonlinear stability. To this end replace the salt perturbation fields ϕ^1 and ϕ^2 by the new generalised variables ψ and ϕ defined by

$$\psi = \phi^1 + \phi^2, \quad \phi = \phi^1 - \phi^2. \tag{3.12}$$

From (3.11) the boundary conditions for ψ and ϕ are $\phi = \psi = 0$ on $z = 0, 1$ and also that ϕ and ψ are periodic on the lateral boundaries of the period cell V.

Equation (3.6) can be rewritten in terms of the new variables as

$$\pi_{,i} = -u_i + \left[R\theta - \frac{1}{2}(R_1 + R_2)\psi - \frac{1}{2}(R_1 - R_2)\phi\right] k_i. \tag{3.13}$$

We also need evolution equations for ψ and ϕ and equations (3.9) and (3.10) can easily be rearranged to give

$$\psi_t + u_i\psi_{,i} = \left(\frac{H_1R_1}{P_1} + \frac{H_2R_2}{P_2}\right)w + \frac{1}{2}\left(\frac{1}{P_1} + \frac{1}{P_2}\right)\Delta\psi + \frac{1}{2}\left(\frac{1}{P_1} - \frac{1}{P_2}\right)\Delta\phi, \quad (3.14)$$

and

$$\phi_t + u_i\phi_{,i} = \left(\frac{H_1R_1}{P_1} - \frac{H_2R_2}{P_2}\right)w + \frac{1}{2}\left(\frac{1}{P_1} - \frac{1}{P_2}\right)\Delta\psi + \frac{1}{2}\left(\frac{1}{P_1} + \frac{1}{P_2}\right)\Delta\phi. \quad (3.15)$$

We wish to form the basic "energy" identities in L^2 combinations of u_i, θ, ψ and ϕ. Thus, we now multiply (3.13) by u_i, (3.8) by θ, (3.14) by ψ, (3.15) by ϕ and integrate over V. Integration by parts and use of the boundary conditions yields

$$\begin{aligned}
0 &= -\|\mathbf{u}\|^2 + R(\theta, w) - \frac{1}{2}(R_1 + R_2)(\psi, w) \\
&\qquad -\frac{1}{2}(R_1 - R_2)(\phi, w) && (3.16)\\
\frac{1}{2}\frac{d}{dt}\|\theta\|^2 &= HR(w, \theta) - \|\nabla\theta\|^2, && (3.17)\\
\frac{1}{2}\frac{d}{dt}\|\psi\|^2 &= \left(\frac{H_1R_1}{P_1} + \frac{H_2R_2}{P_2}\right)(w, \psi) - \frac{1}{2}\left(\frac{1}{P_1} + \frac{1}{P_2}\right)\|\nabla\psi\|^2 \\
&\qquad -\frac{1}{2}\left(\frac{1}{P_1} - \frac{1}{P_2}\right)(\nabla\phi, \nabla\psi), && (3.18)\\
\frac{1}{2}\frac{d}{dt}\|\phi\|^2 &= \left(\frac{H_1R_1}{P_1} - \frac{H_2R_2}{P_2}\right)(w, \phi) - \frac{1}{2}\left(\frac{1}{P_1} + \frac{1}{P_2}\right)(\nabla\psi, \nabla\phi) \\
&\qquad -\frac{1}{2}\left(\frac{1}{P_1} - \frac{1}{P_2}\right)\|\nabla\phi\|^2, && (3.19)
\end{aligned}$$

where $\|\cdot\|$ denotes the $L^2(V)$ norm and $(f, g) = \int_V fg\, dV$.

Now form (3.16) + γ_0 (3.17) + γ_1 (3.18) + γ_2 (3.19), where γ_0, γ_1 and γ_2 are positive coupling parameters to be selected at our discretion. If we define an energy $E(t)$ by

$$E(t) = \frac{\gamma_0}{2}\|\theta\|^2 + \frac{\gamma_1}{2}\|\psi\|^2 + \frac{\gamma_2}{2}\|\phi\|^2,$$

then it follows that

$$\frac{dE}{dt} = \mathcal{I} - \mathcal{D}, \quad (3.20)$$

where the indefinite term $\mathcal{I}$ and the dissipation $\mathcal{D}$ are given by

$$\begin{aligned}\mathcal{I} &= R(1+\gamma_0 H)(w,\theta) \\ &\quad +\Big[-\frac{1}{2}(R_1+R_2)+\gamma_1\Big(\frac{H_1R_1}{P_1}+\frac{H_2R_2}{P_2}\Big)\Big](w,\psi) \\ &\quad +\Big[-\frac{1}{2}(R_1-R_2)+\gamma_2\Big(\frac{H_1R_1}{P_1}-\frac{H_2R_2}{P_2}\Big)\Big](w,\phi), \qquad (3.21)\\ \mathcal{D} &= \|\mathbf{u}\|^2+\gamma_0\|\nabla\theta\|^2+\mathcal{D}_1(\psi,\phi). \qquad (3.22)\end{aligned}$$

In (3.22) the function $\mathcal{D}_1$ is given by

$$\begin{aligned}\mathcal{D}_1(\psi,\phi) &= \frac{\gamma_1(P_1+P_2)}{2P_1P_2}\|\nabla\psi\|^2+\frac{(\gamma_1+\gamma_2)(P_2-P_1)}{2P_1P_2}(\nabla\phi,\nabla\psi) \\ &\quad +\frac{\gamma_2(P_1+P_2)}{2P_1P_2}\|\nabla\phi\|^2. \qquad (3.23)\end{aligned}$$

In order to show nonlinear stability in a similar manner as the argument leading to equation (2.48) we need $\mathcal{D}_1$ to be definite positive. Clearly the middle term in equation (3.23) may be positive or negative. However, completing the square in $\mathcal{D}_1$ yields,

$$\begin{aligned}\mathcal{D}_1 &= \frac{\gamma_1(P_1+P_2)}{2P_1P_2}\Bigg[\|\nabla\left(\psi+\frac{(\gamma_1+\gamma_2)(P_2-P_1)}{2\gamma_1(P_1+P_2)}\phi\right)\|^2 \\ &\quad -\frac{(\gamma_1+\gamma_2)^2(P_2-P_1)^2-4\gamma_1\gamma_2(P_1+P_2)^2}{4\gamma_1^2(P_1+P_2)^2}\|\nabla\phi\|^2\Bigg]. \qquad (3.24)\end{aligned}$$

So, the condition

$$(\gamma_1+\gamma_2)^2(P_2-P_1)^2-4\gamma_1\gamma_2(P_1+P_2)^2<0 \qquad (3.25)$$

implies that $\mathcal{D}_1$ is a definite positive function of ψ and ϕ. In the arguments below we select γ_1 and γ_2 to ensure this is so. With this condition enforced then nonlinear stability can be obtained as follows. By rearrangement of (3.20),

$$\frac{dE}{dt}=\mathcal{I}-\mathcal{D}=-\mathcal{D}\left(1-\frac{\mathcal{I}}{\mathcal{D}}\right).$$

If we now define

$$\frac{1}{\Lambda}=\max_{\mathcal{H}}\frac{\mathcal{I}}{\mathcal{D}}, \qquad (3.26)$$

where $\mathcal{H}$ is the space of admissible functions, then

$$\frac{dE}{dt}\leq-\mathcal{D}(1-\frac{1}{\Lambda}).$$

If now $\Lambda > 1$ then $1 - \dfrac{1}{\Lambda} = a > 0$ and so

$$\frac{dE}{dt} \leq -a\mathcal{D}.$$

The Poincaré inequalities $\pi\|\theta\| \leq \|\nabla\theta\|, \quad \pi\|\psi\| \leq \|\nabla\psi\|, \quad \pi\|\phi\| \leq \|\nabla\phi\|$ may be used in the inequality above to deduce

$$\frac{dE}{dt} \leq -\frac{a\pi^2}{c_0}E,$$

where c_0 is a positive computable constant depending on $\gamma_0, \gamma_1, \gamma_2, P_1$ and P_2. This last inequality can then be integrated to show nonlinear exponential stability.

The problem remains to find the maximum in (3.26).

In order to clear the denominator of the maximisation problem of the coupling parameter γ_0 the transformation $\sqrt{\gamma_0}\,\theta \to \theta$ is made and the Euler–Lagrange equations for this maximum are then

$$\begin{aligned}\left\{\frac{R(1+\gamma_0 H)}{\sqrt{\gamma_0}}\theta + \left[-\frac{1}{2}(R_1+R_2) + \gamma_1\left(\frac{H_1R_1}{P_1} + \frac{H_2R_2}{P_2}\right)\right]\psi\right. \\ \left. + \left[-\frac{1}{2}(R_1-R_2) + \gamma_1\left(\frac{H_1R_1}{P_1} - \frac{H_2R_2}{P_2}\right)\right]\phi\right\} k_i - \frac{2}{\Lambda}u_i &= \varpi_{,i},\end{aligned} \tag{3.27}$$

$$\frac{R(1+\gamma_0 H)}{\sqrt{\gamma_0}} + \frac{2}{\Lambda}\Delta\theta = 0, \tag{3.28}$$

$$\begin{aligned}&\left[-\frac{1}{2}(R_1+R_2) + \gamma_1\left(\frac{H_1R_1}{P_1} + \frac{H_2R_2}{P_2}\right)\right]w \\ &+\frac{1}{\Lambda}\left[\gamma_1\left(\frac{1}{P_1}+\frac{1}{P_2}\right)\Delta\psi + \frac{1}{2}(\gamma_1+\gamma_2)\left(\frac{1}{P_1}-\frac{1}{P_2}\right)\Delta\phi\right] = 0,\end{aligned} \tag{3.29}$$

$$\begin{aligned}&\left[-\frac{1}{2}(R_1-R_2) + \gamma_2\left(\frac{H_1R_1}{P_1} - \frac{H_2R_2}{P_2}\right)\right]w \\ &+\frac{1}{\Lambda}\left[\gamma_2\left(\frac{1}{P_1}+\frac{1}{P_2}\right)\Delta\phi + \frac{1}{2}(\gamma_1+\gamma_2)\left(\frac{1}{P_1}-\frac{1}{P_2}\right)\Delta\psi\right] = 0,\end{aligned} \tag{3.30}$$

where ϖ is a Lagrange multiplier introduced because $\mathbf{u}$ is divergence free.

If $H = 1, H_1 = H_2 = -1$, then all effects are destabilizing and the nonlinear energy boundary is the same as the linear stability boundary, see section 2.3. The focus of this chapter is the situation where salt concentration 1 is stabilizing and the other effects are destabilizing in the conduction state. This is the case $H = H_1 = 1, \ H_2 = -1$. This was studied according to linear stability methods and the standard kinetic energy method in chapter 2.

To draw conclusions from equations (3.27)–(3.30) consider $R_1, R_2, P_1, P_2, \gamma_1$ and γ_2 to be fixed and use parametric differentiation to investigate the variation of R with γ_0. Denote by f, g and h the functions

$$f(\gamma_0) = \frac{1+\gamma_0}{\sqrt{\gamma_0}}, \tag{3.31}$$

$$g(\gamma_1) = -\frac{1}{2}(R_1 + R_2) + \gamma_1 \left(\frac{R_1}{P_1} - \frac{R_2}{P_2}\right), \tag{3.32}$$

$$h(\gamma_2) = -\frac{1}{2}(R_1 - R_2) + \gamma_2 \left(\frac{R_1}{P_1} + \frac{R_2}{P_2}\right). \tag{3.33}$$

At the stability limit $\Lambda \to 1$. Setting $\Lambda = 1$ in (3.27)–(3.30) will therefore yield the optimum results. In that case

$$[fR\theta + g\psi + h\phi]\, k_i - 2u_i = \varpi_{,i}, \tag{3.34}$$

$$Rfw + 2\Delta\theta = 0, \tag{3.35}$$

$$gw + \gamma_1 \left(\frac{1}{P_1} + \frac{1}{P_2}\right) \Delta\psi + \frac{1}{2}(\gamma_1 + \gamma_2) \left(\frac{1}{P_1} - \frac{1}{P_2}\right) \Delta\phi = 0, \tag{3.36}$$

$$hw + \gamma_2 \left(\frac{1}{P_1} + \frac{1}{P_2}\right) \Delta\phi + \frac{1}{2}(\gamma_1 + \gamma_2) \left(\frac{1}{P_1} - \frac{1}{P_2}\right) \Delta\psi = 0. \tag{3.37}$$

Using parametric differentiation on (3.34)–(3.37) it can be shown that

$$\left(f\frac{\partial R}{\partial \gamma_0} + R\frac{\partial f}{\partial \gamma_0}\right)(\theta, w) = 0. \tag{3.38}$$

At the optimum value of R, $\dfrac{\partial R}{\partial \gamma_0} = 0$ and it can also be shown that, from (3.35), $Rf(w,\theta) = 2\|\nabla\theta\|^2$. So, equation (3.38) becomes

$$\frac{\partial f}{\partial \gamma_0} \frac{2\|\nabla\theta\|^2}{f} = 0,$$

and since $f > 0$ we must have $\dfrac{\partial f}{\partial \gamma_0} = 0$ at the optimum value of γ_0. From (3.31)

$$\frac{\partial f}{\partial \gamma_0} = \frac{\gamma_0 - 1}{2\gamma_0^{\frac{3}{2}}},$$

and so $\gamma_0 = 1$ at the optimum value.

If we now set $\gamma_0 = 1$ in (3.34)–(3.37) we obtain

$$[2R\theta + g\psi + h\phi]\, k_i - 2u_i = \varpi_{,i}, \tag{3.39}$$

$$Rw + \Delta\theta = 0, \tag{3.40}$$

$$gw + \gamma_1\left(\frac{1}{P_1} + \frac{1}{P_2}\right)\Delta\psi + \frac{1}{2}(\gamma_1 + \gamma_2)\left(\frac{1}{P_1} - \frac{1}{P_2}\right)\Delta\phi = 0, \tag{3.41}$$

$$hw + \gamma_2\left(\frac{1}{P_1} + \frac{1}{P_2}\right)\Delta\phi + \frac{1}{2}(\gamma_1 + \gamma_2)\left(\frac{1}{P_1} - \frac{1}{P_2}\right)\Delta\psi = 0. \tag{3.42}$$

Taking the third component of the double curl of (3.39) and then assuming a normal mode representation results in

$$2Ra^2\Theta + ga^2\Psi + ha^2\Phi + 2(D^2 - a^2)W = 0,$$

$$RW + (D^2 - a^2)\Theta = 0,$$

$$gW + \gamma_1\left(\frac{1}{P_1} + \frac{1}{P_2}\right)(D^2 - a^2)\Psi + \frac{1}{2}(\gamma_1 + \gamma_2)\left(\frac{1}{P_1} - \frac{1}{P_2}\right)(D^2 - a^2)\Phi = 0,$$

$$hW + \gamma_2\left(\frac{1}{P_1} + \frac{1}{P_2}\right)(D^2 - a^2)\Phi + \frac{1}{2}(\gamma_1 + \gamma_2)\left(\frac{1}{P_1} - \frac{1}{P_2}\right)(D^2 - a^2)\Psi = 0,$$

where a^2 is a wavenumber and $D = \dfrac{d}{dz}$.

From the boundary conditions (3.11), the appropriate z–dependence for W, Θ, Ψ and Φ is $\sin n\pi z$. We are left with

$$2Ra^2\Theta + ga^2\Psi + ha^2\Phi + 2(n^2\pi^2 + a^2)W = 0, \tag{3.43}$$

$$RW - (n^2\pi^2 + a^2)\Theta = 0, \tag{3.44}$$

$$gW - \gamma_1\left(\frac{1}{P_1} + \frac{1}{P_2}\right)(n^2\pi^2 + a^2)\Psi - \frac{1}{2}(\gamma_1 + \gamma_2)\left(\frac{1}{P_1} - \frac{1}{P_2}\right)(n^2\pi^2 + a^2)\Phi = 0, \tag{3.45}$$

$$hW - \gamma_2\left(\frac{1}{P_1} + \frac{1}{P_2}\right)(n^2\pi^2 + a^2)\Phi - \frac{1}{2}(\gamma_1 + \gamma_2)\left(\frac{1}{P_1} - \frac{1}{P_2}\right)(n^2\pi^2 + a^2)\Psi = 0. \tag{3.46}$$

For non–zero solutions of (3.43)–(3.46) to exist the determinant of system (3.43)–(3.46) must be zero. We find

$$(R^2a^2 - y_n^2)A + 2P_1P_2a^2(P_1 + P_2)(g^2\gamma_2 + h^2\gamma_1) - 2P_1P_2gha^2(P_2 - P_1)(\gamma_1 + \gamma_2) = 0, \tag{3.47}$$

where we have set $y_n = n^2\pi^2 + a^2$ and the term A is defined by

$$A = 4\gamma_1\gamma_2(P_1 + P_2)^2 - (\gamma_1 + \gamma_2)^2(P_2 - P_1)^2.$$

Notice that, from (3.25), $A > 0$. Upon rearranging, equation (3.47) becomes,

$$R^2 = \frac{y_n^2}{a^2} + \frac{2P_1P_2(P_1 + P_2)(g^2\gamma_2 + h^2\gamma_1)}{A} - \frac{2P_1P_2gh(P_2 - P_1)(\gamma_1 + \gamma_2)}{A}. \tag{3.48}$$

Now the right–hand side is minimised over n and a to find the following energy boundary,

$$R^2 = 4\pi^2 + \frac{2P_1P_2}{A}\left[gh(P_2 - P_1)(\gamma_1 + \gamma_2) - (P_1 + P_2)(g^2\gamma_2 + h^2\gamma_1)\right]. \qquad (3.49)$$

3.4 Results

In chapter 2 the following sets of parameter values were shown to give rise to the unusual neutral curves described in the introduction:

$$P_1 = 4.545454, P_2 = 4.761904, R_1 = \sqrt{284}, \sqrt{184}, \sqrt{130.5}$$

(in the present notation).

The classical energy method presented in section 2.4 yields the following nonlinear stability boundary:

$$R^2 + R_2^2 = 4\pi^2. \qquad (3.50)$$

The new nonlinear stability results are given in curves (b) of figures (3.1)–(3.3). They represent nonlinear stability for all initial data values and are thus very useful. To obtain curves (b) we fix R_2 and plot the curve in (3.49) for γ_1 and γ_2 satisfying the constraint (3.25). The envelope of all such curves gives rise to each of curves (b) in figures (3.1)–(3.3). In addition the linear stability boundary from section 2.3 and the "standard" energy curves given by equation (3.50) are also plotted, as curves (c) and (a), respectively, in figures (3.1)–(3.3). The multi–valued region on the linear instability curves (c), i.e. the "kink" region is due to the existence of the isolated heart–shaped oscillatory neutral curves described in the introduction.

In figures (3.1)–(3.3) the region below curves (b) represents the region where the conduction solution is always stable. Above curves (c) the solution is always unstable. the region between (b) and (c) is where possible subcritical instabilities may occur. These are to be expected from the work of Proctor (1981) and Hansen and Yuen (1989).

The present work can be seen to be a considerable improvement on the nonlinear results of section 2.4. In particular the energy boundary has been extended to include the region along the R_2–axis that pertains to the isolated oscillatory curves.

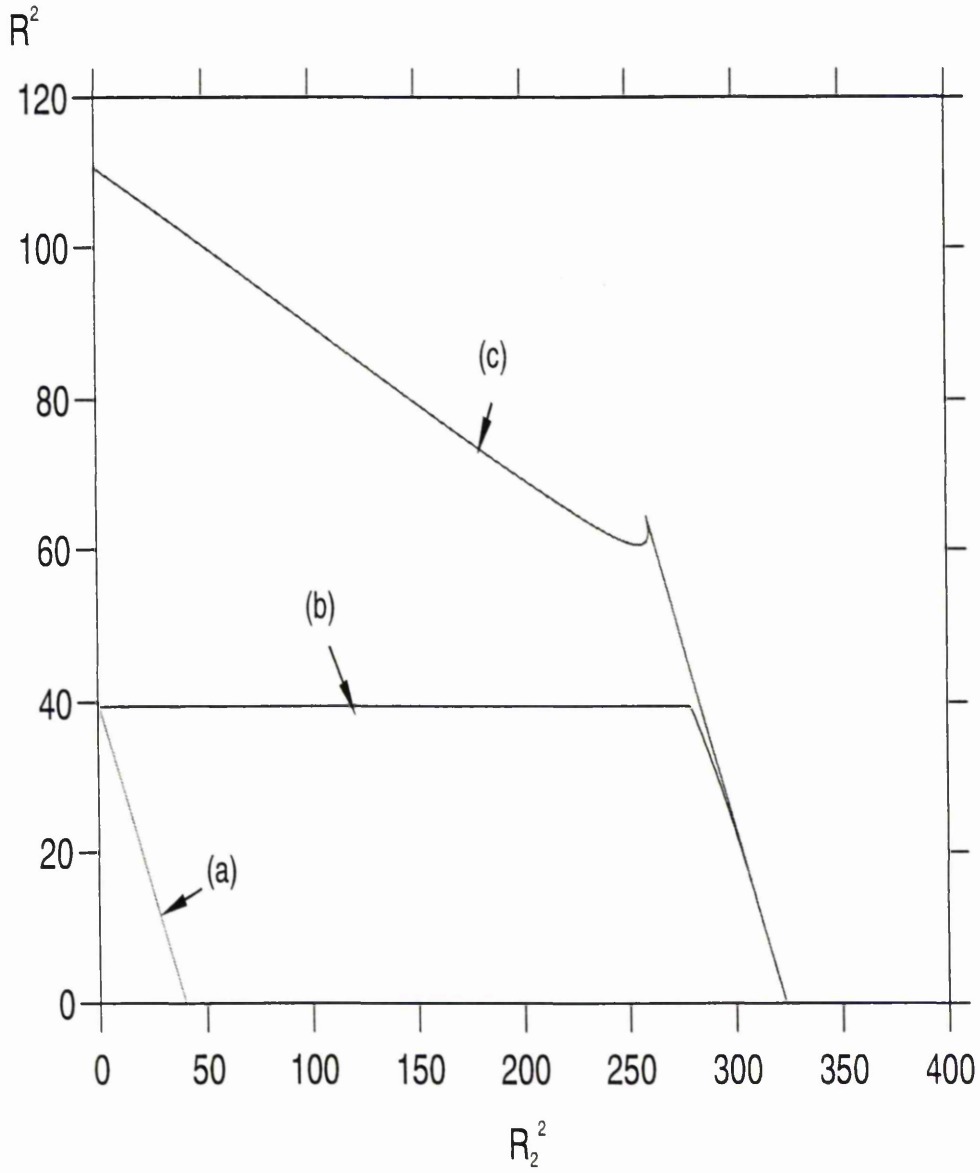

Figure 3.1: (a) Energy boundary from chapter 2 (equation (3.50)). (b) Energy boundary from equation (3.49). (c) Linear instability boundary from chapter 2. For all curves $P_1 = 4.545454, P_2 = 4.761904, R_1^2 = 284$.

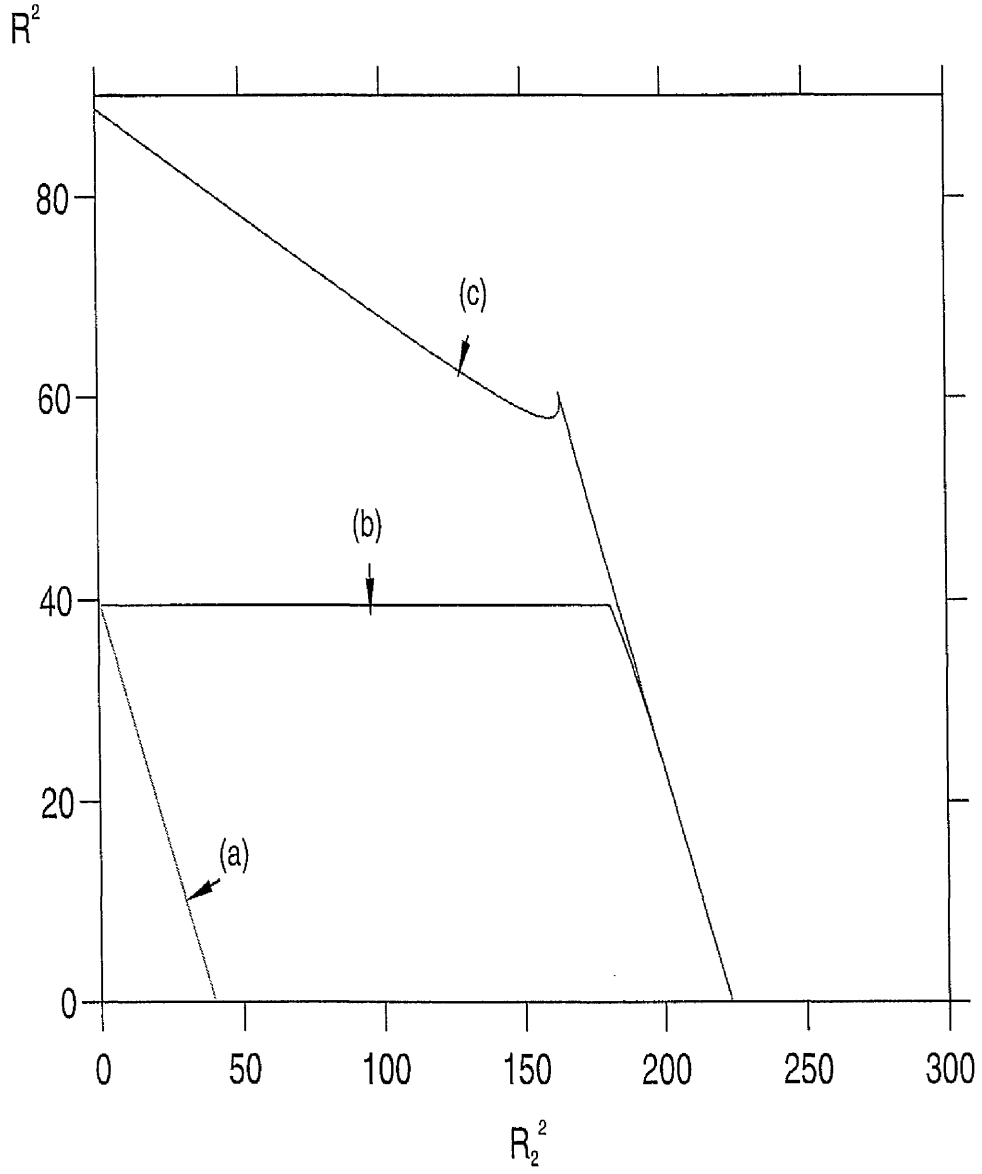

Figure 3.2: (a) Energy boundary from chapter 2 (equation (3.50)). (b) Energy boundary from equation (3.49). (c) Linear instability boundary from chapter 2. For all curves $P_1 = 4.545454, P_2 = 4.761904, R_1^2 = 184$.

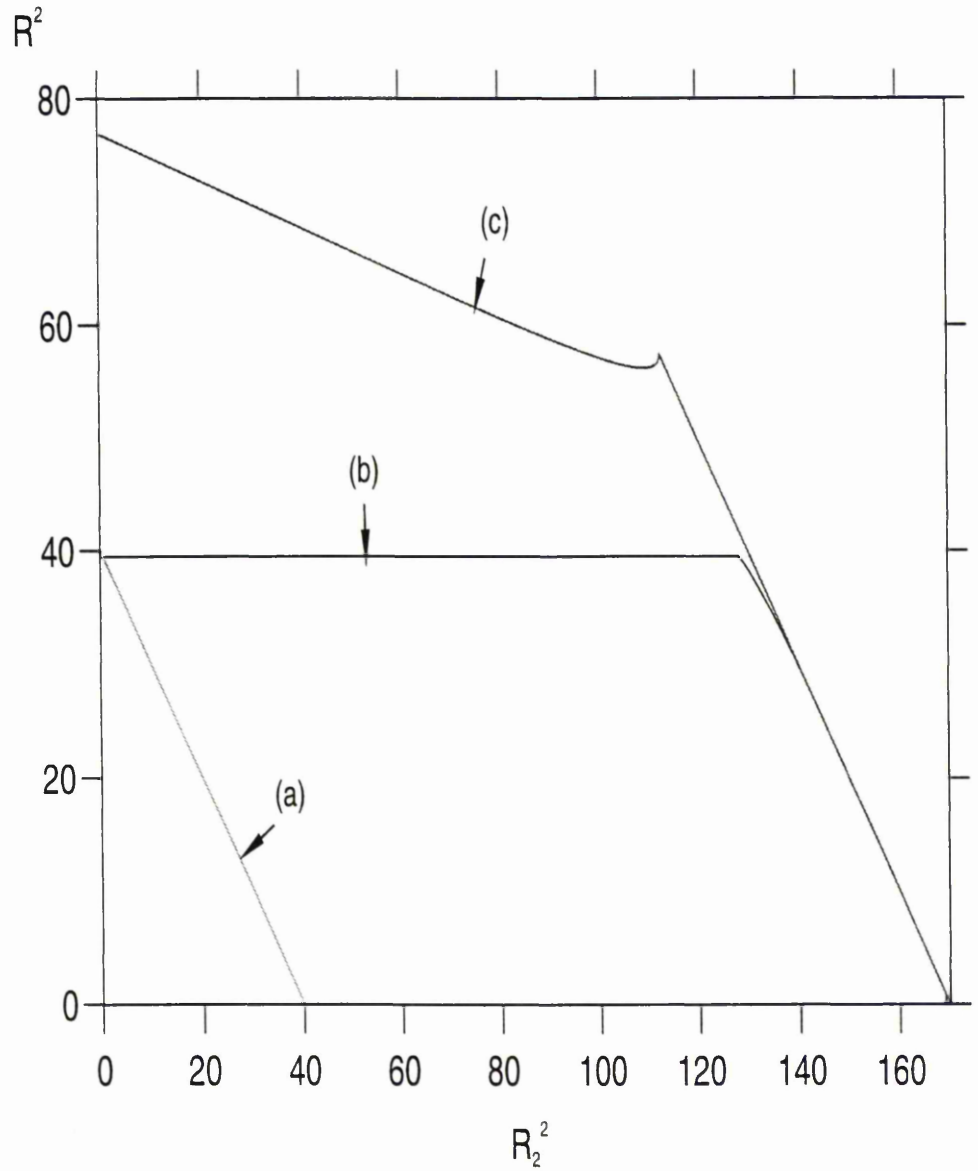

Figure 3.3: (a) Energy boundary from chapter 2 (equation (3.50)). (b) Energy boundary from equation (3.49). (c) Linear instability boundary from chapter 2. For all curves $P_1 = 4.545454, P_2 = 4.761904, R_1^2 = 130.5$.

Chapter 4

Penetrative convection and multi–component diffusion in a porous medium

4.1 Introduction

In chapters 2 and 3 the stability (linear and nonlinear) of triple diffusive porous convection was investigated. Highly unusual linear stability results were obtained, notably the fact that, for some fixed values of the diffusivity ratios, Prandtl number and two of the three Rayleigh numbers, three values of the third Rayleigh number may be required in order to specify the linear stability criteria. This is due to the existence of an isolated, symmetric heart–shaped oscillatory curve lying below the stationary curve. One consequence of the *perfect* heart shape of the oscillatory neutral curves is that instability could occur at the same thermal Rayleigh number but different wavenumbers. There are two factors that cast doubt over the experimental observation of this result. Firstly, nonlinear effects. Instability has been predicted as occurring at the twin maxima of the "lobes" of the oscillatory neutral curve. However the critical Rayleigh number at which this occurs is not a minimum but instead lies in a region where nonlinear effects are likely to be of importance. Work by Proctor (1981) and Hansen and Yuen (1989) on the double diffusive fluid problem shows that subcritical instability can occur at values of the thermal Rayleigh

number much less than that predicted by linear theory. Rudraiah, Shivakumara and Friedrich (1986) find a similar result in considering the effect of rotation on the double diffusive porous problem. In order to investigate the nonlinear stability of the triple diffusive problem an application of the classical energy method that yields unconditional nonlinear stability is presented in chapter 2. A generalised energy method that yields sharper results is given in chapter 3. Secondly, there is the relevance of the equation of state. In chapters 2 and 3 an equation of state in which the density is linearly dependent upon temperature is adopted, i.e. the Boussinesq approximation. The density of a fluid will not be a linear function of temperature in reality and so in the present chapter an equation of state that is quadratic in temperature is adopted in order to investigate the triple diffusive problem. This quadratic temperature law allows the introduction of the phenomenon of penetrative convection — a term used to describe the situation when a stable layer exists next to an unstable layer. When convection begins in the unstable layer the motions penetrate into the stable layer. Penetrative convection has applications in stellar regions (see e.g. Veronis (1963)) and in geophysical problems including modelling thawing subsea permafrost (see e.g. Payne *et al.* (1988)) and patterned ground formation (see e.g. Ray *et al.* (1983), George *et al.* (1989)). Other occurrences of penetrative convection are cited in Veronis (1963), Straughan (1992) and Nield and Bejan (1992).

The analytical method of section 2.3 cannot be used in the present situation as the differential equations that arise in the eigenvalue problem here have coefficients that are functions of the spatial variables. Instead a Chebyshev tau method is employed. This provides quick and accurate results and in addition yields as many eigenvalues as are required, allowing the behaviour of the growth rate and the instability mechanism to be investigated in detail.

The reasons outlined above that necessitated the nonlinear stability analyses of chapters 2 and 3 are equally relevant here. Consequently, the energy method is again used in this chapter to investigate the nonlinear stability of the basic motionless state. The nonlinear equation of state gives rise to quadratic temperature terms in addition to convective nonlinearities. To deal with these a weight is introduced to

the temperature part of the energy, the effect of which is to cancel out the quadratic temperature term. The results presented here have the important advantage that they are unconditional i.e., nonlinear stability is guaranteed for initial perturbations of arbitrary sized amplitude.

This chapter has essentially appeared as Tracey (1997b).

4.2 Governing equations

Consider a fluid–saturated porous layer lying in the infinite three–dimensional region $0 < z < d$. The lower boundary $z = 0$ is held at the fixed temperature $T = 0°C$ while the upper boundary $z = d$ is held at a temperature $T_1 \geq 4°C$. If the fluid under consideration is water then penetrative convection can occur in the fluid layer. This is due to the fact that water has a density maximum at $4°C$ and so the lower part of the layer is gravitationally unstable while the upper part is gravitationally stable. When convection occurs in the lower part of the layer the motions will penetrate into the upper part. Suppose further that the fluid has dissolved in it N different chemical species. Denote the concentration of component α by C^α $(\alpha = 1, \ldots, N)$. The concentration of component α at the lower and upper boundaries is held at C_l^α and C_u^α, respectively. The density is taken to be quadratic in the temperature field and linear in the salt concentration, i.e.

$$\rho = \rho_0 \left(1 - A\,(T-4)^2 + \sum_{\alpha=1}^{N} A_\alpha (C^\alpha - C_0^\alpha) \right),$$

where ρ_0 is the value of the density at a temperature $4°C$ and some reference salt concentrations C_0^α $(\alpha = 1, \ldots, N)$. The constants A and A_α $(\alpha = 1, \ldots, N)$ represent the thermal and solute expansion coefficients, respectively.

The equations of motion which govern flow in a porous medium are largely based on a relation which is a generalisation of empirical observation (c.f. Nield and Bejan (1994)). This relation is known as Darcy's Law and can be written

$$\nabla p = -\frac{\mu}{k}\mathbf{v} + \rho \mathbf{g},$$

where the variables $p, \mu, k, \mathbf{v}$ and $\mathbf{g}$ represent pressure, dynamic viscosity, permeability, seepage velocity and gravitational acceleration, respectively. In addition to

Darcy's Law we have the incompressibility condition and the equations of conservation of temperature and solute. Combining these equations with the Darcy law and the equation of state gives the following system of $5+N$ governing equations:

$$
\begin{aligned}
p_{,i} &= -\frac{\mu}{k}v_i - g\rho_0\left(1 - A(T-4)^2 + \sum_{\alpha=1}^{N} A_\alpha(C^\alpha - C_0^\alpha)\right)k_i, && (4.1)\\
v_{i,i} &= 0, && (4.2)\\
T_{,t} + v_i T_{,i} &= \kappa\Delta T, && (4.3)\\
C^\alpha_{,t} + v_i C^\alpha_{,i} &= \kappa_\alpha \Delta C^\alpha \quad (\alpha = 1,\ldots,N), && (4.4)
\end{aligned}
$$

where indicial notation and the Einstein summation convention have been employed. The vector $\mathbf{k}$ is the unit vector in the z–direction while the variables κ and κ_α represent thermal and solute diffusivity, respectively. The boundary conditions considered are

$$
\begin{aligned}
&\text{at } z = 0,\ T = 0°C,\ C^\alpha = C_l^\alpha\ (\alpha = 1,\ldots,N),\ v_3 = 0,\\
&\text{at } z = d,\ T = T_1 \geq 4°C,\ C^\alpha = C_u^\alpha\ (\alpha = 1,\ldots,N),\ v_3 = 0.
\end{aligned}
\qquad (4.5)
$$

The experimental realisation of prescribing these boundary conditions for the salt concentrations has been investigated by Krishnamurti and Howard (1983).

The steady solution $(\bar{v}_i, \bar{p}, \bar{T}, \bar{C}^\alpha)$ of (4.1)–(4.5) on which we will perform a linear stability analysis is given by

$$
\begin{aligned}
\bar{v}_i &= 0,\\
\bar{T} &= \frac{T_1}{d}z,\\
\bar{C}^\alpha &= C_l^\alpha - \frac{\Delta C^\alpha}{d}z\ (\Delta C^\alpha = C_l^\alpha - C_u^\alpha, \alpha = 1,\ldots,N),
\end{aligned}
\qquad (4.6)
$$

and the steady pressure $\bar{p}$ can be obtained from (4.1).

In order to investigate the linear stability of this basic solution we introduce perturbations $(u_i, \pi, \theta, \phi^\alpha)$ to $(\bar{v}_i, \bar{p}, \bar{T}, \bar{C}^\alpha)$ via

$$v_i = \bar{v}_i + u_i, p = \bar{p} + \pi, T = \bar{T} + \theta, C^\alpha = \bar{C}^\alpha + \phi^\alpha.$$

The resultant perturbation equations are non–dimensionalised using the following scalings:

$$t = t^*\frac{d^2}{\kappa},\ \mathbf{u} = \mathbf{u}^*\frac{\kappa}{d},\ \pi = \pi^*\frac{\mu\kappa}{k},\ \mathbf{x} = \mathbf{x}^* d,$$

$$\theta = \theta^* T^{\#},\ \phi^\alpha = (\phi^\alpha)^* \Phi^\alpha,\ \xi = \frac{4}{T_1},$$

$$T^{\#} = \left(\frac{\mu\kappa}{A\rho_o g k d}\right)^{1/2},\ \Phi^\alpha = \left(\frac{\mu\kappa P^\alpha |\triangle C^\alpha|}{A_\alpha \rho_o g k d}\right)^{1/2},$$

$$R = T_1 \left(\frac{A\rho_o g k d}{\mu\kappa}\right)^{1/2},\ R_\alpha = \left(\frac{A_\alpha \rho_o g k d P^\alpha |\triangle C^\alpha|}{\mu\kappa}\right)^{1/2},$$

$$H_\alpha = \mathrm{sgn}(\triangle C^\alpha),\ P_\alpha = \frac{\kappa}{\kappa_\alpha}.$$

Here R and R_α are the Rayleigh and salt Rayleigh numbers and P_α are salt Prandtl numbers.

The nonlinear perturbation equations are then, in non–dimensional form (dropping the asterisks),

$$\pi_{,i} = -u_i - \left[2R(\xi - z)\theta + \sum_{\alpha=1}^{N} R_\alpha \phi^\alpha - \theta^2\right] k_i, \tag{4.7}$$

$$u_{i,i} = 0, \tag{4.8}$$

$$\theta_{,t} + u_i \theta_{,i} = -Rw + \Delta\theta, \tag{4.9}$$

$$P_\alpha \left(\phi^\alpha_{,t} + u_i \phi^\alpha_{,i}\right) = H_\alpha R_\alpha w + \Delta\phi^\alpha \qquad (\alpha = 1, \ldots, N), \tag{4.10}$$

where $w = u_3$. The boundary conditions which follow from (4.5) for the perturbed quantities are

$$w = \theta = \phi^\alpha\ (\alpha = 1, \ldots, N) = 0 \quad \text{at } z = 0, 1. \tag{4.11}$$

4.3 Linear stability analysis

Equations (4.7)–(4.10) are linearised by neglecting terms containing products of the perturbed quantities. A time dependence of $e^{\sigma t}$ is introduced by substituting

$$\begin{aligned} \mathbf{u}(\mathbf{x}, t) &= \mathbf{u}(\mathbf{x}) e^{\sigma t}, \\ \theta(\mathbf{x}, t) &= \theta(\mathbf{x}) e^{\sigma t}, \\ \phi^\alpha(\mathbf{x}, t) &= \phi^\alpha(\mathbf{x}) e^{\sigma t} \quad (\alpha = 1, \ldots, N). \end{aligned}$$

The pressure term is eliminated by taking curlcurl of equations (4.7) and then selecting the third component. This gives

$$\Delta w = -2R(\xi - z)\Delta^*\theta - \sum_{\alpha=1}^{N} R_\alpha \Delta^* \phi^\alpha, \tag{4.12}$$

$$\sigma\theta = -Rw + \Delta\theta, \tag{4.13}$$

$$P_\alpha \sigma \phi^\alpha = H_\alpha R_\alpha w + \Delta\phi^\alpha \qquad (\alpha = 1, \ldots, N), \tag{4.14}$$

where $\Delta^* = \dfrac{\partial^2}{\partial x^2} + \dfrac{\partial^2}{\partial y^2}$ is the horizontal Laplacian.

A normal mode representation is assumed, i.e.

$$\begin{aligned} w &= W(z)\exp[i(mx+ny)], \\ \theta &= \Theta(z)\exp[i(mx+ny)], \\ \phi^\alpha &= \Phi^\alpha(z)\exp[i(mx+ny)], \qquad (\alpha = 1, \ldots, N), \end{aligned}$$

and the following transformations are made in order to put the equations in a form like chapter 2,

$$R\theta \to \theta, R_\alpha \phi^\alpha \to \phi^\alpha, R^2 \to R, H_\alpha R_\alpha^2 \to -R_\alpha. \tag{4.15}$$

Attention is now focussed on the case of two salt fields, i.e. $N = 2$. The resultant equations are

$$(D^2 - k^2)W - 2(\xi - z)k^2\Theta - k^2\Phi^1 - k^2\Phi^2 = 0, \tag{4.16}$$

$$(D^2 - k^2)\Theta - RW = \sigma\Theta, \tag{4.17}$$

$$(D^2 - k^2)\Phi^1 - R_1 W = P_1\sigma\Phi^1, \tag{4.18}$$

$$(D^2 - k^2)\Phi^2 - R_2 W = P_2\sigma\Phi^2, \tag{4.19}$$

where $k^2 = m^2 + n^2$ is a wavenumber and $D = \dfrac{d}{dz}$. The appropriate boundary conditions are, from (4.11),

$$W = \Theta = \Phi^1 = \Phi^2 = 0, \quad z = 0, 1. \tag{4.20}$$

The presence of a z-dependent term in (4.16) rules out the possibility of using the analytical method of chapter 2. Instead, a Chebyshev tau method was used to solve system (4.16)–(4.20). This method is described in appendix A. Numerical results are presented in section 4.5.

4.4 Nonlinear stability analysis

An analysis of the nonlinear stability of the basic solution is now presented by making use of the energy method. The nonlinear perturbation equations are, from (4.7)–(4.10),

$$\pi_{,i} = -u_i - \left[2R(\xi - z)\theta + R_1\phi + R_2\psi - \theta^2\right] k_i, \tag{4.21}$$

$$u_{i,i} = 0, \tag{4.22}$$

$$\theta_{,t} + u_i\theta_{,i} = -Rw + \Delta\theta, \tag{4.23}$$

$$P_1\left(\phi_{,t} + u_i\phi_{,i}\right) = H_1R_1w + \Delta\phi, \tag{4.24}$$

$$P_2\left(\psi_{,t} + u_i\psi_{,i}\right) = H_2R_2w + \Delta\psi, \tag{4.25}$$

where, for later convenience, the following transformations have been used

$$\phi^1 \to \phi, \quad \phi^2 \to \psi.$$

Let V denote a period cell for the solution. The boundary conditions considered are,

$$w = \theta = \phi = \psi = 0 \quad \text{on } z = 0, 1, \tag{4.26}$$

and further that u_i, θ, ϕ, ψ and π are periodic on the lateral boundaries of V.

To commence multiply (4.21) by u_i, (4.24) by ϕ, (4.25) by ψ and integrate over V. Integration by parts and use of the boundary conditions yields

$$0 = -\|\mathbf{u}\|^2 - 2R\langle(\xi - z)\theta w\rangle - R_1\langle\phi w\rangle - R_2\langle\psi w\rangle + \langle\theta^2 w\rangle, \tag{4.27}$$

$$\frac{d}{dt}\frac{P_1}{2}\|\phi\|^2 = H_1R_1\langle w\phi\rangle - \|\nabla\phi\|^2, \tag{4.28}$$

$$\frac{d}{dt}\frac{P_2}{2}\|\psi\|^2 = H_2R_2\langle w\psi\rangle - \|\nabla\psi\|^2, \tag{4.29}$$

where $\|\cdot\|$ denotes the $L^2(V)$ norm and $\langle f\rangle = \int_V f\, dV$. In order to deal with the $\langle\theta^2 w\rangle$ term in equation (4.27) a technique used by Payne and Straughan (1987) is introduced. A weighted energy relation is formed by multiplying (4.23) by $(\mu - 2z)\theta$, where $\mu > 2$ is a coupling parameter to be selected at our discretion, and integrating

over V. Selecting $\mu > 2$ ensures that $\mu - 2z > 0$. The weighted relation is

$$\frac{d}{dt}\langle\frac{1}{2}(\mu-2z)\theta^2\rangle + \langle(\mu-2z)\theta u_i\theta_{,i}\rangle = \langle(\mu-2z)\theta(-Rw+\Delta\theta)\rangle.$$

Integration by parts and use of the boundary conditions then gives

$$\frac{d}{dt}\langle\frac{1}{2}\hat{\mu}\theta^2\rangle = -\langle w\theta^2\rangle - R\langle\hat{\mu}w\theta\rangle - \langle\hat{\mu}|\nabla\theta|^2\rangle, \tag{4.30}$$

where $\hat{\mu} = \mu - 2z$.

If we now form (4.27) + (4.30) + λ_1(4.28) + λ_2(4.29), where λ_1 and λ_2 are positive coupling parameters, then,

$$\begin{aligned} &\frac{d}{dt}\left(\frac{1}{2}\langle\hat{\mu}\theta^2\rangle + \frac{\lambda_1 P_1}{2}\|\phi\|^2 + \frac{\lambda_2 P_2}{2}\|\psi\|^2\right) \\ = \;& -R\langle M\theta w\rangle + (\lambda_1 H_1 - 1)R_1\langle w\phi\rangle + (\lambda_2 H_2 - 1)R_2\langle w\psi\rangle \\ & - \left(\|\mathbf{u}\|^2 + \langle\hat{\mu}|\nabla\theta|^2\rangle + \lambda_1\|\nabla\phi\|^2 + \lambda_2\|\nabla\psi\|^2\right), \end{aligned} \tag{4.31}$$

where $M(z) = \mu + 2\xi - 4z$. The effect of the weight is that the problematic $\langle\theta^2 w\rangle$ term in equation (4.27) is cancelled out by the $-\langle w\theta^2\rangle$ term that arises in equation (4.30).

If we now define an energy

$$E(t) = \frac{1}{2}\langle\hat{\mu}\theta^2\rangle + \frac{\lambda_1 P_1}{2}\|\phi\|^2 + \frac{\lambda_2 P_2}{2}\|\psi\|^2, \tag{4.32}$$

then (4.31) shows that

$$\frac{dE}{dt} = \mathcal{I} - \mathcal{D},$$

where

$$\mathcal{I} = -R\langle M\theta w\rangle + (\lambda_1 H_1 - 1)R_1\langle w\phi\rangle + (\lambda_2 H_2 - 1)R_2\langle w\psi\rangle,$$

$$\mathcal{D} = \|\mathbf{u}\|^2 + \langle\hat{\mu}|\nabla\theta|^2\rangle + \lambda_1\|\nabla\phi\|^2 + \lambda_2\|\nabla\psi\|^2.$$

By rearrangement,

$$\frac{dE}{dt} = \mathcal{I} - \mathcal{D} = -\mathcal{D}\left(1 - \frac{\mathcal{I}}{\mathcal{D}}\right).$$

If we now define

$$\frac{1}{\Lambda} = \max_{\mathcal{H}}\frac{\mathcal{I}}{\mathcal{D}}, \tag{4.33}$$

where $\mathcal{H}$ is the space of admissible functions, then

$$\frac{dE}{dt} \leq -\mathcal{D}(1 - \frac{1}{\Lambda}).$$

If now

$$\Lambda > 1, \tag{4.34}$$

then

$$1 - \frac{1}{\Lambda} = b > 0,$$

and so

$$\frac{dE}{dt} \leq -b\mathcal{D}. \tag{4.35}$$

Use of the Poincaré inequality (see e.g. Straughan (1992)) results in

$$\mathcal{D} \geq cE.$$

where c is a positive constant that arises from the use of the Poincaré inequality. Therefore,

$$\frac{dE}{dt} \leq -bcE, \tag{4.36}$$

which can be integrated to yield

$$E(t) \leq E(0)e^{-bct}.$$

So, if $\Lambda > 1$ then $E(t) \to 0$ as $t \to \infty$ at least exponentially fast and so our steady solution is stable. This fact, together with (4.32), shows that $\|\theta\|, \|\phi\|, \|\psi\| \to 0$. The lack of a time derivative in Darcy's law means that a similar result cannot easily be obtained for $\|\mathbf{u}\|$. However, if equation (4.35) is integrated with respect to time then

$$E(t) + b\int_0^t \mathcal{D}(s)\, ds \leq E(0),$$

which means that, in particular,

$$\int_0^\infty \|\mathbf{u}\|^2\, ds < \infty.$$

So $\|\mathbf{u}\|^2 \in L^1(0,\infty)$. This ensures "practical decay" even though the solution $\mathbf{u}$ may "peak" over vanishingly small intervals as $t \to \infty$. It is difficult, though, to conceive of such a situation physically.

The problem remains to find the maximum in (4.33).

In order to clear the denominator of the maximisation problem of the coupling parameters λ_1 and λ_2, the following transformations are made,

$$\sqrt{\lambda_1}\phi \to \phi,\ \sqrt{\lambda_2}\psi \to \psi.$$

Consider now the case $H_1 = 1, H_2 = -1$. This corresponds to the situation considered in section 4.3 where component 1 is stabilizing while component 2 is destabilizing. The resultant maximisation problem to be considered is

$$\frac{1}{\Lambda} = \max_{\mathcal{H}} \frac{-R\langle M\theta w\rangle + \frac{(\lambda_1 - 1)}{\sqrt{\lambda_1}} R_1 \langle w\phi\rangle - \frac{(\lambda_2 + 1)}{\sqrt{\lambda_2}} R_2 \langle w\psi\rangle}{\|\mathbf{u}\|^2 + \langle \hat{\mu}|\nabla\theta|^2\rangle + \|\nabla\phi\|^2 + \|\nabla\psi\|^2}.$$

The Euler–Lagrange equations for this maximum are as follows

$$\Lambda\left[-\frac{R}{2}M\theta + \left(\frac{\lambda_1 - 1}{2\sqrt{\lambda_1}}\right) R_1\phi - \left(\frac{\lambda_2 + 1}{2\sqrt{\lambda_2}}\right) R_2\psi\right] k_i - u_i = \varpi_{,i} \tag{4.37}$$

$$-\Lambda\frac{R}{2}Mw + \hat{\mu}\Delta\theta - 2\frac{\partial\theta}{\partial z} = 0, \tag{4.38}$$

$$\Lambda\left(\frac{\lambda_1 - 1}{2\sqrt{\lambda_1}}\right) R_1 w + \Delta\phi = 0, \tag{4.39}$$

$$-\Lambda\left(\frac{\lambda_2 + 1}{2\sqrt{\lambda_2}}\right) R_2 w + \Delta\psi = 0. \tag{4.40}$$

where ϖ is a Lagrange multiplier introduced because $\mathbf{u}$ is divergence free. At the stability limit $\Lambda \to 1$. Setting $\Lambda = 1$ in the Euler–Lagrange equations (4.37)–(4.40) will then yield the optimum results. The equations to be solved are now

$$\left[-\frac{R}{2}M\theta + R_1 g\phi - R_2 h\psi\right] k_i - u_i = \varpi_{,i} \tag{4.41}$$

$$-\frac{R}{2}Mw + \hat{\mu}\Delta\theta - 2\frac{\partial\theta}{\partial z} = 0, \tag{4.42}$$

$$R_1 gw + \Delta\phi = 0, \tag{4.43}$$

$$-R_2 hw + \Delta\psi = 0, \tag{4.44}$$

where

$$g = \frac{\lambda_1 - 1}{2\sqrt{\lambda_1}}, h = \frac{\lambda_2 + 1}{2\sqrt{\lambda_2}}. \tag{4.45}$$

We now consider R_1 and R_2 to be fixed and investigate the variation of R, where now

$$R = R(\mu, \lambda_1, \lambda_2, k^2),$$

where k is a wavenumber.

We will now vary each of λ_1, λ_2 and μ in turn and find the optimum values of these coupling parameters. Firstly, we consider λ_1, μ, R_1 and R_2 to be

fixed and investigate the optimum value of λ_2 by using parametric differentiation. Let now superscripts 1 and 2 refer to a solution of (4.41)–(4.44) corresponding to parameters λ_2^1 and λ_2^2 respectively. We now form the inner products $\langle (4.41)^1.\mathbf{u}^2\rangle, \langle (4.41)^2.\mathbf{u}^1\rangle, \langle (4.42)^1\theta^2\rangle, \langle (4.42)^2\theta^1\rangle, \langle (4.43)^1\phi^2\rangle,$
$\langle (4.43)^2\phi^1\rangle, \langle (4.44)^1\psi^2\rangle$ and $\langle (4.44)^2, \psi^1\rangle$ and obtain the equations

$$-\frac{R^1}{2}\langle M\theta^1 w^2\rangle + R_1 g\langle \phi^1 w^2\rangle - R_2 h^1\langle \psi^1 w^2\rangle = \langle \mathbf{u}^1.\mathbf{u}^2\rangle, \tag{4.46}$$

$$-\frac{R^2}{2}\langle M\theta^2 w^1\rangle + R_1 g\langle \phi^2 w^1\rangle - R_2 h^2\langle \psi^2 w^1\rangle = \langle \mathbf{u}^2.\mathbf{u}^1\rangle, \tag{4.47}$$

$$-\frac{R^1}{2}\langle M w^1\theta^2\rangle = \langle \hat{\mu}\nabla\theta^1.\nabla\theta^2\rangle, \tag{4.48}$$

$$-\frac{R^2}{2}\langle M w^2\theta^1\rangle = \langle \hat{\mu}\nabla\theta^2.\nabla\theta^1\rangle, \tag{4.49}$$

$$R_1 g\langle w^1\phi^2\rangle = \langle \nabla\phi^1.\nabla\phi^2\rangle, \tag{4.50}$$

$$R_1 g\langle w^2\phi^1\rangle = \langle \nabla\phi^2.\nabla\phi^1\rangle, \tag{4.51}$$

$$-R_2 h^1\langle w^1\psi^2\rangle = \langle \nabla\psi^1.\nabla\psi^2\rangle, \tag{4.52}$$

$$-R_2 h^2\langle w^2\psi^1\rangle = \langle \nabla\psi^2.\nabla\psi^1\rangle. \tag{4.53}$$

To proceed, form (4.46)+(4.48)−(4.47)−(4.49)+(4.50)−(4.51)+(4.52)−(4.53) to find

$$-\frac{1}{2}\langle M(R^1 - R^2)(\theta^1 w^2 + \theta^2 w^1)\rangle - R_2(h^1 - h^2)\langle w^1\psi^2 + \psi^2 w^1\rangle = 0.$$

Divide this by $\lambda_2^1 - \lambda_2^2$ and then let $\lambda_2^1 \to \lambda_2^2$ to obtain,

$$-\frac{\partial R}{\partial \lambda_2}\langle M\theta w\rangle - 2R_2\frac{\partial h}{\partial \lambda_2}\langle w\psi\rangle = 0. \tag{4.54}$$

However, using (4.42) and (4.44) it can be shown that

$$\frac{2}{R}\langle\hat{\mu}|\nabla\theta|^2\rangle\frac{\partial R}{\partial\lambda_2} = -2R_2\frac{\partial h}{\partial\lambda_2}\frac{\|\nabla\psi\|^2}{hR_2}. \tag{4.55}$$

At the optimum value of λ_2, $\dfrac{\partial R}{\partial\lambda_2} = 0$ and so from (4.55),

$$2\frac{\partial h}{\partial\lambda_2}\frac{\|\nabla\psi\|^2}{h} = 0,$$

and since $h > 0$, we have $\dfrac{\partial h}{\partial\lambda_2} = 0$. From (4.45),

$$\frac{\partial h}{\partial\lambda_2} = \frac{\lambda_2 - 1}{4\lambda_2^{\frac{3}{2}}}.$$

So,

$$\frac{\partial R}{\partial\lambda_2} = 0 \Rightarrow \lambda_2 = 1. \tag{4.56}$$

If we now fix λ_2 and μ and vary λ_1 then a similar argument to the above shows that

$$-\frac{\partial R}{\partial\lambda_1}\langle M\theta w\rangle + 2R_1\frac{\partial g}{\partial\lambda_1}\langle w\phi\rangle = 0.$$

Using equations (4.41), (4.43) and (4.45), this can be rearranged to show

$$\frac{2}{R}\langle\hat{\mu}|\nabla\theta|^2\rangle\frac{\partial R}{\partial\lambda_1} = -\frac{\lambda_1 + 1}{\lambda_1(\lambda_1 - 1)}\|\nabla\phi\|^2.$$

So the system is singular at $\lambda_1 = 1$. While we cannot find a solution for $\dfrac{\partial R}{\partial\lambda_1} = 0$, note that

$$\lambda_1 > 1 \Rightarrow \frac{\partial R}{\partial\lambda_1} < 0, \;\; \lambda_1 < 1 \Rightarrow \frac{\partial R}{\partial\lambda_1} > 0,$$

which suggests that the best value is $\lambda_1 = 1$.

If now λ_1 and λ_2 are held constant and the variation in μ is considered an argument such as the above does not lead to a result for the optimum value of μ. Instead, the value

$$\max_{\mu\geq 2}\min_{k^2} R(\mu, k^2) \tag{4.57}$$

is found numerically.

The optimum values $\lambda_1 = \lambda_2 = 1$ are substituted into equations (4.41), the effect of which is that the ϕ equation drops out. This means that the ϕ equation does not provide any information and that the energy results are unlikely to be close to the

linear stability results when the terms involving ϕ are of any significance. We are left with three equations

$$\left(-\frac{R}{2}M\theta - R_2\psi\right)k_i - u_i = \varpi_{,i}, \tag{4.58}$$

$$-\frac{R}{2}Mw - 2\frac{\partial\theta}{\partial z} + \hat{\mu}\Delta\theta = 0, \tag{4.59}$$

$$-R_2 w + \Delta\psi = 0. \tag{4.60}$$

The solenoidal term $\varpi_{,i}$ is eliminated by taking curlcurl of equation (4.58) and then selecting the third component. Normal modes are assumed and the transformations (4.15) are made, resulting in the system

$$(D^2 - k^2)W = \frac{1}{2}Mk^2\Theta + k^2\Psi, \tag{4.61}$$

$$(D^2 - k^2)\Theta = \frac{2}{\hat{\mu}}D\Theta + \frac{RM}{2\hat{\mu}}W, \tag{4.62}$$

$$(D^2 - k^2)\Psi = R_2 W, \tag{4.63}$$

where $D = \dfrac{d}{dz}$ and $k^2 = m^2 + n^2$ is the wavenumber. The boundary conditions on W, Θ and Ψ follow from (4.26) and are

$$W = \Theta = \Psi = 0 \quad \text{at} \quad z = 0, 1. \tag{4.64}$$

For fixed values of R_2 equations (4.61)–(4.64) form an eigenvalue problem with eigenvalue R. The compound matrix method was used to solve this. Details of this method may be found in e.g. Straughan (1992). For the maximisation and minimisation problems in (4.57) the golden section search was employed (see e.g. Cheney and Kincaid (1985)). Numerical results are presented in section 4.5.

4.5 Numerical results

4.5.1 Linear Stability

The main interest of the linear stability analysis is the nature of the disconnected oscillatory neutral curves described in the introduction. In the problem where the equation of state is linear in the temperature field (chapter 2) an analytical solution may be obtained which allows the various parameter ranges to be searched in a much

less time–consuming manner than solving the equations numerically. In the present work attention is focussed on the situation where the salt concentration with the larger diffusion coefficient (salt field 1) is gravitationally stable while the salt field with the smaller diffusion coefficient (salt field 2) is destabilising. In chapter 2 the following parameters were shown to give rise to the disconnected oscillatory neutral curves:

$$R_1 \in (-287, -285), R_2 \in (259, 261), P_1 = 4.545454, P_2 = 4.761904.$$

Figure 4.1 shows the (R^{crit}, R_2) stability boundary for $T_1 = 4°C, R_1 = -286, P_1 = 4.545454$, $P_2 = 4.761904$. There are three regions of interest. To the left of the cusp $(R_2 < 260.4)$ there is a region of oscillatory onset. Here oscillatory instability first occurs at a smaller value of R than does steady instability and there is a single critical value of R. To the right of the point of infinite slope $(R_2 > 261.67)$ instability occurs with real growth rate. Here oscillatory instability does not occur and again there is one critical value of R. The intervening region is the most interesting and is shown in the right–hand graph of figure 4.1. Here three values of R^{crit} are required to fully specify the linear instability criteria. Oscillatory instability sets in first at the lowest critical Rayleigh number. Then there is a region of oscillatory instability until the middle critical Rayleigh number is reached. At this point the system becomes linearly stable again until the third critical Rayleigh number is reached. Here stationary instability sets in and the system remains linearly unstable for all higher values of R. At higher temperatures (figure 4.2) a similar (R^{crit}, R_2) stability boundary is seen, with the presence of a multi–valued region (the "kink-region"). A similar multi–valued curve is found when considering R_2 fixed and varying R_1. An explanation for these stability boundaries can be obtained by considering the R, k neutral curves.

Figures 4.3 and 4.4 show a selection of (R, k) neutral curves for $T_1 = 4°C, R_2 = 261, P_1 = 4.545454, P_2 = 4.761904$. Setting $T_1 = 4°C$ means that the whole of the layer is destabilising in the conduction state. For $R_1 = -287, -286.6$ the oscillatory curve is attached to the stationary curve at two bifurcation points. As the bifurcation points are approached along the oscillatory curve the frequency tends to zero. At $R_1 = -286$ the bifurcation points have moved closer together and finally coalesced

and a disconnected oscillatory neutral curve has been formed. As R_1 is increased further the oscillatory curve moves wholly beneath the stationary curve and becomes increasingly smaller until it collapses to a point and disappears. At $R_1 = -285.1$ (not shown) only the stationary curve is found. These results are similar to those found in chapter 2. However, in that chapter the disconnected oscillatory curves were *perfectly* symmetric heart–shapes. It can be clearly seen that the oscillatory curves in the present work are not perfectly heart–shaped — the maximum of the left hand lobe is greater than that of the right hand lobe. For values of $R_1 = -285.4, -285.3$ the oscillatory curve can be seen to lie wholly below the stationary curve and so three critical values of the thermal Raleigh number are required to fully specify the linear stability criteria. Oscillatory instability sets in first at the lowest critical thermal Rayleigh number. Then there is a region of oscillatory instability until the middle critical thermal Rayleigh number is reached. At this point the system becomes linearly stable again until the third critical thermal Rayleigh number is reached. Here stationary instability sets in and the system remains linearly unstable for all higher values of R.

Figure 4.5 shows two neutral curves for $T_1 = 5°C$. The departure from a perfect heart shape is clearly more pronounced than for $T_1 = 4°C$. Figure 4.6 shows that for $T_1 = 6°C$ the skewness has again increased. For $T_1 = 7°C$ (figure 4.7), the increased skewness results in a new effect at smaller values of R_1. At values of $R_1 = -292, -291.5$ the minimum on the oscillatory curve is clearly less than the minimum on the stationary curve. At $R_1 = -290.1$ the role of minimum has been reversed and now the minimum on the stationary curve is smaller than the minimum on the oscillatory curve. At a value of R_1 between -291.5 and -290.1 the minimum on each curve occurs at the same value of R. This value was computed to be

$$R_1 = -291.067,$$

with minimum thermal Rayleigh number

$$R_{\min} = 228.0107,$$

and corresponding wavenumbers

$$k^{\text{osc}} = 3.77, \quad k^{\text{stat}} = 4.62.$$

[In fact, for

$$R_1 = -291.066,$$

$$R_{\min}^{\text{osc}} = 228.0131, \quad k^{\text{osc}} = 3.77,$$

$$R_{\min}^{\text{stat}} = 228.0090, \quad k^{\text{stat}} = 4.62,$$

while, for

$$R_1 = -291.067,$$

$$R_{\min}^{\text{osc}} = 228.0107, \quad k^{\text{osc}} = 3.77,$$

$$R_{\min}^{\text{stat}} = 228.0111, \quad k^{\text{stat}} = 4.62. \ ]$$

These results predict the onset of oscillatory instability and the onset of stationary instability at the same value of R but different wavenumbers.

As the upper temperature is increased, the minimum on the oscillatory curve occurs at increasingly smaller values of the wavenumber while the minimum on the stationary curve moves to the right as T_1 is increased.

One considerable advantage of the Chebyshev tau — QZ algorithm method employed here is that it yields more eigenvalues than just the leading one. This allows us to investigate the behaviour of the growth rate in more detail. Over the range of values of R indicated in figures 4.3–4.6 the leading three eigenvalues always consist of a complex conjugate pair and a real eigenvalue. The behaviour of the real part of the growth rate $\sigma = \sigma_r + i\sigma_i$ is shown in figures 4.8 and 4.9. In both figures the complex conjugate pair is initially the leading eigenvalue. As R is increased σ_r reaches a maximum for the complex conjugate pair and then starts to decrease. The real eigenvalue then takes over and becomes the leading eigenvalue.

The Chebyshev tau method also yields the eigenfunctions. Figure 4.10 shows the eigenfunctions for the case $T_1 = 7°C, R = 228.0107, R_1 = -291.067, R_2 = 261, k = 4.62$, i.e. at the minimum on the stationary curve when the minima on the stationary and oscillatory neutral curves coincide. The normalised eigenfunctions Φ^1 and Φ^2 are the same as the Θ eigenfunction. That this should be so can be seen from equations (4.17)–(4.20) with $\sigma = 0$. These three equations can be solved to show that

$$\Theta = RG(z), \quad \Phi^\alpha = R_\alpha G(z) \quad (\alpha = 1, 2),$$

where

$$G(z) = F(z) - F(1)\frac{\sinh kz}{\sinh k},$$

with

$$F(z) = \int_0^z e^{k(\xi - z)} \int_0^\xi e^{k(\xi - \mu)} W(\mu)\ d\mu d\xi.$$

So, when Θ and Φ^α are normalised they will be identical. At the minimum on the oscillatory curve the eigenfunctions for W and Φ^α (shown in figure 4.11) are similar but not identical. This can be seen by setting $\sigma_r = 0$ in equations (4.17)–(4.20), obtaining

$$((D^2 - k^2)^2 + \sigma_i^2)\Theta_r = R(D^2 - k^2)W_r - \sigma_i R W_i,$$

$$((D^2 - k^2)^2 + P_\alpha \sigma_i^2)\Phi_r^\alpha = R_\alpha(D^2 - k^2)W_r - \sigma_i P_\alpha R_\alpha W_i,$$

while similar equations exist for Θ_i, Φ_i^α.

In figures 4.10 and 4.11 the penetrative effect (W becoming negative) can be clearly seen.

4.5.2 Nonlinear results

In figure 4.12 the solution of the eigenvalue problem (4.61)–(4.64) for $T_1 = 4°C$ is plotted together with the (R, R_2) linear stability boundary for $R_1 = -261$ and $R_1 = -100$. The energy results are clearly closer to the linear results for smaller (in modulus) values of R_1. This is not surprising as the terms involving the first salt concentration drop out of the energy analysis and so do not yield any information. Whenever the stabilizing salt field is of any consequence the energy results may be far from the linear results. Also at $R_1 = -100$ the disconnected oscillatory curves are not found. The energy results do have the advantage that they are unconditional, i.e. for perturbations of any initial amplitude nonlinear exponential stability is assured.

At higher temperatures (figures 4.13–4.15) a similar result can be seen. The energy results are closer for smaller absolute values of R_1, however at the smaller values of R_1 the disconnected oscillatory curves are not found.

4.6 Discussion

In the present work a linear stability analysis is presented that yields several interesting results. The existence of disconnected oscillatory neutral curves produces a finite interval of stable values of R, the thermal Rayleigh number, as well as the normal semi–infinite range. The penetrative effect has skewed these oscillatory curves away from the *perfect* heart–shaped curves found in chapter 2. There it was stated that oscillatory instability could occur at the same thermal Rayleigh number but differing wavenumbers at the maxima on the lobes of the heart–shaped curve. The skewed nature of the oscillatory curves produced here by the quadratic equation of state means that this effect is not seen. McKay and Straughan (1992) argue that the density of a fluid is never a linear function of temperature. Consequently the perfect heart–shapes are unlikely to be observed experimentally.

An alternative result which may be seen experimentally is observed here. The effect shown in figure 4.7 whereby oscillatory and stationary instability set in at two different wavenumbers but the same thermal Rayleigh number is a completely original phenomenon in porous convection. By increasing R_1 one should see instability change from being initiated by oscillatory convection with wavenumber $k = 3.77$ to a stationary instability with wavenumber $k = 4.62$. For values of $R = 228.0107, R_1 = -291.067$ the present analysis predicts that one should find instability occurring in two different cell sizes.

There are two factors in the present problem that could give rise to subcritical instabilities. Firstly, the nonlinear term that arises in the velocity equation from the quadratic equation of state, and secondly the competition between the different stratifying effects. These factors show the need for the nonlinear stability analysis of section 4.4. Unconditional nonlinear stability is obtained and L^2 decay is shown for the temperature and solute perturbations. Although the use of Darcy's Law means that L^2 decay for the velocity cannot be easily proved, in section 4.4 it is shown that the velocity satisfies a condition which ensures "practical decay".

The classical kinetic energy results presented here are somewhat disappointing in that the energy boundary may be far away from the linear stability boundary. As explained in section 4.5 this is due to the terms involving the stabilising salt field

dropping out of the analysis. To overcome this a generalised energy method in the vein of chapter 3 may be constructed. Work to this end is in progress.

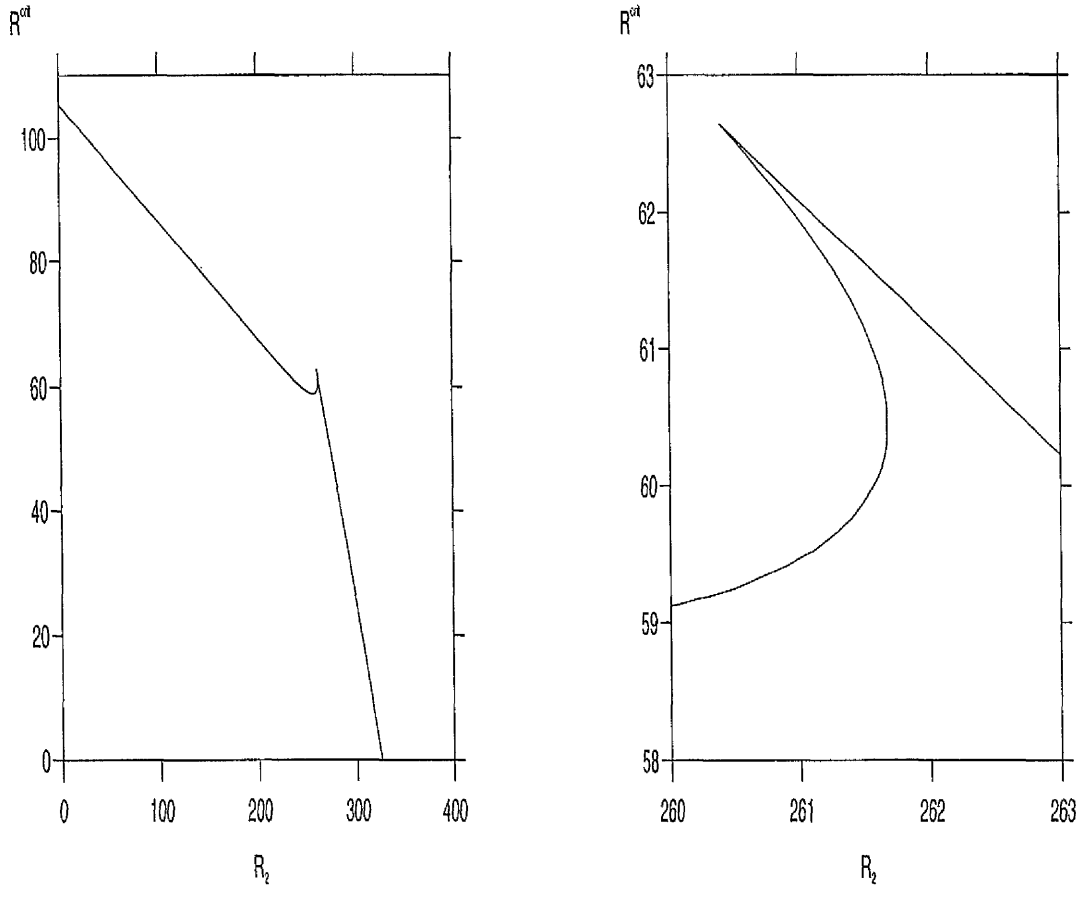

Figure 4.1: (R^{crit}, R_2) stability boundary for $T_1 = 4°C, R_1 = -286.0$, $P_1 = 4.545454$, $P_2 = 4.761904$. The right–hand graph shows the multi–valued region in more detail.

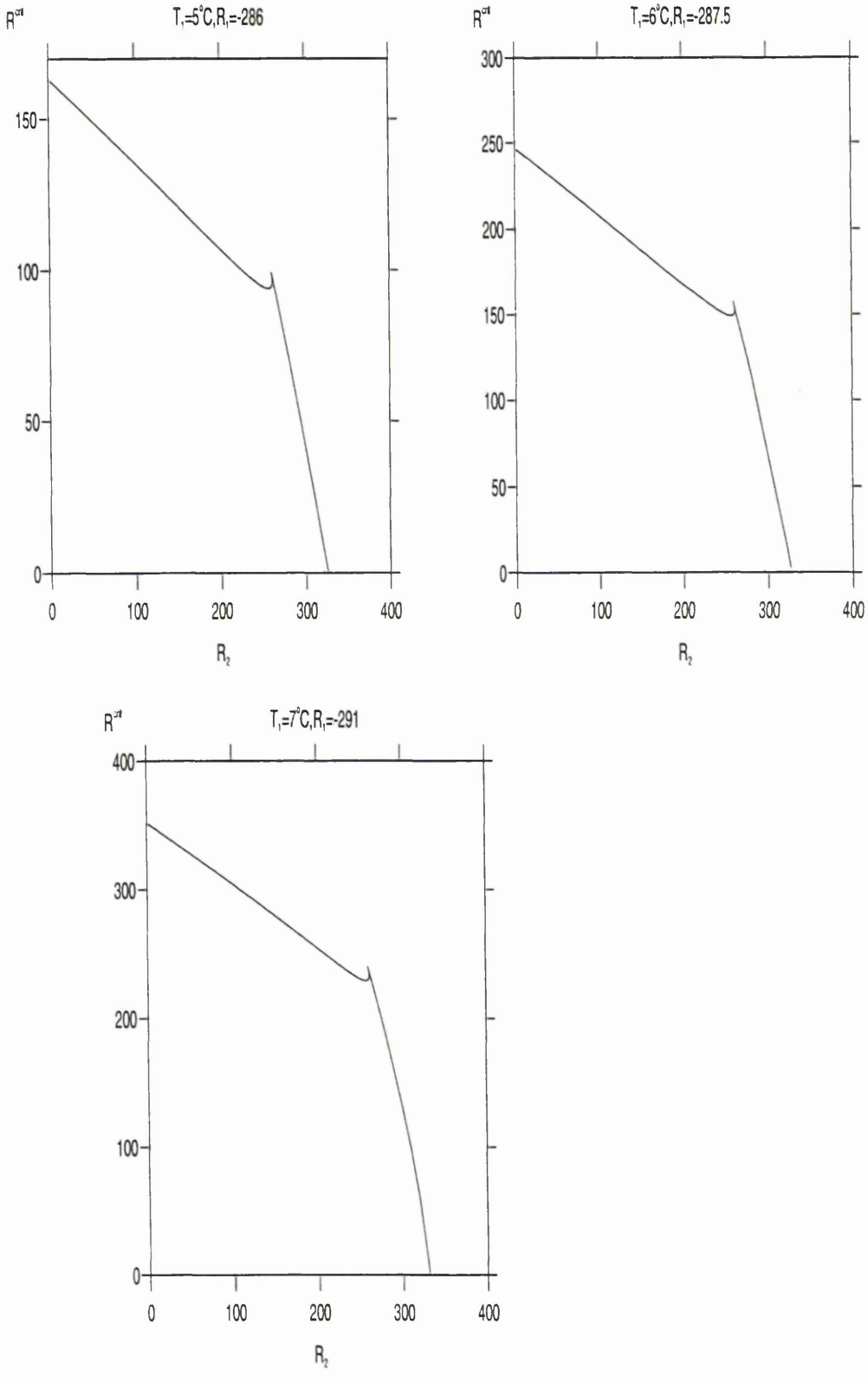

Figure 4.2: (R^{crit}, R_2) stability boundaries for $T_1 = 5°C, R_1 = -286, T_1 = 6°C, R_1 = -287.5$ and $T_1 = 7°, R_1 = -291$

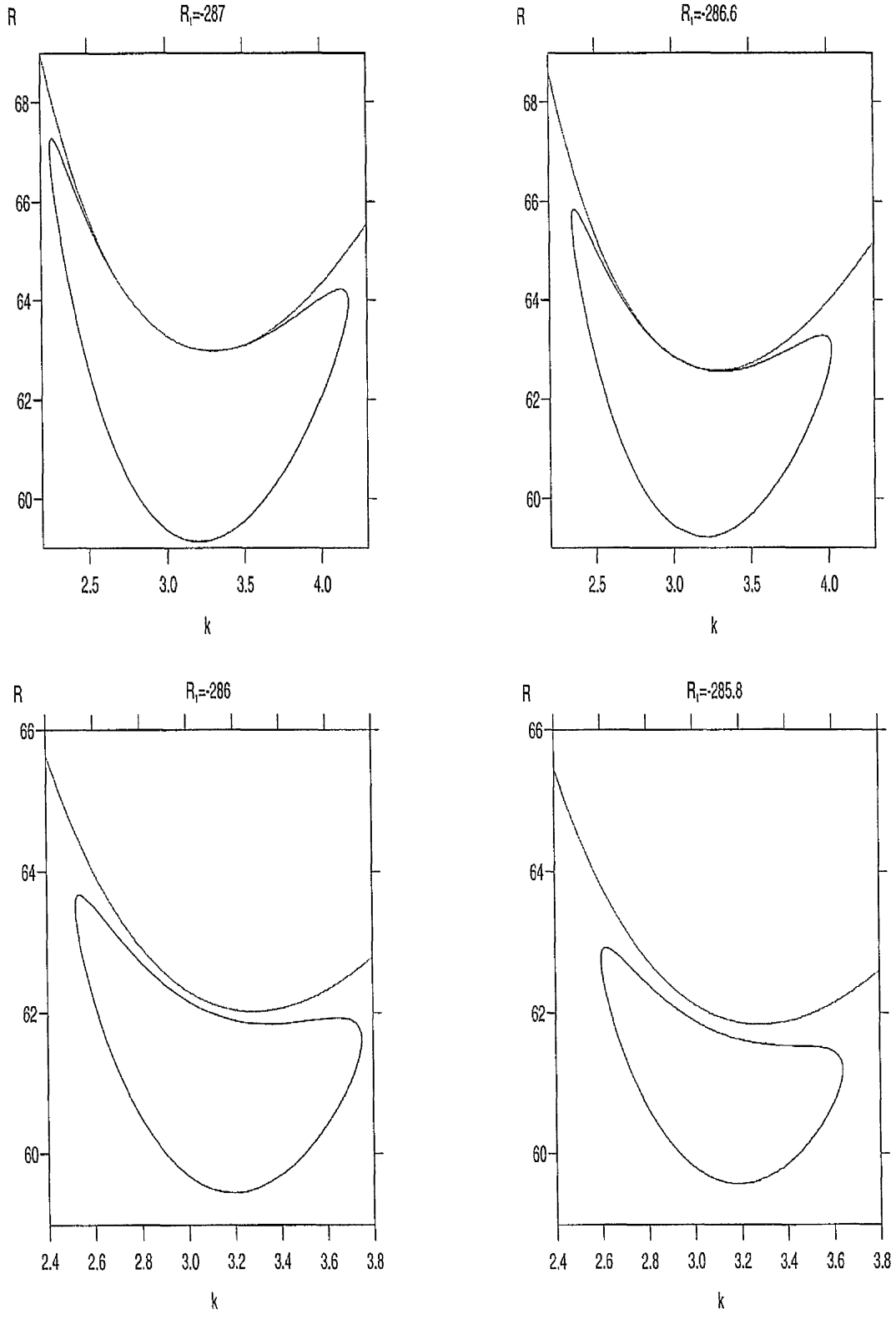

Figure 4.3: (R, k) neutral curves for $T_1 = 4°C, R_2 = 261, P_1 = 4.545454, P_2 = 4.761904$.

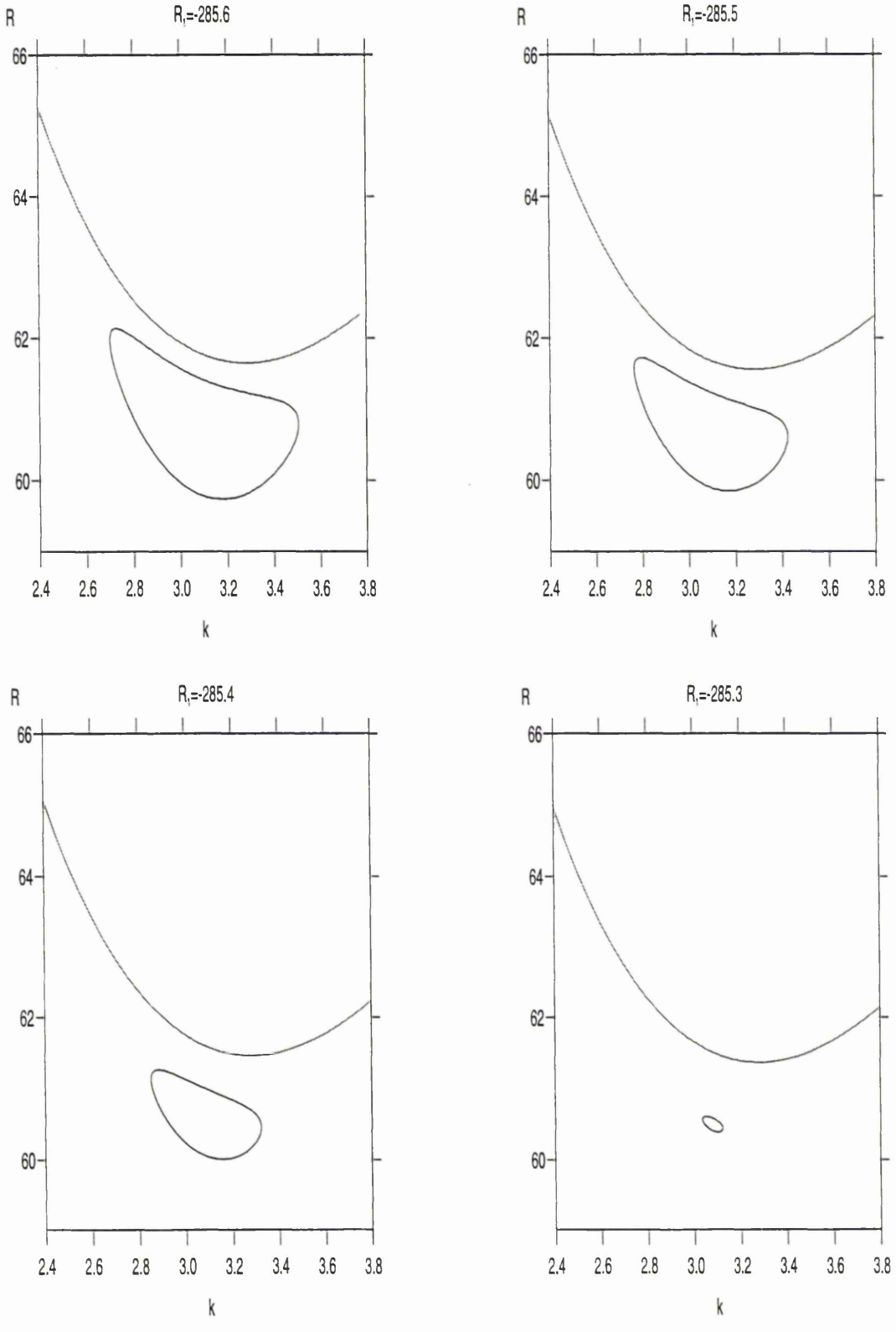

Figure 4.4: (R, k) neutral curves for $T_1 = 4°C, R_2 = 261, P_1 = 4.545454, P_2 = 4.761904$.

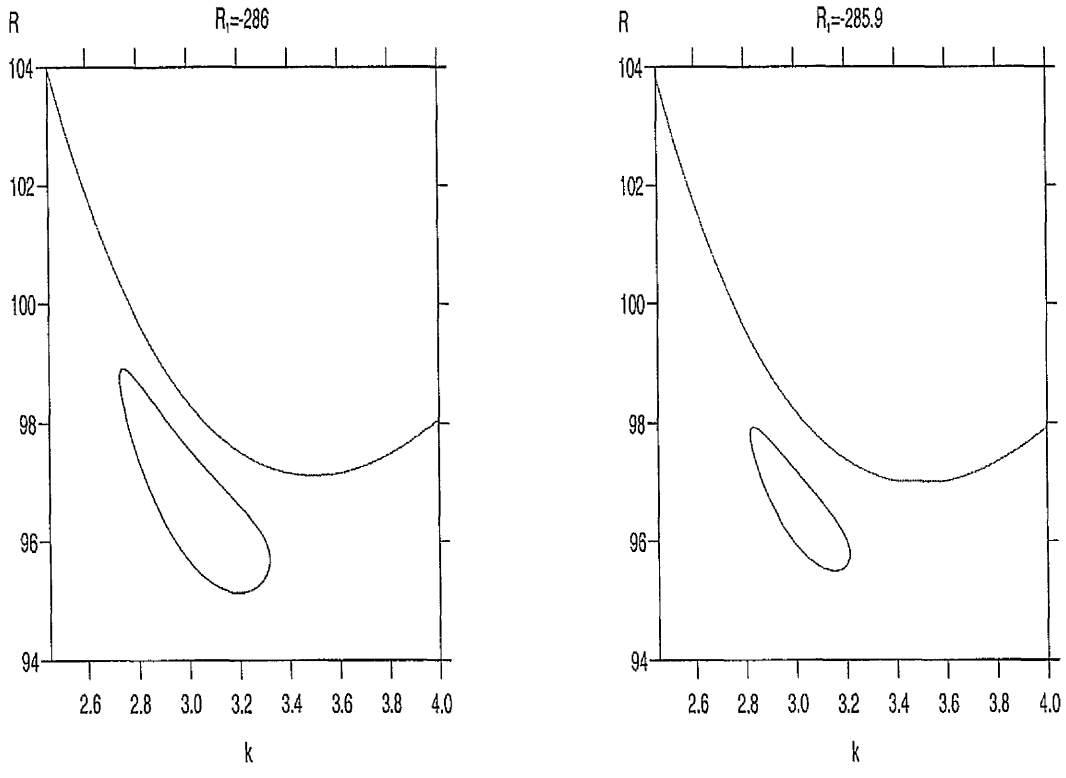

Figure 4.5: (R, k) neutral curves for $T_1 = 5°C, R_2 = 261, P_1 = 4.545454, P_2 = 4.761904$.

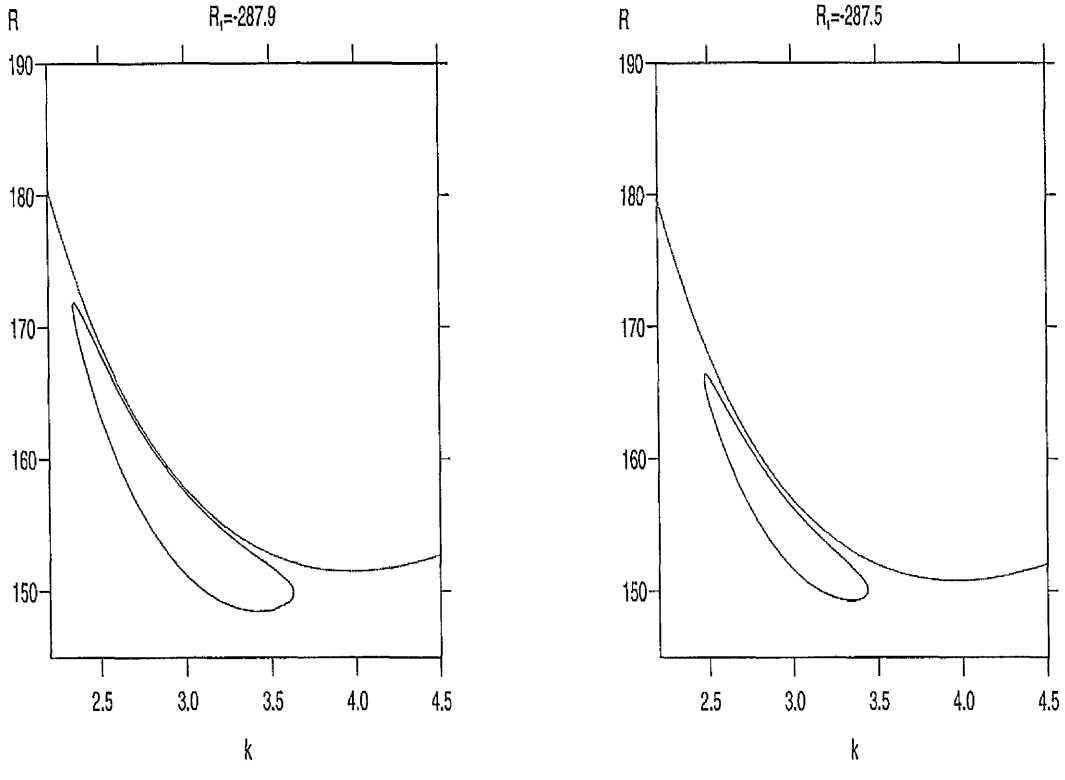

Figure 4.6: (R, k) neutral curves for $T_1 = 6°C, R_2 = 261, P_1 = 4.545454, P_2 = 4.761904$.

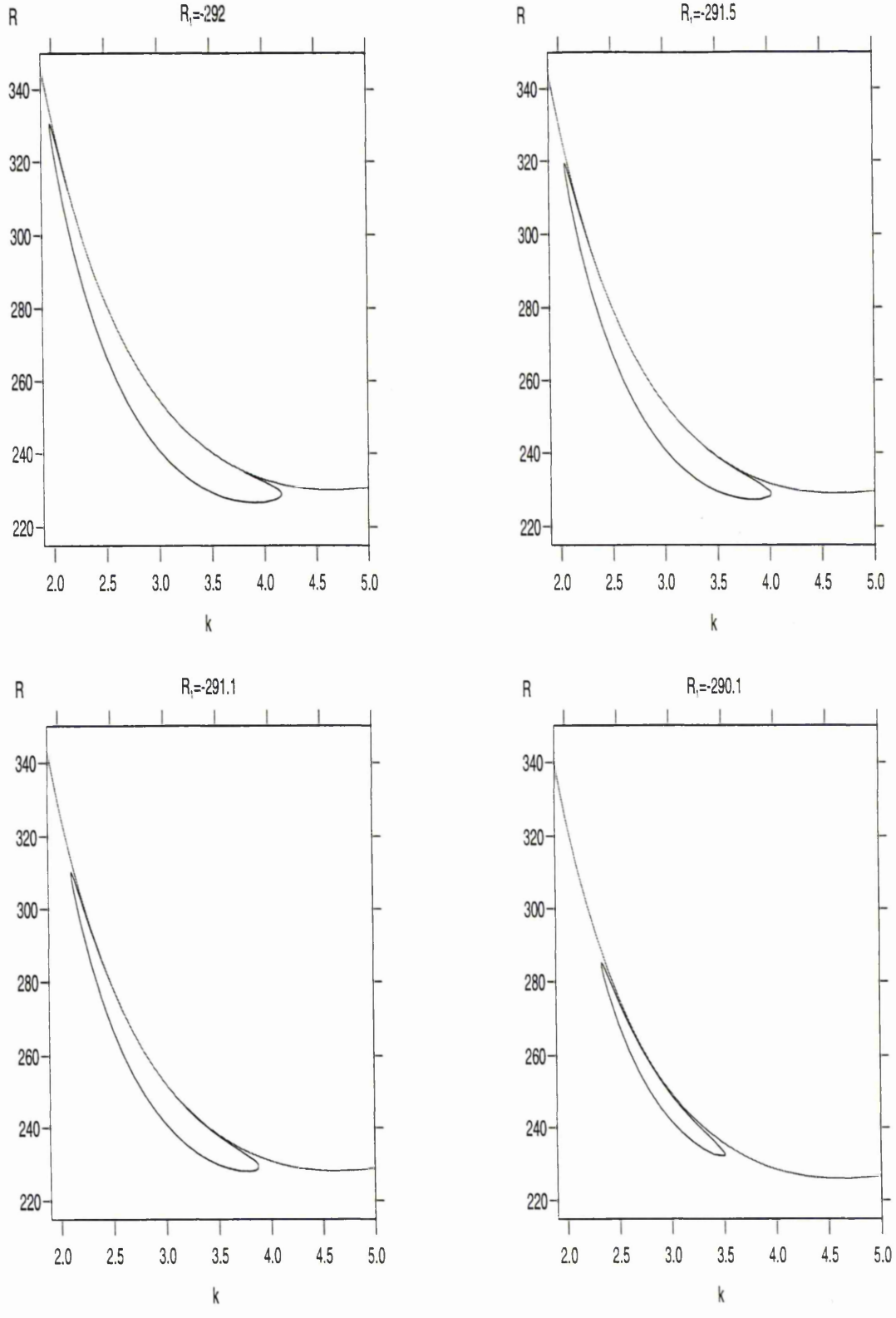

Figure 4.7: (R, k) neutral curves for $T_1 = 7°C, R_2 = 261, P_1 = 4.545454, P_2 = 4.761904$.

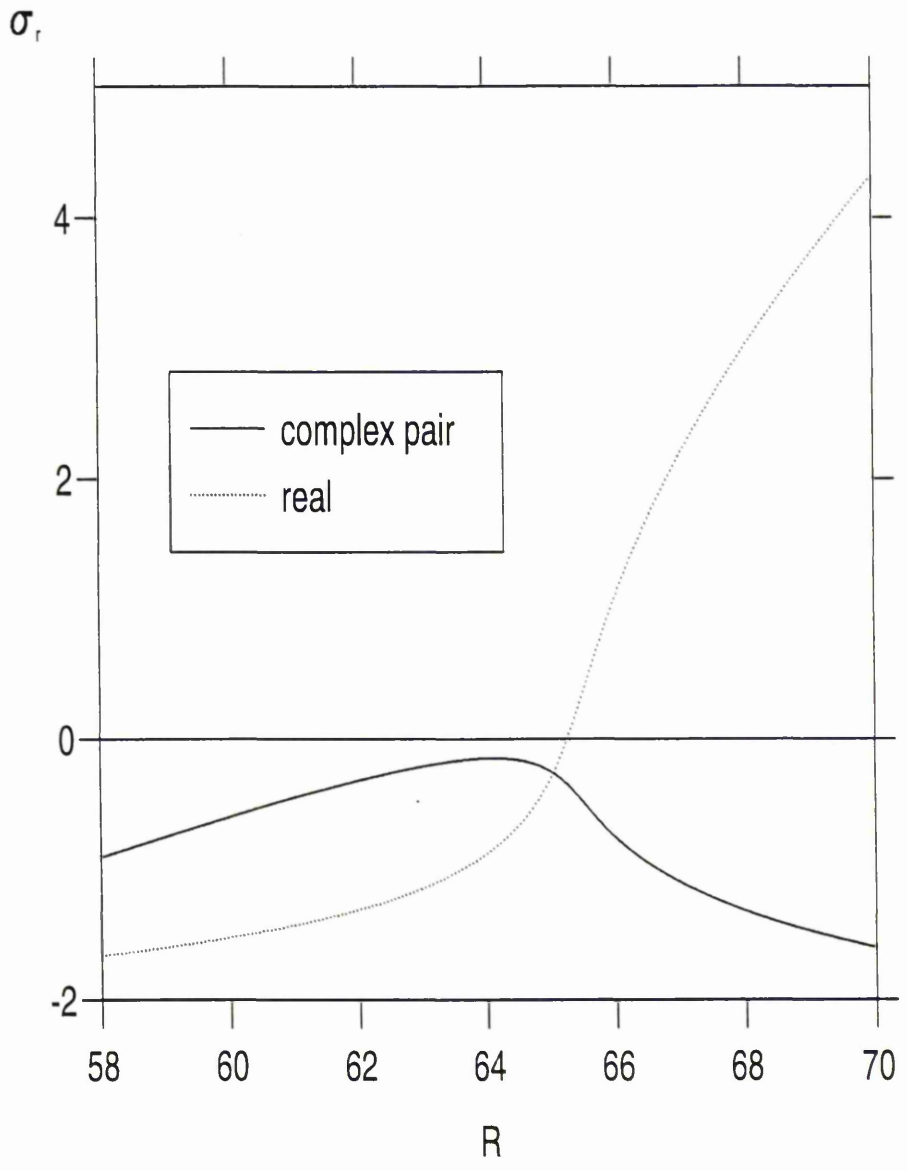

Figure 4.8: Graph of σ_r against R for $T_1 = 4°C, R_1 = -285.6, R_2 = 261, P_1 = 4.545454, P_2 = 4.761904, k = 2.4$.

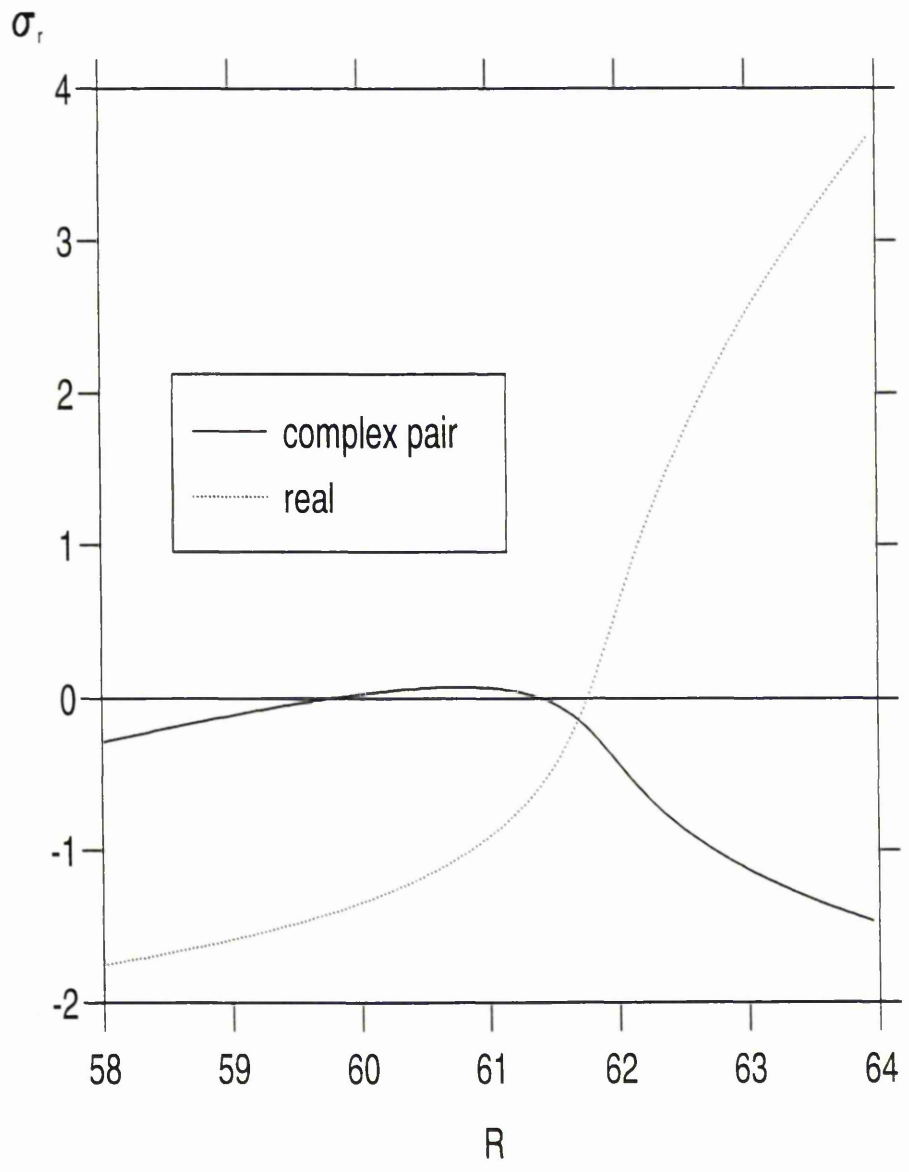

Figure 4.9: Graph of σ_r against R for $T_1 = 4°C, R_1 = -285.6, R_2 = 261, P_1 = 4.545454, P_2 = 4.761904, k = 3.1$.

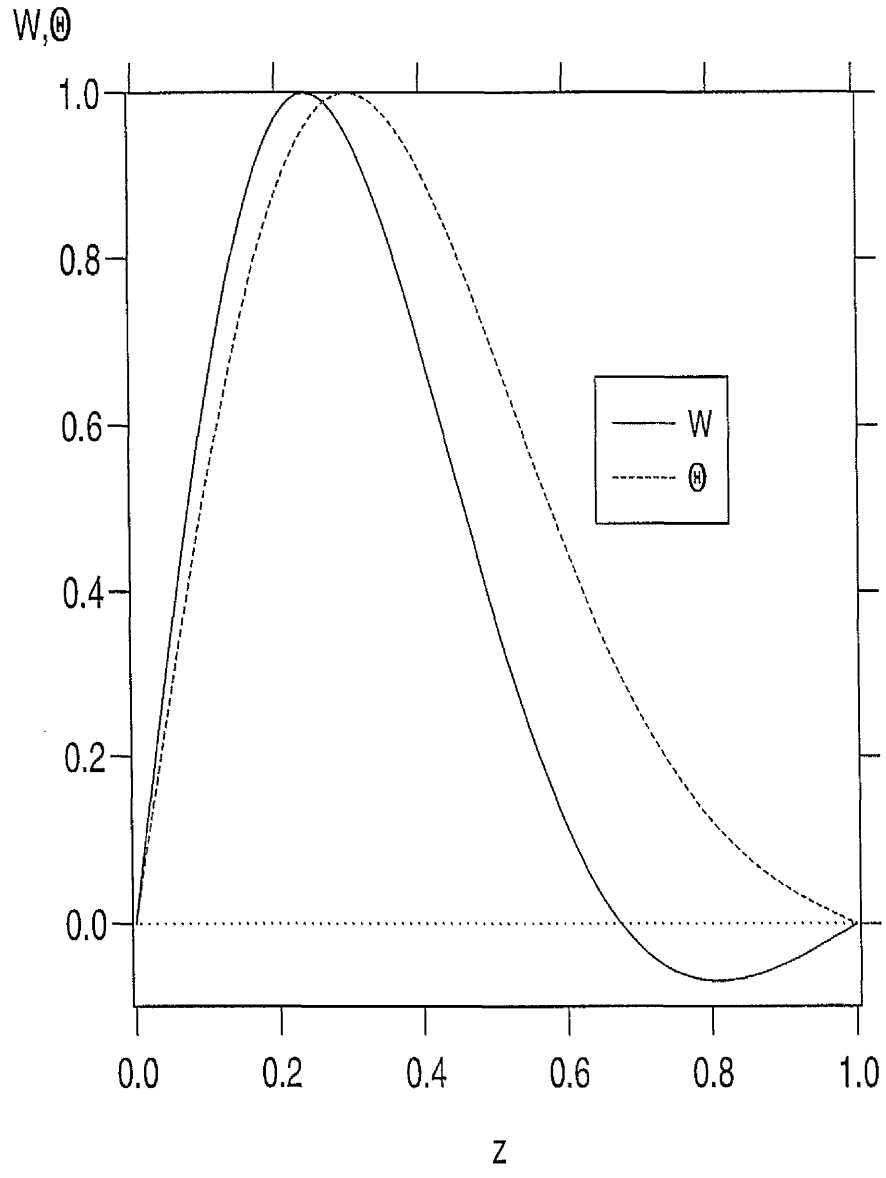

Figure 4.10: Plot of eigenfunctions for $T_1 = 7°C, R = 228.0107, R_1 = -291.067.6, R_2 = 261, P_1 = 4.545454, P_2 = 4.761904, k = 4.62$, i.e. at the minimum of the stationary curve. The Φ^1 and Φ^2 eigenfunctions are identical to the Θ eigenfunction.

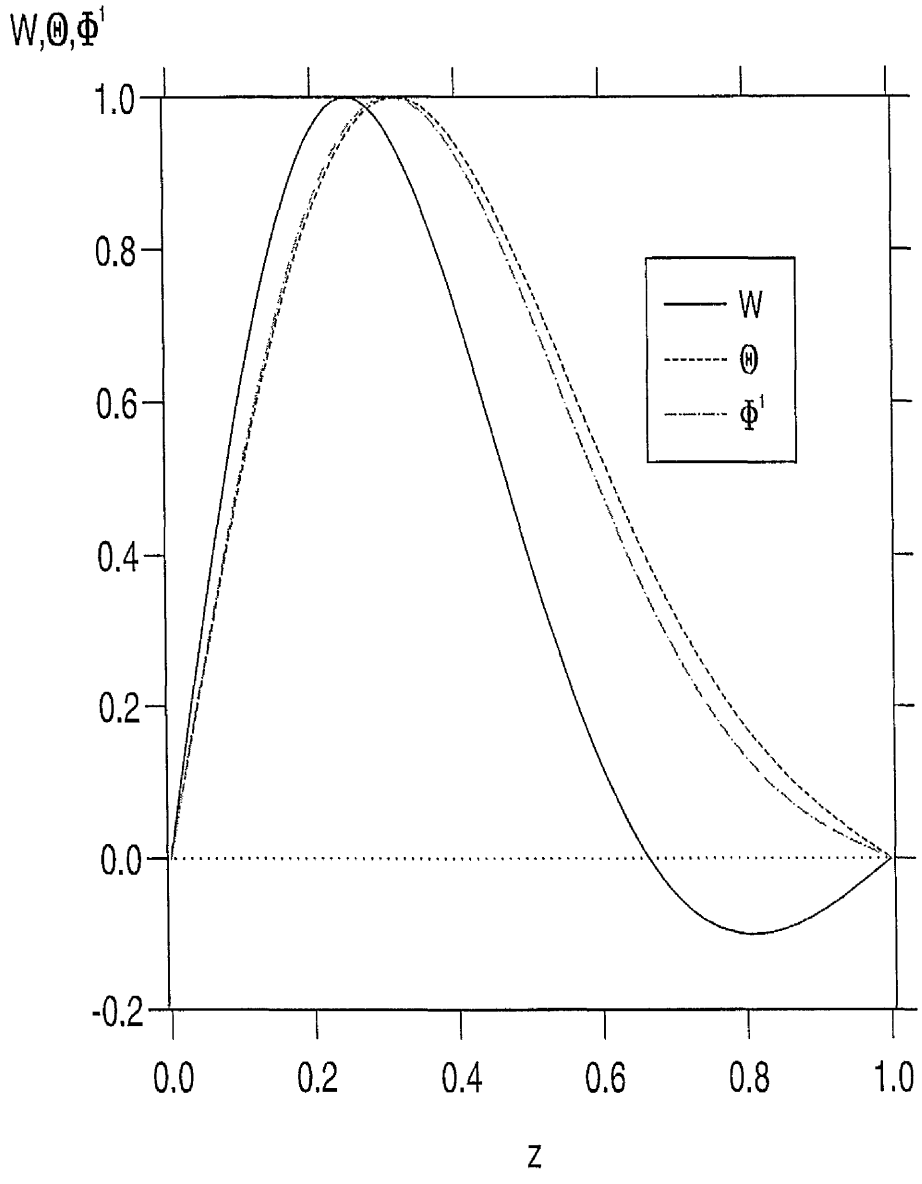

Figure 4.11: Plot of eigenfunctions for $T_1 = 7°C, R = 228.0107, R_1 = -291.067.6, R_2 = 261, P_1 = 4.545454, P_2 = 4.761904, k = 3.77$ i.e. at the minimum on the oscillatory curve. The Φ^2 eigenfunction is very similar to the Φ^1 curve.

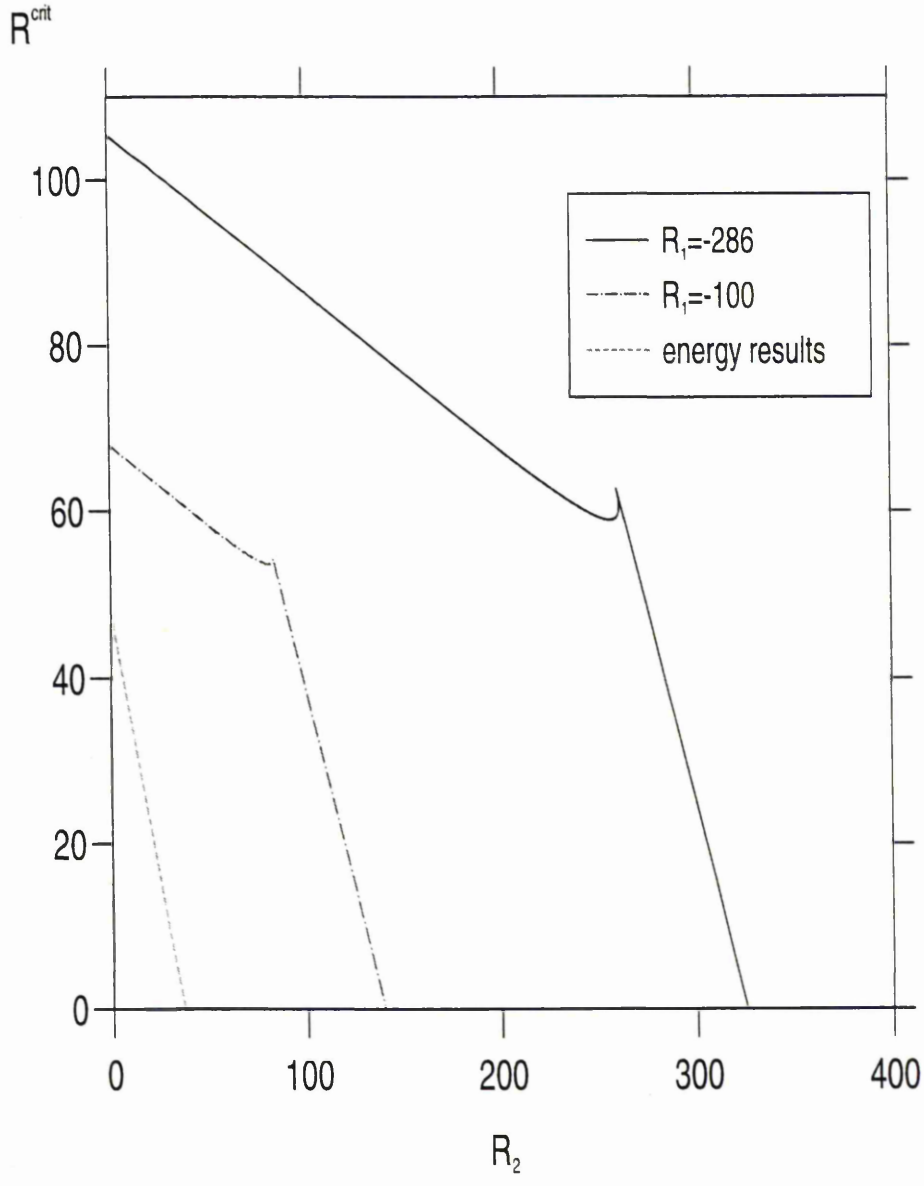

Figure 4.12: Plot of the energy stability boundary for $T_1 = 4°C$ together with the linear instability boundaries for $R_1 = -261$ and $R_1 = -100$. Also $P_1 = 4.545454, P_2 = 4.761904$.

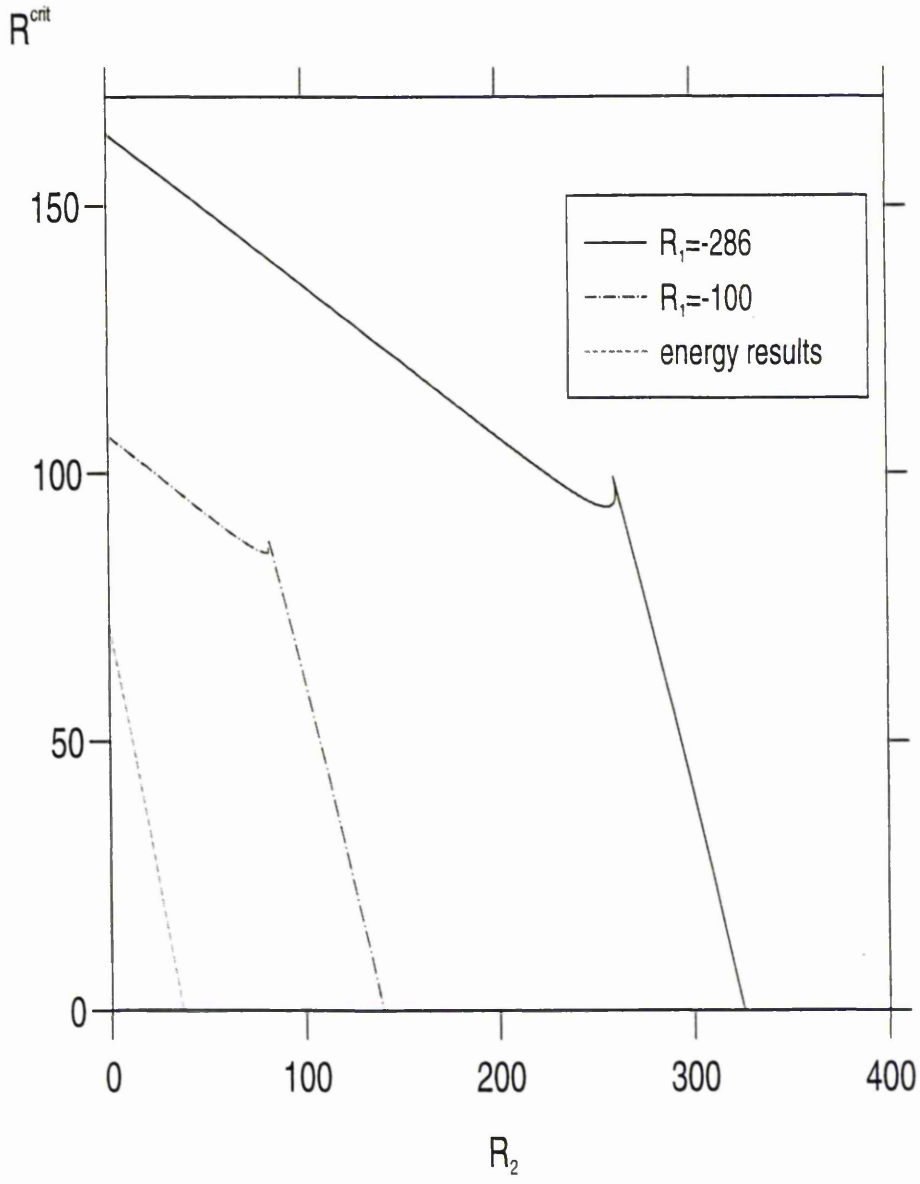

Figure 4.13: Plot of the energy stability boundary for $T_1 = 5°C$ together with the linear instability boundaries for $R_1 = -261$ and $R_1 = -100$. Also $P_1 = 4.545454, P_2 = 4.761904$.

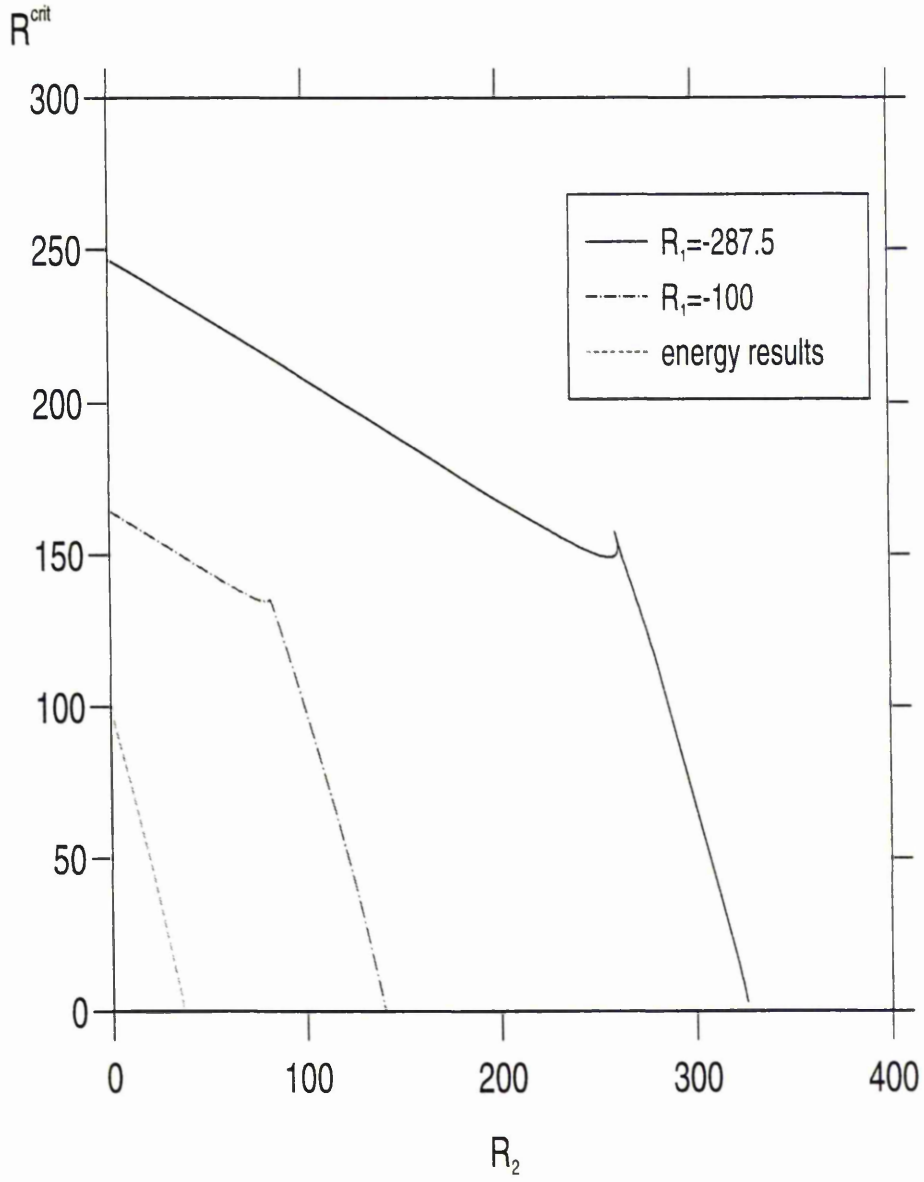

Figure 4.14: Plot of the energy stability boundary for $T_1 = 6°C$ together with the linear instability boundaries for $R_1 = -287.5$ and $R_1 = -100$. Also $P_1 = 4.545454, P_2 = 4.761904$.

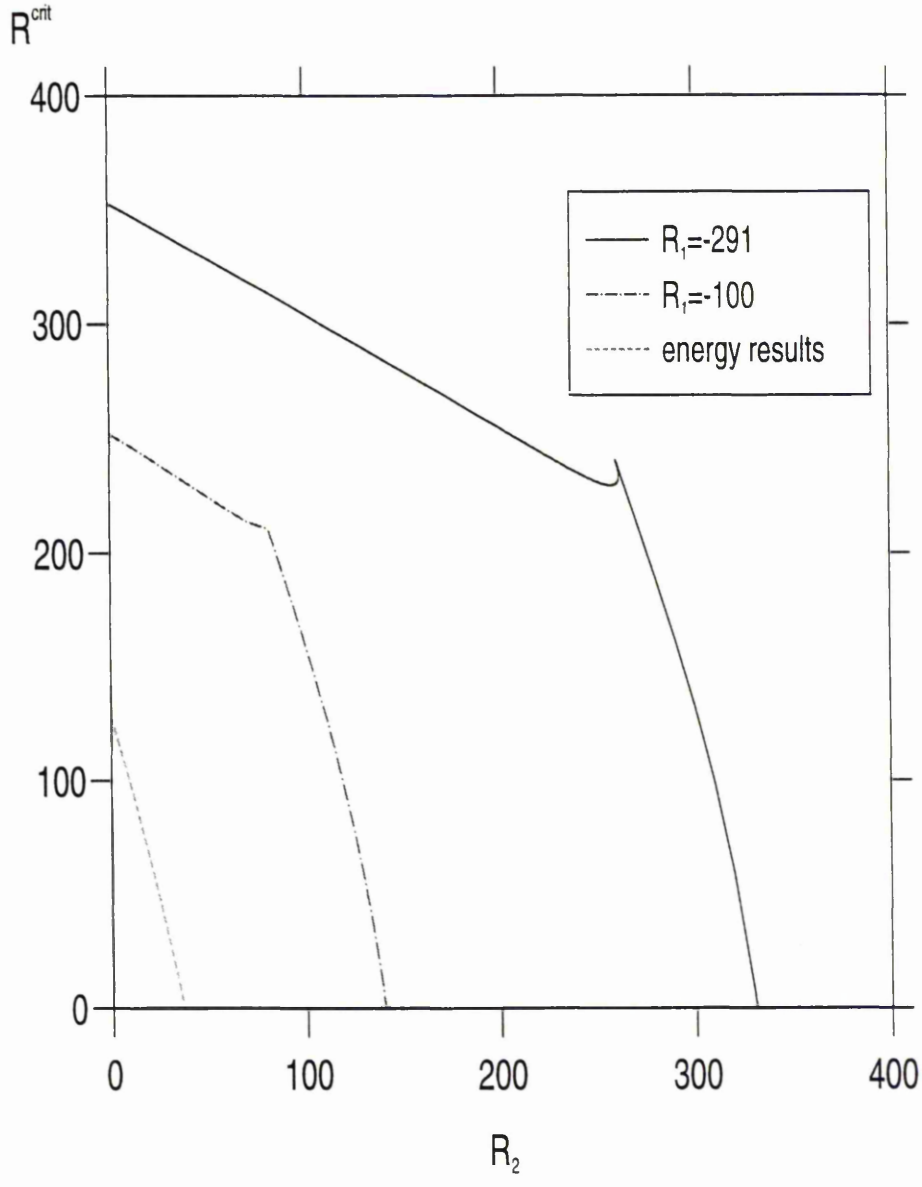

Figure 4.15: Plot of the energy stability boundary for $T_1 = 7°C$ together with the linear instability boundaries for $R_1 = -291$ and $R_1 = -100$. Also $P_1 = 4.545454$, $P_2 = 4.761904$.

Chapter 5

Multi–component convection–diffusion with internal heating or cooling

5.1 Introduction

In the previous chapter penetrative convection was introduced into the multi–component porous problem by having the equation of state quadratic in temperature, i.e.

$$\rho = \rho_0 \left(1 - A\left(T - T_0\right)^2\right) \tag{5.1}$$

where T is the temperature and ρ_0 and T_0 are reference values. If the temperature at the lower boundary is held fixed at a temperature $T < T_0$ and the upper boundary is fixed at a temperature greater than T_0 then a gravitationally stable layer will be created above a layer of gravitationally unstable fluid. When convection occurs in the lower layer the motions will penetrate into the upper layer. One of the motivating factors for the previous chapter was the paper of Straughan and Walker (1997) where a quadratic buoyancy law was used in the analogous fluid problem to that studied in chapter 4.

An alternative model of penetrative convection can be constructed by introducing an internal heat source. One can again produce an unstable layer next to a stable layer. An internal heat source has been employed in various fluid problems, for

instance, in modelling the motion of the plates that form the Earth's crust. A suggested source of the energy required to maintain the movement of these plates is from the radioactive decay within the Earth's mantle of Uranium and Potassium isotopes (see, e.g. McKenzie, Roberts and Weiss (1974)).

In this chapter we will use an internal heat source model of penetrative convection to investigate the stability of the motionless state in a triple diffusive fluid layer. Here a viscous fluid layer, rather than the fluid–saturated porous layer of previous chapters, is considered. The reason for this change is that we wish to make comparisons with the quadratic buoyancy law model of penetrative convection used by Straughan and Walker (1997). Straughan and Walker (1997) were partly motivated by the numerical technique of removing the boundary condition rows in the Chebyshev tau method first used by Haidvogel and Zang (1979) (and employed here in chapter 4). As noted in Appendix A, this method only works for free boundary conditions and consequently Straughan and Walker (1997) only considered the case of an infinite layer with free upper and lower boundaries. A more physically realistic problem can be obtained by using fixed boundaries and so the cases of "fixed–free" and "fixed–fixed" boundary conditions will be studied here. Clearly this extends the problem beyond that studied by Straughan and Walker (1997). The effect of rigid boundaries on the non–penetrative triple diffusive fluid problem has already been studied by Lopez *et al.* (1990). Those authors found that the perfectly symmetric neutral curves found by Pearlstein *et al.* (1989) were slightly skewed away from symmetry in a similar manner to the penetrative effect described by Straughan and Walker (1997).

In this chapter it will be shown that there is a strong connection between the linearised internal heat sink problem and the linearised quadratic buoyancy law model — namely that one is the adjoint of the other. The connection between the heat source and sink problems is also discussed.

A further enhancement that would make the problem more physically realistic is the inclusion of adiabatic sidewalls and so this chapter concludes by including such sidewalls and considering their stabilizing effect.

5.2 Governing equations

The problem to be considered is that of the onset of convection in an incompressible fluid confined to the infinite horizontal layer $z \in (0, d)$. The fluid has dissolved in it two different chemical species and also contains an internal heat source. The lower and upper boundaries $z = 0$ and $z = d$ are held at fixed temperatures T_l and T_u, respectively. Denote the concentration of component α by C^α $(\alpha = 1, 2)$. The concentration of component α at the lower and upper boundaries is held at C_l^α and C_u^α respectively.

The equation of state is assumed to be linear in both the temperature and salt concentrations, i.e.

$$\rho = \rho_0 \left(1 - A\left(T - T_0\right) + A_1 \left(C^1 - C_0^1\right) + A_2 \left(C^2 - C_0^2\right)\right),$$

where ρ_0, T_0 and C_0^α $(\alpha = 1, 2)$ are reference values of density, temperature and salt concentration respectively. The constants A and A_α $(\alpha = 1, 2)$ represent the thermal and solute expansion coefficients respectively.

This situation can be described by seven partial differential equations for the velocity, pressure, temperature and salt concentrations. The density is assumed constant, ρ_0, everywhere except in the body force and the equations are

$$\begin{aligned}
\rho_0 \left(v_{i,t} + v_j v_{i,j}\right) &= -p_{,i} + \rho_0 \nu \Delta v_i - g\rho_0(1 - A(T - T_0) \\
&\quad + A_1(C^1 - C_0^1) + A_2(C^2 - C_0^2))k_i, \qquad (5.2) \\
v_{i,i} &= 0, \qquad (5.3) \\
T_{,t} + v_i T_{,i} &= \kappa \Delta T + Q(z), \qquad (5.4) \\
C_{,t}^\alpha + v_i C_{,i}^\alpha &= \kappa_\alpha \Delta C^\alpha \ (\alpha = 1, 2). \qquad (5.5)
\end{aligned}$$

where indicial notation and the Einstein summation convention have been employed. The vector $\mathbf{k}$ is the unit vector in the z–direction and the variables v_i, p, ν, g, κ and κ_α represent velocity, pressure, viscosity, gravity, thermal diffusivity and solutal diffusivity, respectively. $Q(z)$ is the internal heat source term.

These equations are supplemented by boundary conditions on $z = 0$ and $z = d$. Three separate cases are considered, namely 1. free lower and upper surfaces, 2. rigid lower and free upper surfaces and 3. rigid lower and upper surfaces. A discussion of

these boundary conditions may be found in, e.g., Drazin and Reid (1981) pp. 40-44. Here these boundaries are held at fixed temperatures and salt concentrations. The boundary conditions are then

1. free–free boundaries

$$\begin{aligned} &\text{On } z=0,\ v_3=0,\ v_{1,z}=v_{2,z}=0,\ T=T_l,\ C^\alpha=C_l^\alpha\ (\alpha=1,2),\\ &\text{on } z=d,\ v_3=0,\ v_{1,z}=v_{2,z}=0,\ T=T_u,\ C^\alpha=C_u^\alpha\ (\alpha=1,2), \end{aligned} \tag{5.6}$$

2. fixed–free boundaries

$$\begin{aligned} &\text{On } z=0,\ \mathbf{v}(\mathbf{x})=\mathbf{0},\ T=T_l,\ C^\alpha=C_l^\alpha\ (\alpha=1,2),\\ &\text{on } z=d,\ v_3=0,\ v_{1,z}=v_{2,z}=0,\ T=T_u,\ C^\alpha=C_u^\alpha\ (\alpha=1,2), \end{aligned} \tag{5.7}$$

3. fixed–fixed boundaries

$$\begin{aligned} &\text{On } z=0,\ \mathbf{v}(\mathbf{x})=\mathbf{0},\ T=T_l,\ C^\alpha=C_l^\alpha\ (\alpha=1,2),\\ &\text{on } z=d,\ \mathbf{v}(\mathbf{x})=\mathbf{0},\ T=T_u,\ C^\alpha=C_u^\alpha\ (\alpha=1,2). \end{aligned} \tag{5.8}$$

We consider a motionless steady solution $(\bar{v}_i, \bar{p}, \bar{T}, \bar{C}^\alpha)$ of (5.2)–(5.8) in which $\bar{T}$ and $\bar{C}^\alpha$ are functions of z only. From (5.4) and (5.5),

$$\frac{1}{\rho_0}\bar{p}_{,z} = -g\left(1 - A\left(\bar{T}-T_0\right) + A_1\left(\bar{C}^1 - C_0^1\right) + A_2\left(\bar{C}^2 - C_0^2\right)\right), \tag{5.9}$$

$$\frac{d^2\bar{T}}{dz^2} = -\frac{1}{\kappa}Q(z), \tag{5.10}$$

$$\frac{d^2\bar{C}^\alpha}{dz^2} = 0. \tag{5.11}$$

At this point attention is restricted to the case where $Q(z) = Q$, a constant. Consider the integral form of the conservation of heat equation, namely,

$$\frac{d}{dt}\int_V T\,dV = -\oint_{\partial V} \mathbf{q}.\mathbf{n}\,dA + \int_V Q\,dV,$$

where V is the fluid layer $z \in (0,1)$ and $\mathbf{q}$ and $\mathbf{n}$ are the heat flux into and the unit normal to this volume. Notice that, in the absence of any heat flux into the volume, a positive value of Q will give rise to an increase in the temperature of the layer and so describes an internal heat *source*. Clearly a negative value of Q describes an internal heat *sink*.

With Q assumed constant the basic state considered is, from (5.9)–(5.11),

$$\begin{aligned} \bar{T} &= \frac{Qd^2}{\kappa}\left(\frac{z}{2d} - \frac{z^2}{2d^2}\right) + T_l - \frac{\delta T}{d}z, \\ \bar{C}^\alpha &= C_l^\alpha - \frac{\delta C^\alpha}{d}z, \end{aligned} \tag{5.12}$$

where $\delta T = T_l - T_u, \delta C^\alpha = C_l^\alpha - C_u^\alpha$. From (5.9), the steady pressure $\bar{p}$ is also a function of z only, namely

$$\frac{d\bar{p}}{dz} = -\rho_0 g\left(1 - A\left(\bar{T} - T_0\right) + A_1\left(\bar{C}^1 - C_0^1\right) + A_2\left(\bar{C}^2 - C_0^2\right)\right).$$

Figure 5.1 shows sketches of the steady–state temperature for fixed T_l, T_u, κ, d and various values of Q.

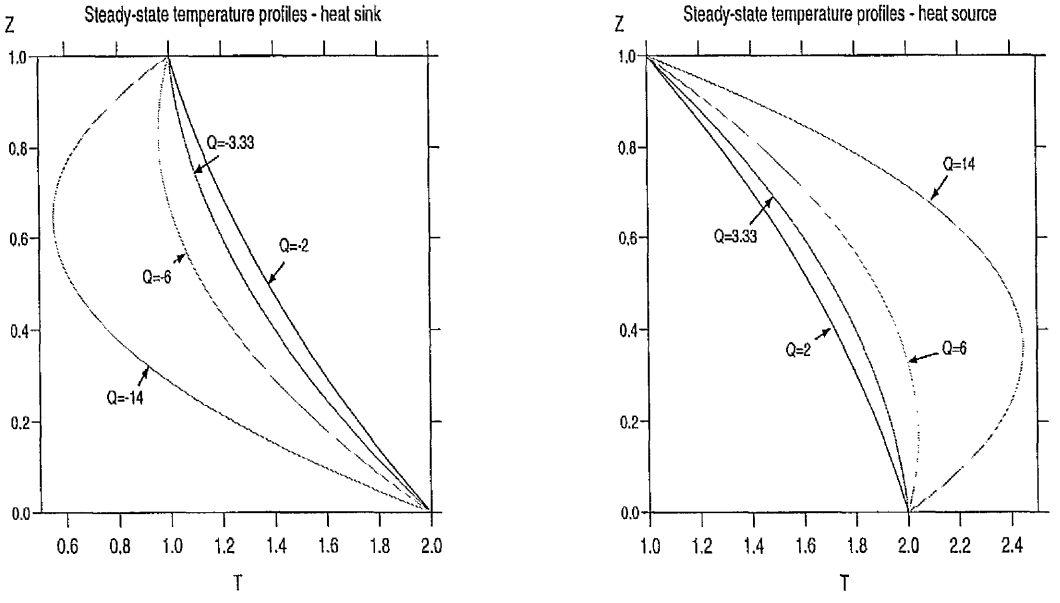

Figure 5.1: Steady-state temperature profiles for $T_l = 2, T_u = 1, d = 1, \kappa = 2$. In the left–hand graph negative values of Q are plotted, corresponding to an internal heat *sink*. The right–hand graph shows positive values of Q, corresponding to an internal heat *source*.

In order to investigate the linear stability of this basic solution we introduce perturbations $(u_i, \pi, \theta, \phi^\alpha)$ to $(\bar{v}_i, \bar{p}, \bar{T}, \bar{C}^\alpha)$ via

$$v_i = \bar{v}_i + u_i, p = \bar{p} + \pi, T = \bar{T} + \theta, C^\alpha = \bar{C}^\alpha + \phi^\alpha. \tag{5.13}$$

The resultant perturbation equations are non–dimensionalised using the following scalings:

$$t = t^* \frac{d^2}{\kappa},\ \mathbf{u} = \mathbf{u}^* \frac{\nu}{d},\ \pi = \pi^* \frac{\nu^2 \rho_0}{d^2},\ \mathbf{x} = \mathbf{x}^* d,$$

$$\theta = \theta^* T^{\#},\ \phi^\alpha = (\phi^\alpha)^* \Phi^\alpha,$$

$$T^{\#} = \left(\frac{\nu^3 |\delta T|}{Ag\kappa d^3}\right)^{1/2},\ \Phi^\alpha = \left(\frac{\nu^3 |\delta C^\alpha|}{A_\alpha g \kappa d^3}\right)^{1/2},$$

$$R = \left(\frac{Agd^3 |\delta T|}{\nu\kappa}\right)^{1/2},\ R_\alpha = \left(\frac{A_\alpha g d^3 |\delta C^\alpha|}{\nu\kappa}\right)^{1/2},$$

$$Pr = \frac{\kappa}{\nu}, Q = Q^* \frac{\kappa \delta T}{d^2}, \tau_\alpha = \frac{\kappa_\alpha}{\kappa},$$

$$\delta T = T_l - T_u, H = \mathrm{sgn}(\delta T), H_\alpha = \mathrm{sgn}(\delta C^\alpha).$$

Here R and R_α are thermal and solute Rayleigh numbers and Pr is the Prandtl number.

The non–dimensional nonlinear perturbation equations are then (dropping the asterisks),

$$Pr^{-1}\, u_{i,t} + u_j u_{i,j} = -\pi_{,i} + \Delta u_i + \left[R\theta - R_1 \phi^1 - R_2 \phi^2\right] k_i, \tag{5.14}$$

$$u_{i,i} = 0, \tag{5.15}$$

$$\theta_{,t} + Pr\, u_i \theta_{,i} = HRw(1 - h(z)) + \Delta\theta, \tag{5.16}$$

$$\phi^1_{,t} + Pr\, u_i \phi^1_{,i} = H_1 R_1 w + \tau_1 \Delta \phi^1, \tag{5.17}$$

$$\phi^2_{,t} + Pr\, u_i \phi^2_{,i} = H_2 R_2 w + \tau_2 \Delta \phi^2, \tag{5.18}$$

where $h(z) = \dfrac{Q}{2}(1 - 2z)$ and $w = u_3$. The perturbation boundary conditions are

1. free–free boundary conditions,

$$w = \frac{\partial^2 w}{\partial z^2} = \theta = \phi_1 = \phi_2 = 0 \ \text{ at } \ z = 0, 1, \tag{5.19}$$

2. fixed–free boundary conditions,

$$\begin{aligned} \theta = \phi_1 = \phi_2 = 0 \ \text{ at } \ z = 0, 1, \\ w = \frac{\partial w}{\partial z} = 0 \ \text{ at } \ z = 0, \\ w = \frac{\partial^2 w}{\partial z^2} = 0 \ \text{ at } \ z = 1, \end{aligned} \tag{5.20}$$

3. fixed–fixed boundary conditions,

$$w = \frac{\partial w}{\partial z} = \theta = \phi^1 = \phi^2 = 0 \text{ at } z = 0, 1. \tag{5.21}$$

5.3 Linear stability analysis

Equations (5.14)–(5.18) are linearised by neglecting terms containing products of the perturbed quantities. A time dependence of $e^{\sigma t}$ is introduced by substituting

$$\begin{aligned} \mathbf{u}(\mathbf{x}, t) &= \mathbf{u}(\mathbf{x})e^{\sigma t}, \\ \theta(\mathbf{x}, t) &= \theta(\mathbf{x})e^{\sigma t}, \\ \phi^\alpha(\mathbf{x}, t) &= \phi^\alpha(\mathbf{x})e^{\sigma t} \quad (\alpha = 1, 2). \end{aligned}$$

In order to put the resulting system in a form like that of Pearlstein *et al.* (1989) the following transformations are made

$$R\theta \to \theta, R_\alpha \phi^\alpha \to \phi^\alpha, HR^2 \to R, H_\alpha R_\alpha^2 \to -R_\alpha,$$

resulting in

$$Pr^{-1}\,\sigma u_i = -\pi_{,i} + \Delta u_i + \theta k_i - \phi^1 k_i - \phi^2 k_i, \tag{5.22}$$

$$\sigma\theta = Rw(1 - h(z)) + \Delta\theta, \tag{5.23}$$

$$\sigma\phi^1 = -R_1 w + \tau_1 \Delta\phi^1, \tag{5.24}$$

$$\sigma\phi^2 = -R_2 w + \tau_2 \Delta\phi^2, \tag{5.25}$$

It will now be shown that the present system is the adjoint of the linearised version of the nonlinear buoyancy law problem studied by Straughan and Walker (1997). The adjoint, A^*, of an $n \times n$ matrix A is defined by the following relation

$$(\mathbf{x}, A\mathbf{y}) = (A^*\mathbf{x}, \mathbf{y}),$$

for all n-vectors $\mathbf{x}$ and $\mathbf{y}$. The inner product $(\mathbf{x}, \mathbf{y})$ is formed by multiplying together the corresponding elements of $\mathbf{x}$ and the conjugate of $\mathbf{y}$, $\bar{\mathbf{y}}$, summing the results and

integrating over the fluid layer $z \in (0,1)$. If the two systems can be shown to be adjoint then the eigenvalues of the present problem will be identical to that of Straughan and Walker (1997).

Equations (3.6) of Straughan and Walker (1997) are (specialising to the case of 2 salt fields)

$$Pr^{-1}\,\sigma u_i = -\pi_{,i} + \Delta u_i - 2M\theta k_i - \phi^1 k_i - \phi^2 k_i, \tag{5.26}$$

$$\sigma\theta = -Rw + \Delta\theta, \tag{5.27}$$

$$\sigma\phi^1 = -R_1 w + \tau_1 \Delta\phi^1, \tag{5.28}$$

$$\sigma\phi^2 = -R_2 w + \tau_2 \Delta\phi^2, \tag{5.29}$$

where $M(z) = \xi - z$, with $\xi = \dfrac{4}{T_u}$.

Notice first that the term $R(1-h)$ in equation (5.23) can be rearranged as follows:

$$R(1-h) = R(1 - \frac{Q}{2}(1-2z)) = R(1 - \frac{Q}{2} + Qz).$$

It will be shown shortly that only negative values of Q (i.e. an internal heat sink) allow the present system to be identified as the adjoint of the Straughan and Walker (1997) system . So, if we restrict attention to the case $Q < 0$ and set $J = -Q > 0$ then

$$\begin{aligned} R(1 - \frac{Q}{2} + Qz) &= \frac{RJ}{2}(\frac{2}{J} + 1 - 2z) \\ &= \hat{R}(2\xi - 2z) \\ &\equiv 2MR \end{aligned}$$

if we set

$$2\xi = \frac{2}{J} + 1, \qquad \hat{R} = \frac{JR}{2}. \tag{5.30}$$

If we make the identifications from equation (5.30) and then apply the transformation $\theta \to -\theta$ to equations (5.22) and (5.23) we get the following system

$$Pr^{-1}\,\sigma u_i = -\pi_{,i} + \Delta u_i - \theta k_i - \phi^1 k_i - \phi^2 k_i, \tag{5.31}$$

$$\sigma\theta = -2MRw + \Delta\theta, \tag{5.32}$$

$$\sigma\phi^1 = -R_1 w + \tau_1 \Delta\phi^1, \tag{5.33}$$

$$\sigma\phi^2 = -R_2 w + \tau_2 \Delta\phi^2. \tag{5.34}$$

The following transformations are made to equations (5.26)–(5.29) and also to equations (5.31)–(5.34) in order to allow us to identify one system as the adjoint of the other:

$$\theta \to R^{1/2}\theta, \phi^1 \to R_1^{1/2}\phi^1, \phi^2 \to R_2^{1/2}\phi^2,$$

and then

$$R^{1/2} \to R, R_1^{1/2} \to R_1, R_2^{1/2} \to R_2.$$

The resultant equations can then be written as, for the Straughan and Walker (1997) system,

$$\sigma B\Psi = A_{T^2}\Psi \tag{5.35}$$

where $B = \text{diag}(0, Pr^{-1}I, Pr^{-1}I, Pr^{-1}I, I, I, I), \Psi = (\pi, u, v, w, \theta, \phi^1, \phi^2)^T$ and

$$A_{T^2} = \begin{pmatrix} -\frac{\partial}{\partial x} & \Delta & 0 & 0 & 0 & 0 & 0 \\ -\frac{\partial}{\partial y} & 0 & \Delta & 0 & 0 & 0 & 0 \\ -\frac{\partial}{\partial z} & 0 & 0 & \Delta & -2MR & -R_1 & -R_2 \\ 0 & 0 & 0 & -R & \Delta & 0 & 0 \\ 0 & 0 & 0 & -R_1 & 0 & \tau_1\Delta & 0 \\ 0 & 0 & 0 & -R_2 & 0 & 0 & \tau_2\Delta \end{pmatrix},$$

while for the present internal heat sink system we have

$$\sigma B\Psi = A_Q\Psi, \tag{5.36}$$

with B and Ψ as before, and

$$A_Q = \begin{pmatrix} -\frac{\partial}{\partial x} & \Delta & 0 & 0 & 0 & 0 & 0 \\ -\frac{\partial}{\partial y} & 0 & \Delta & 0 & 0 & 0 & 0 \\ -\frac{\partial}{\partial z} & 0 & 0 & \Delta & -R & -R_1 & -R_2 \\ 0 & 0 & 0 & -2MR & \Delta & 0 & 0 \\ 0 & 0 & 0 & -R_1 & 0 & \tau_1\Delta & 0 \\ 0 & 0 & 0 & -R_2 & 0 & 0 & \tau_2\Delta \end{pmatrix}.$$

Now let subscripts (1) and (2) refer to two different solutions of equations (5.26)–(5.29) or (5.22)–(5.25). We form the inner product $(\Psi_{(1)}, A_{T^2}\Psi_{(2)})$ (with the intention of equating this to $(A_Q\Psi_{(1)}, \Psi_{(2)})$, thereby showing that A_Q is the adjoint of A_{T^2}). Integration by parts then yields

$$\begin{aligned}(\Psi_{(1)}, A_{T^2}\Psi_{(2)}) \;=\; & -(\nabla\mathbf{u}_{(1)}, \nabla\mathbf{u}_{(2)}) - 2R(w_{(1)}, M\theta_{(2)}) - R_1(w_{(1)}, \phi^1_{(2)}) - R_2(w_{(1)}, \phi^2_{(2)}) \\ & -R(\theta_{(1)}, w_{(2)}) - (\nabla\theta_{(1)}, \nabla\theta_{(2)}) \\ & -R_1(\phi^1_{(1)}, w_{(2)}) - \tau_1(\nabla\phi^1_{(1)}, \nabla\phi^1_{(2)}) \\ & -R_2(\phi^2_{(1)}, w_{(2)}) - \tau_2(\nabla\phi^2_{(1)}, \nabla\phi^2_{(2)}).\end{aligned} \tag{5.37}$$

In a similar manner it can be shown that

$$\begin{aligned}(A_Q\Psi_{(1)}, \Psi_{(2)}) \;=\; & -(\nabla\mathbf{u}_{(1)}, \nabla\mathbf{u}_{(2)}) - R(\theta_{(1)}, w_{(2)}) - R_1(\phi^1_{(1)}, w_{(2)}) - R_2(\phi^2_{(1)}, w_{(2)}) \\ & -2R(w_{(1)}M, \theta_{(2)}) - (\nabla\theta_{(1)}, \nabla\theta_{(2)}) \\ & -R_1(w_{(1)}, \phi^1_{(2)}) - \tau_1(\nabla\phi^1_{(1)}, \nabla\phi^2_{(2)}) \\ & -R_2(w_{(1)}, \phi^2_{(2)}) - \tau_2(\nabla\phi^2_{(1)}, \nabla\phi^2_{(2)}).\end{aligned} \tag{5.38}$$

Close inspection will show equations (5.37) and (5.38) to be identical. So, by making the identifications in (5.30) we have shown the linearised version of the nonlinear buoyancy law problem of Straughan and Walker (1997) to be the adjoint of the present linearised internal heat sink problem. Equation (5.30) allows the following table of comparisons to be deduced:

Upper temperature in T^2 problem	Strength of heat sink in Q problem
4	-2
5	-3.33
6	-6
7	-14
8	no equivalence

The method used to solve equations (5.22)–(5.25) is now described. The pressure term is eliminated by taking curlcurl of equations (5.22) and then selecting the third

component. This gives

$$
\begin{aligned}
-Pr^{-1}\sigma\Delta w &= -\Delta^2 w - \Delta^*\theta + \Delta^*\phi^1 + \Delta^*\phi^2, && (5.39)\\
\sigma\theta &= Rw(1-h(z)) + \Delta\theta, && (5.40)\\
\sigma\phi^1 &= -R_1 w + \tau_1\Delta\phi^1, && (5.41)\\
\sigma\phi^2 &= -R_2 w + \tau_2\Delta\phi^2. && (5.42)
\end{aligned}
$$

A normal mode representation is assumed, i.e.

$$
\begin{aligned}
w &= W(z)\exp[i(mx+ny)], && (5.43)\\
\theta &= \Theta(z)\exp[i(mx+ny)], && (5.44)\\
\phi^1 &= \Phi^1(z)\exp[i(mx+ny)], && (5.45)\\
\phi^2 &= \Phi^2(z)\exp[i(mx+ny)], && (5.46)
\end{aligned}
$$

and the system becomes

$$
\begin{aligned}
Pr^{-1}\sigma(D^2-k^2)W &= (D^2-k^2)^2 W - k^2\Theta + k^2\Phi^1 + k^2\Phi^2, && (5.47)\\
\sigma\Theta &= RW(1-h(z)) + (D^2-k^2)\Theta, && (5.48)\\
\frac{\sigma}{\tau_1}\Phi^1 &= -\frac{R_1}{\tau_1}W + (D^2-k^2)\Phi^1, && (5.49)\\
\frac{\sigma}{\tau_2}\Phi^2 &= -\frac{R_2}{\tau_2}W + (D^2-k^2)\Phi^2, && (5.50)
\end{aligned}
$$

where $D = \dfrac{d}{dz}$ and $k^2 = m^2 + n^2$ is a wavenumber. The boundary conditions are

1. free–free boundary conditions,

$$W = D^2 W = \Theta = \Phi_1 = \Phi_2 = 0 \text{ at } z = 0, 1, \qquad (5.51)$$

2. fixed–free boundary conditions,

$$
\begin{aligned}
&\Theta = \Phi_1 = \Phi_2 = 0 \text{ at } z = 0, 1,\\
&W = DW = 0 \text{ at } z = 0, \qquad (5.52)\\
&W = D^2 W = 0 \text{ at } z = 1,
\end{aligned}
$$

3. fixed–fixed boundary conditions,

$$W = DW = \Theta = \Phi^1 = \Phi^2 = 0 \text{ at } z = 0, 1. \tag{5.53}$$

A Chebyshev tau method was used to solve this system. Details can be found in Appendix A. Numerical results follow in the next section.

Before we present the results notice that it is straightforward to show that equations (5.47)–(5.50) remain unchanged under the transformations $Q \to -Q$ and $z \to 1 - z$. For free-free and fixed–fixed boundaries the $z \to 1 - z$ transformation has no noticeable effect — the boundaries may have interchanged but since the boundary conditions are identical this does not matter. So, in the free–free and fixed–fixed cases one can expect identical results whether working with a heat source or a heat sink. However, for the other case, fixed–free, the transformation $z \to 1 - z$ does have a discernible effect. The boundary conditions transform as

$$W(0) = DW(0) = 0 \to W(1) = DW(1) = 0,$$

while

$$W(1) = D^2W(1) = 0 \to W(0) = D^2W(0) = 0.$$

Clearly the transformed system is different from the original, the boundary conditions being for a free–fixed rather than fixed–free problem.

So, to summarise the work of this section, we have shown the present linearised internal heat sink problem to be the adjoint of the linearised quadratic buoyancy law problem of Straughan and Walker (1997). We have also shown that the heat source and sink problems are equivalent when the boundary conditions at the upper and lower boundaries are identical. The heat source and sink problems are not equivalent, however, when dealing with mixed boundary conditions. The numerical results following reflect these facts.

5.4 Results

5.4.1 Free–free boundary conditions

As described in section 5.2 this problem is precisely analogous to that of Straughan and Walker (1997). Clearly, identical results would be expected. In order to check

the veracity of the numerical method some of the results of Straughan and Walker (1997) are reproduced.

Straughan and Walker (1997) use the following parameters, first investigated by Pearlstein *et al.* (1989):

$$R_2 = 814.1119, \tau_1 = 0.22, \tau_2 = 0.21, Pr = 10.2.$$

In the non–penetrative work of Pearlstein *et al.* (1989) these values, with $R_1 = -945$, give rise to a perfectly symmetric heart–shaped oscillatory neutral curve lying beneath the stationary curve. These values result in a steady state that is gravitationally stabilising in the first salt field and destabilizing in the second salt field. Here, $R_1 = -945$ and $Q = 2$ (analogous to $T_1 = 4°C$) give an oscillatory curve that is slightly skewed away from symmetry (shown in figure 5.2). As in chapters 2 and 4, three critical Rayleigh numbers are required to describe the linear stability criteria. The skewing that has resulted from the internal heat source term means that the situation envisaged by Pearlstein *et al.* (1989) whereby oscillatory convection occurs at a given thermal Rayleigh number but differing wavenumbers at the twin maxima on the heart–shaped curve is not recovered here.

As the penetrative effect is increased (by increasing Q) the skewing effect becomes more noticeable (figures 5.2 and 5.3). At $Q = 14$ an effect similar to that found by Straughan and Walker (1997) (and described in chapter 3 for the equivalent porous problem) at $T_1 = 7°C$ is found. For $R_1 = -956$ the minimum on the oscillatory curve is less than the minimum on the stationary curve but at $R_1 = -950.5$ the minimum on the stationary curve is smaller. At some value of $R_1 \in (-956, -950.5)$ the minima should occur at the same Rayleigh number. This value was calculated to be

$$R_1 = -950.965$$

with

$$R_{\min} = 822.6$$

and

$$k_{\text{osc}} = 2.27, \quad k_{\text{stat}} = 2.66.$$

[In fact, for

$$R_1 = -950.965,$$

$$R_{\min}^{\text{osc}} = 822.593, \quad k^{\text{osc}} = 2.27,$$

$$R_{\min}^{\text{stat}} = 822.598 \quad k^{\text{stat}} = 2.66,$$

while, for

$$R_1 = -950.964$$

$$R_{\min}^{\text{osc}} = 822.605, \quad k^{\text{osc}} = 2.27,$$

$$R_{\min}^{\text{stat}} = 822.595, \quad k^{\text{stat}} = 2.66.]$$

By scaling the Rayleigh number here by the factor $J/2$ described in 5.2, identical results to Straughan and Walker (1997) may be obtained.

As expected the sign of Q has no effect on the critical Rayleigh numbers — the heat source and sink problems are equivalent. The W and Θ eigenfunctions shown in figure 5.4 reflect this equivalence — the transformation $z \to 1 - z$ interchanges the source and sink eigenfunctions.

5.4.2 Fixed–free boundary conditions

The lower boundary $z = 0$ is now held fixed. In order to find disconnected oscillatory curves lower values of R_1 than in section 5.4.1 have to be investigated, i.e. the stabilising effect of the first salt field needs to be greater to produce the disconnected curves. The thermal Rayleigh numbers at which instability occurs are also greater than for the free–free case.

Similar results to section 5.4.1 are found, namely the existence of disconnected oscillatory neutral curves. These curves (figures 5.5 and 5.6) are clearly skewed again. As the penetrative effect is increased the departure from a symmetric shape becomes more pronounced. At $Q = 14$, as before, the parameters can be arranged so that the minima on the oscillatory and stationary curves are at the same Rayleigh numbers. For this problem the minima on the oscillatory and stationary curves coincide for

$$R_1 = -979.758$$

with

$$R_{\min} = 909.9$$

and

$$k_{\text{osc}} = 2.62, \quad k_{\text{stat}} = 2.87.$$

[In fact, for

$$R_1 = -979.758,$$

$$R_{\min}^{\text{osc}} = 909.930, \quad k^{\text{osc}} = 2.62,$$

$$R_{\min}^{\text{stat}} = 909.935 \quad k^{\text{stat}} = 2.87,$$

while, for

$$R_1 = -979.757$$

$$R_{\min}^{\text{osc}} = 909.947, \quad k^{\text{osc}} = 2.62,$$

$$R_{\min}^{\text{stat}} = 909.933, \quad k^{\text{stat}} = 2.87. \ ]$$

For all values of Q considered, the wavenumbers at which instability occurs are larger than for the free–free problem.

Here, as expected, the heat sink results are different from the heat source problem. Some sink R–k neutral curves are shown in figures 5.7 and 5.8. It is noticeable that the oscillatory curve is more skewed than in the source problem and the twin minima effect can be recovered for $Q = -6$, i.e. the sink does not have to be as strong as the source to produce this effect.

5.4.3 Fixed–fixed boundary conditions

Now both lower and upper boundaries are held fixed. For the same values of R_2, τ_1 and τ_2 as before disconnected oscillatory neutral curves are not found (see figures 5.9 and 5.10). The oscillatory curve is a single–valued curve attached to the stationary curve at two points. As R_1 is increased these points move closer together until eventually the oscillatory curve disappears and only stationary instability is found. As the penetrative effect is increased the oscillatory curves can be seen to become more and more skewed but disconnected curves are still not found. The critical thermal Rayleigh numbers and wavenumbers at which instability occurs are greater

then in sections 5.4.1 and 5.4.2. This is to be expected from the work of Lopez *et al.* (1990). For values of the transport parameters close to those of Pearlstein *et al.* (1990) they obtained instability at a thermal Rayleigh number of approximately 3000 as compared to the free–free values of about 1000 from Pearlstein *et al.* (1990).

As in the free–free case the eigenvalues are identical for both the heat source and heat sink problems.

5.5 Convection in a box

In order to produce a problem which may be able to be replicated experimentally, the effect of adiabatic impenetrable sidewalls is now investigated. We will investigate the internal heat source problem in a rectangular box where the fluid is allowed to slip on the sidewalls. Following the method of Rosenblat, Homsy and Davis (1982), the boundary conditions on the sidewalls are, for perturbation variables defined as in (5.13),

$$u = w_x = v_x = \theta_x = \phi^1_x = \phi^2_x = 0 \quad \text{on} \quad x = 0, a_1, \quad 0 \le y \le a_2, \quad 0 \le z \le 1, \tag{5.54}$$

$$v = w_y = u_y = \theta_y = \phi^1_y = \phi^2_y = 0 \quad \text{on} \quad y = 0, a_2, \quad 0 \le x \le a_1, \quad 0 \le z \le 1. \tag{5.55}$$

Rather than the normal mode expansion of (5.43)–(5.46) we now seek separable solutions of form

$$w = W(z)\cos\left(\frac{m_1\pi x}{a_1}\right)\cos\left(\frac{m_2\pi y}{a_2}\right), \tag{5.56}$$

$$\theta = \Theta(z)\cos\left(\frac{m_1\pi x}{a_1}\right)\cos\left(\frac{m_2\pi y}{a_2}\right), \tag{5.57}$$

$$\phi^1 = \Phi^1(z)\cos\left(\frac{m_1\pi x}{a_1}\right)\cos\left(\frac{m_2\pi y}{a_2}\right), \tag{5.58}$$

$$\phi^2 = \Phi^2(z)\cos\left(\frac{m_1\pi x}{a_1}\right)\cos\left(\frac{m_2\pi y}{a_2}\right), \tag{5.59}$$

where m_1 and m_2 run over all non–negative integers.

The inclusion of the sidewalls produces the same governing equations, namely

(5.22)–(5.25), but with k replaced by an effective wavenumber λ defined by

$$\lambda^2 = \left[\left(\frac{m_1}{a_1}\right)^2 + \left(\frac{m_2}{a_2}\right)^2\right]\pi^2. \tag{5.60}$$

Numerically, we fix a_1 and a_2 and restrict the wavenumber to values satisfying (5.60) for some pair of values (m_1, m_2).

5.5.1 Convection in a box – results

With a view to future work (including the effects of surface tension at the upper boundary) attention is focussed on the fix-free sink problem.

Figure 5.11 shows the critical Rayleigh number, minimised over the wavenumber, as a function of a_1 for fixed $a_2 = 1$. The other parameters are held fixed at $Q = -6, Pr = 10.2, R_1 = -987.271, R_2 = 814.1119, \tau_1 = 0.22, \tau_2 = 0.21$. The figure shows the sequence of modes $m_2 = 0, m_1 = 1, 2, 3, 4$. The mode having the lowest critical Rayleigh number is clearly dependent on box size. The "kink" region at the minima on each of the curves indicates the mode of instability switching between stationary and oscillatory onset. Notice that the minima on these curves occurs at 1975.2 — the value for an infinite layer. Away from these minima the sidewalls have a stabilizing effect.

For sufficiently large box sizes one can recover the twin minima effect. Figure 5.12 shows a section of the R–λ neutral curve for $a_1 = a_2 = 6$ and $Q = -6, Pr = 10.2, R_1 = -987.03, R_2 = 814.1119, \tau_1 = 0.22, \tau_2 = 0.21$. The twin minima effect is again recovered at

$$R = 1976.5, \quad \lambda^{\text{osc}} = 2.6698, \quad \lambda^{\text{stat}} = 3.0531.$$

Conclusions

In this chapter it has been shown the linearised internal heat sink problem is the adjoint of the linearised quadratic buoyancy law problem studied by Straughan and Walker (1997). The relationship between the heat source and sink problems has also been explained. It has been shown that the inclusion of adiabatic sidewalls will have a stabilizing effect and that the twin minima effect can be recovered. This last result

is, I believe, worthy of experimental investigation. It is unlikely that one would be able to obtain the critical values of the stability parameters to sufficient accuracy as to observe convection occurring simultaneously at two different wavenumbers. However, it should be possible to set up an experiment where increasing R_1 causes the mode of instability to change from oscillatory convection at a small wavenumber to stationary convection at a larger wavenumber.

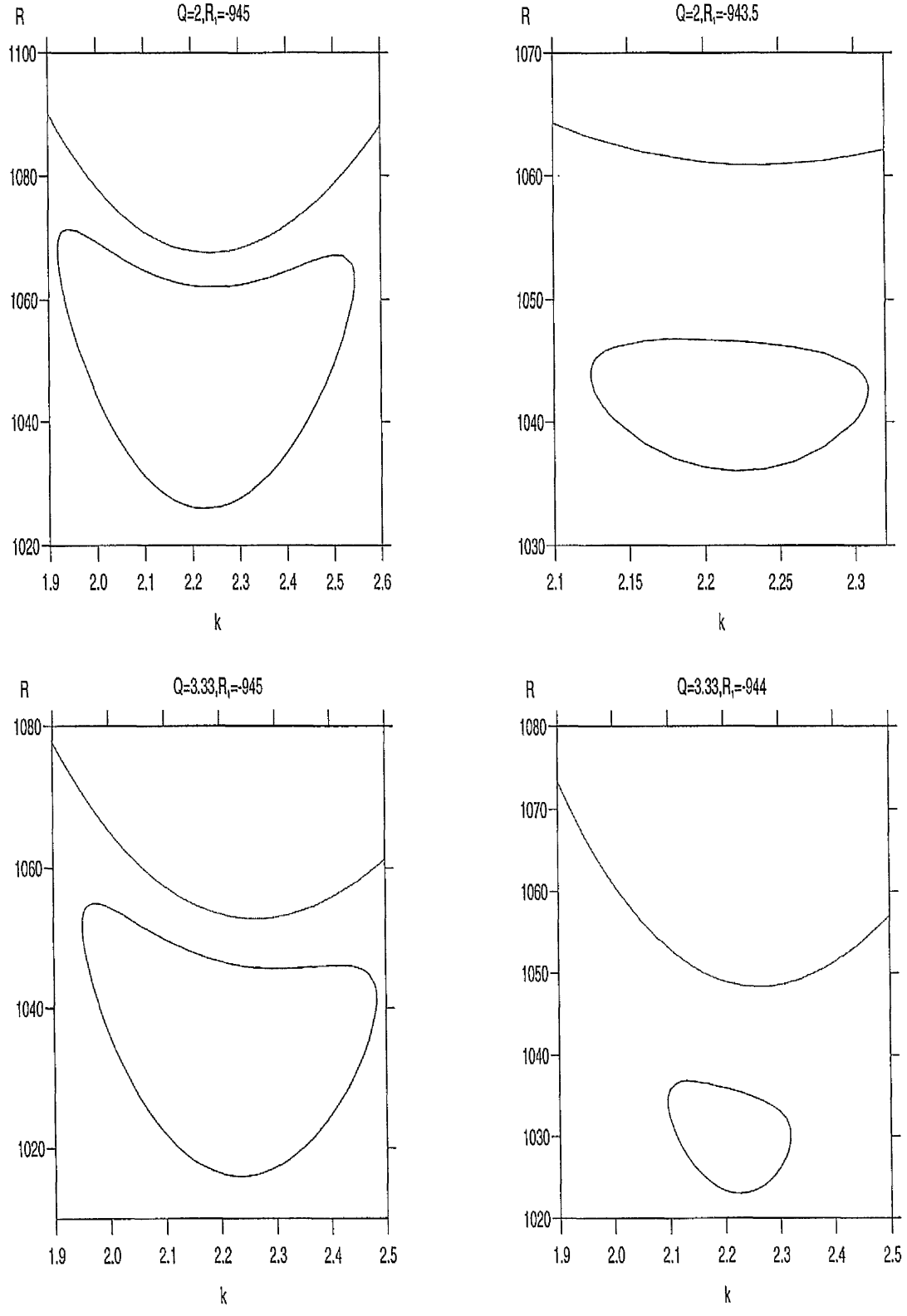

Figure 5.2: Some R–k neutral curves for free–free boundary conditions for the parameters $R_2 = 814.1119, \tau_1 = 0.22, \tau_2 = 0.21, Pr = 10.2$. The positive values of Q denote an internal heat *source*.

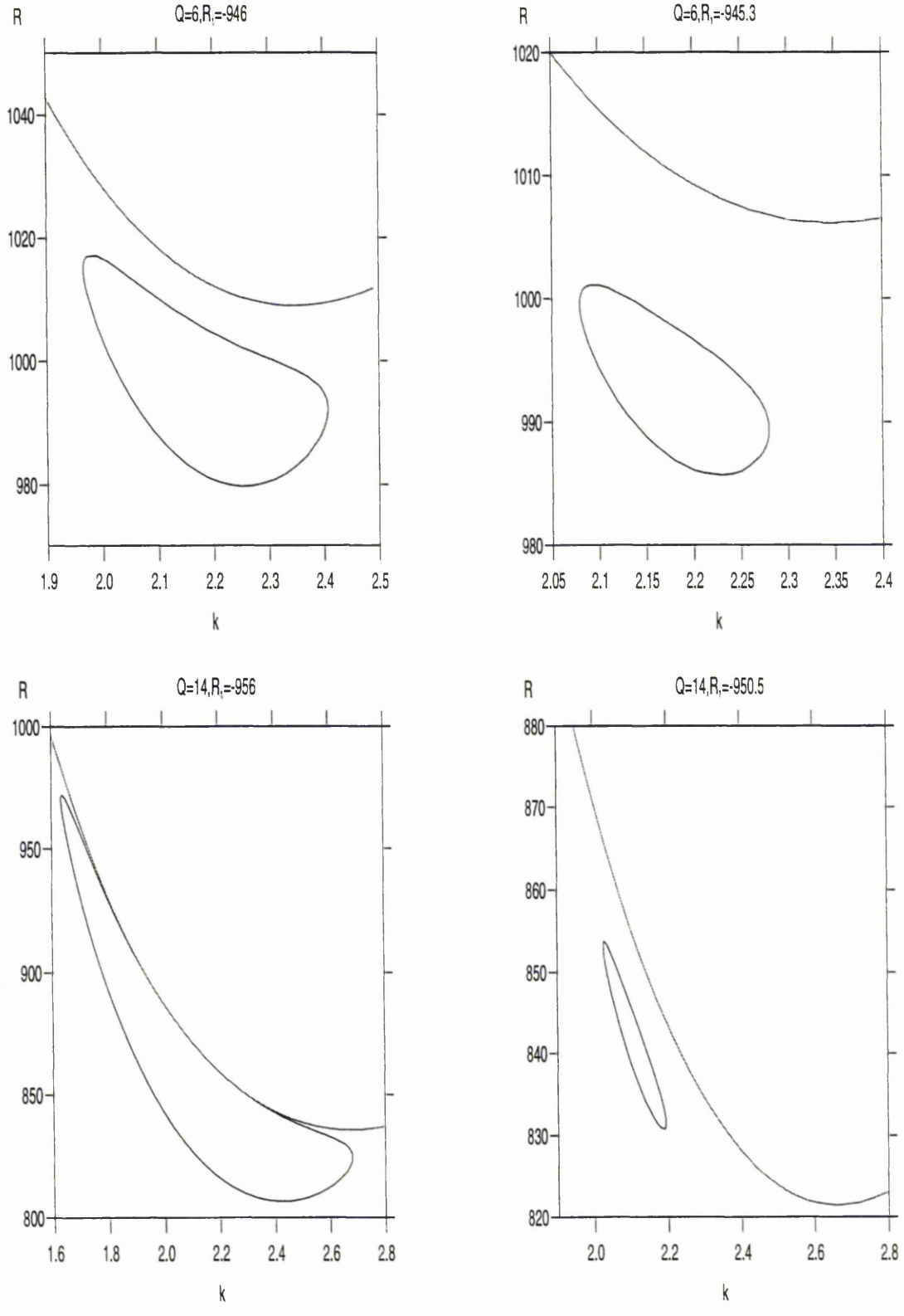

Figure 5.3: Some R–k neutral curves for free–free boundary conditions for the parameters $R_2 = 814.1119, \tau_1 = 0.22, \tau_2 = 0.21, Pr = 10.2$. The positive values of Q denote an internal heat *source*.

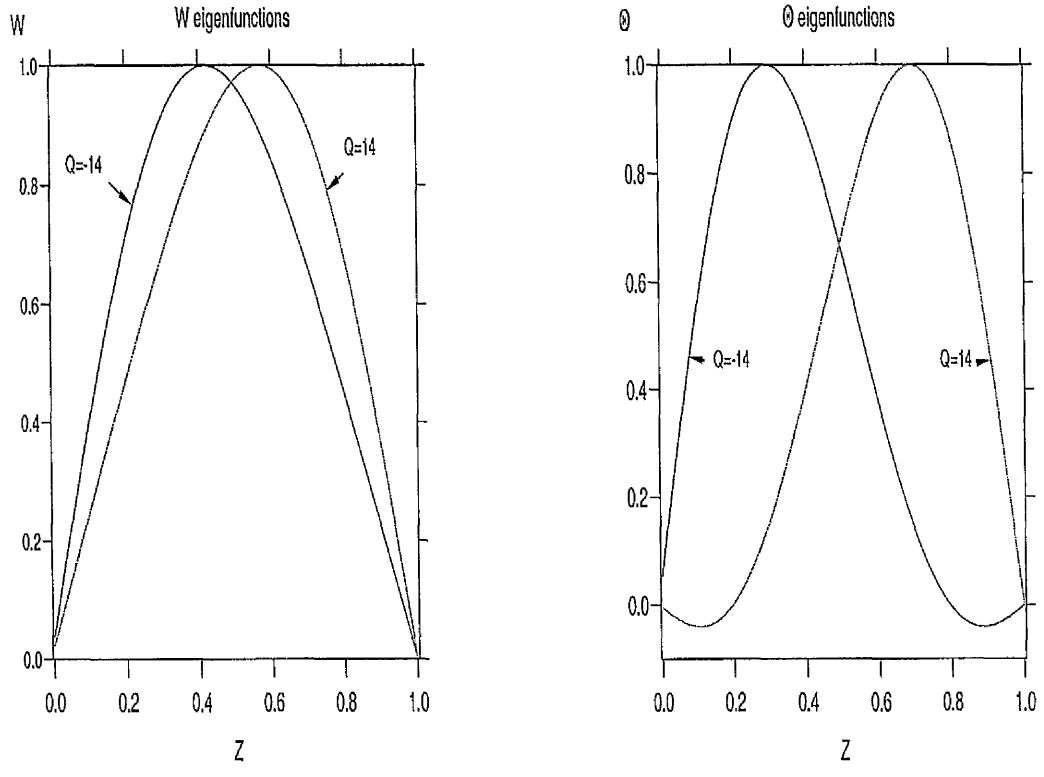

Figure 5.4: W and Θ eigenfunctions for free–free boundary conditions for the parameters $k = 2.27, R = 822.606, R_1 = -950.965, R_2 = 814.1119, \tau_1 = 0.22, \tau_2 = 0.21, Pr = 10.2$. Notice that the source and sink eigenfunctions interchange under the transformation $z \to 1 - z$.

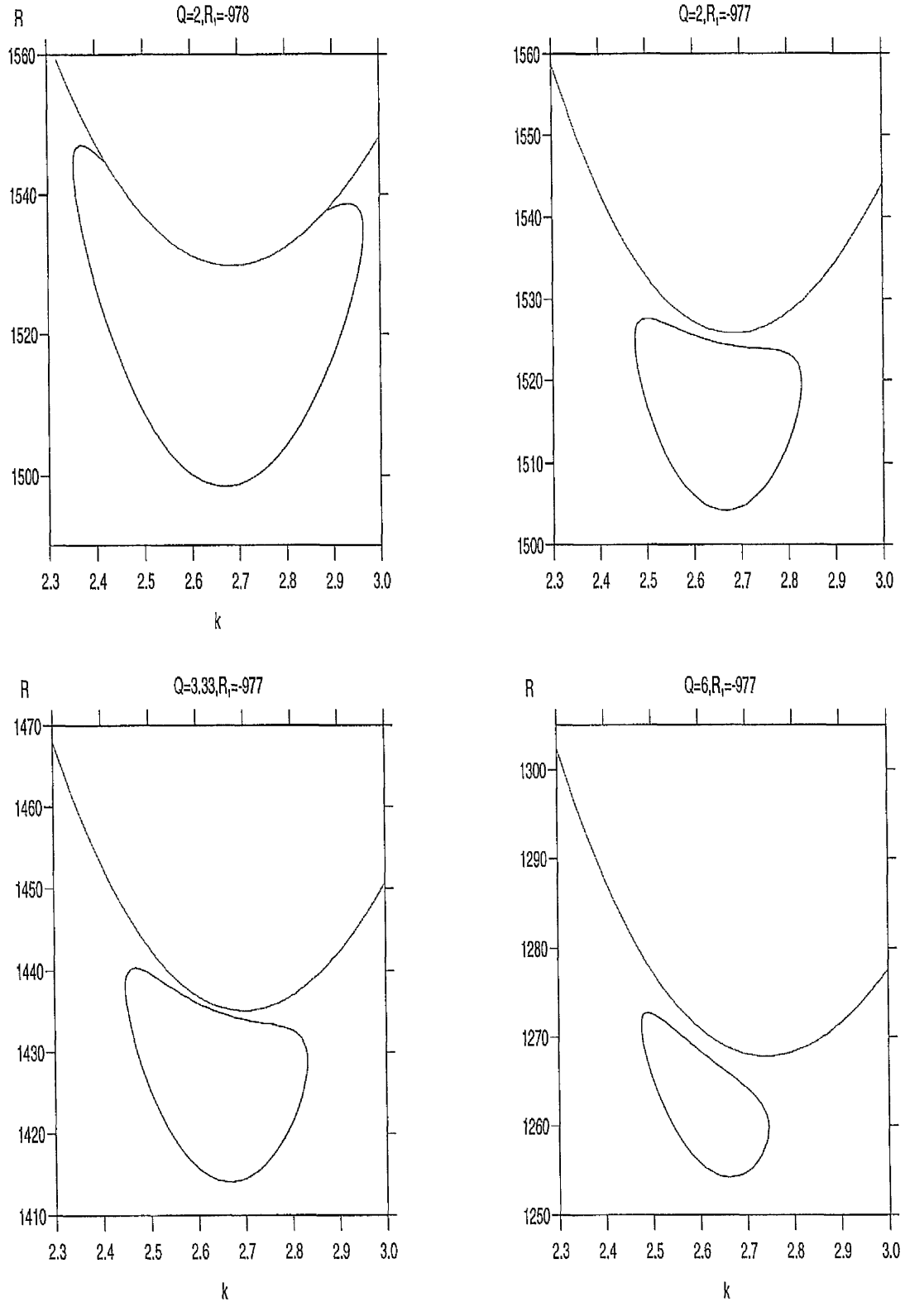

Figure 5.5: Some R–k neutral curves for fixed–free boundary conditions for the parameters $R_2 = 814.1119, \tau_1 = 0.22, \tau_2 = 0.21, Pr = 10.2$. The positive values of Q denote an internal heat *source*.

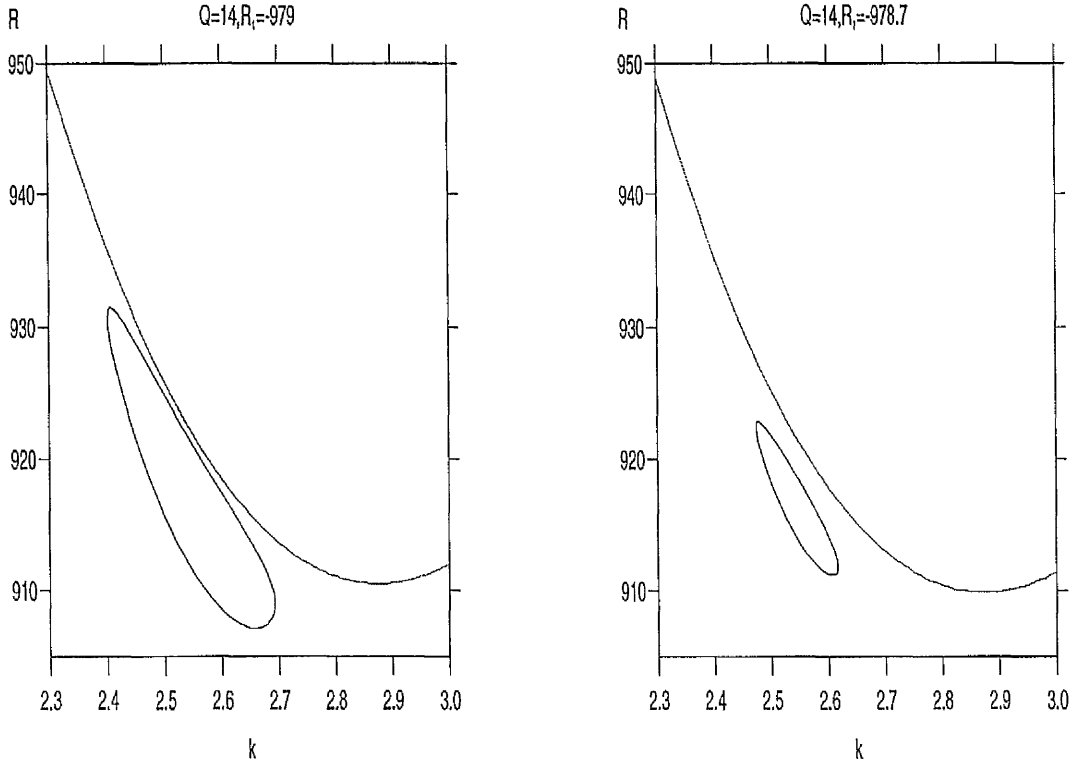

Figure 5.6: Some R–k neutral curves for fixed–free boundary conditions for the parameters $R_2 = 814.1119, \tau_1 = 0.22, \tau_2 = 0.21, Pr = 10.2$. The positive values of Q denote an internal heat *source*.

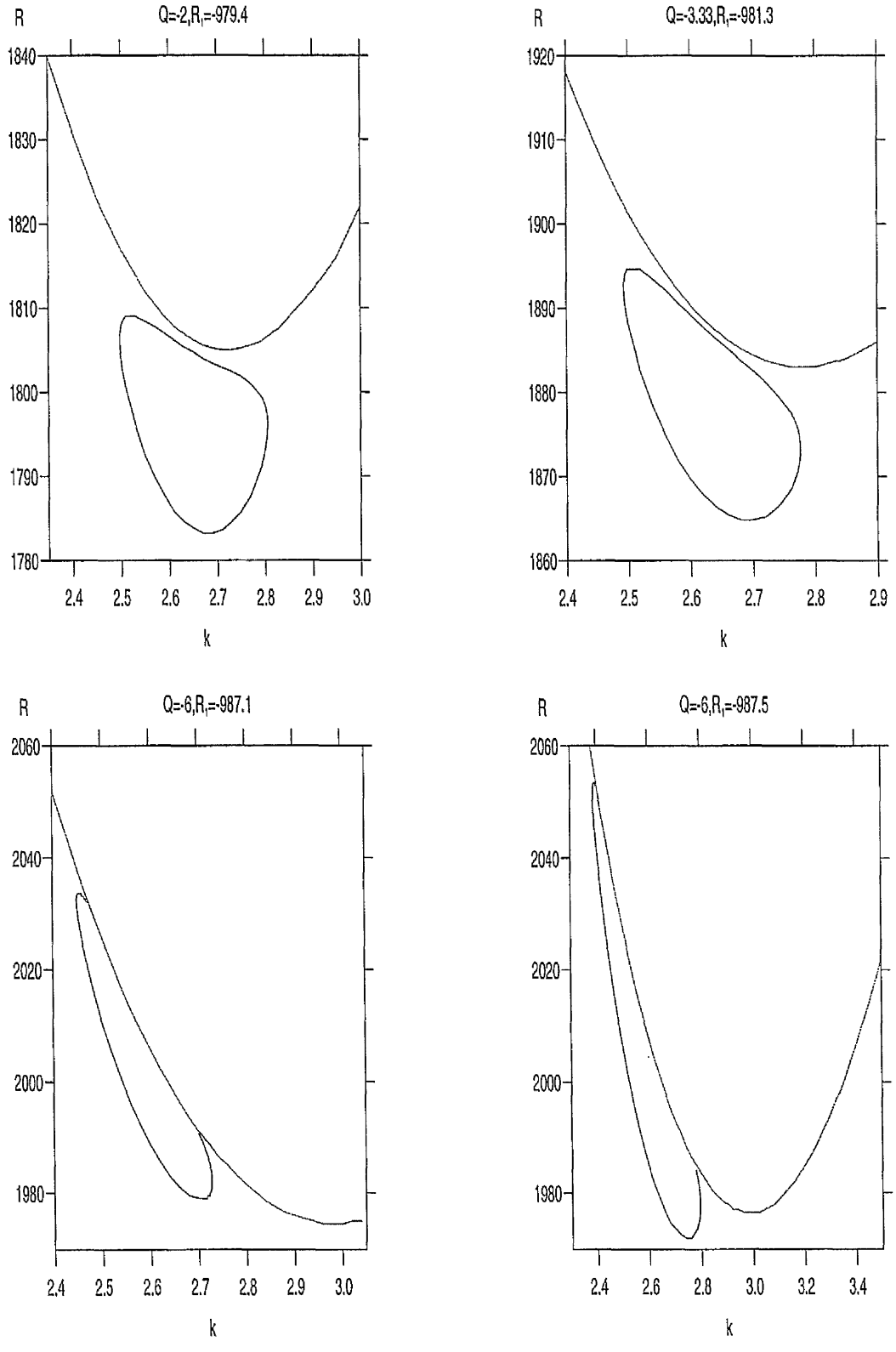

Figure 5.7: Some R-k neutral curves for fixed–free boundary conditions for the parameters $R_2 = 814.1119, \tau_1 = 0.22, \tau_2 = 0.21, Pr = 10.2$. The negative values of Q denote an internal heat *sink*.

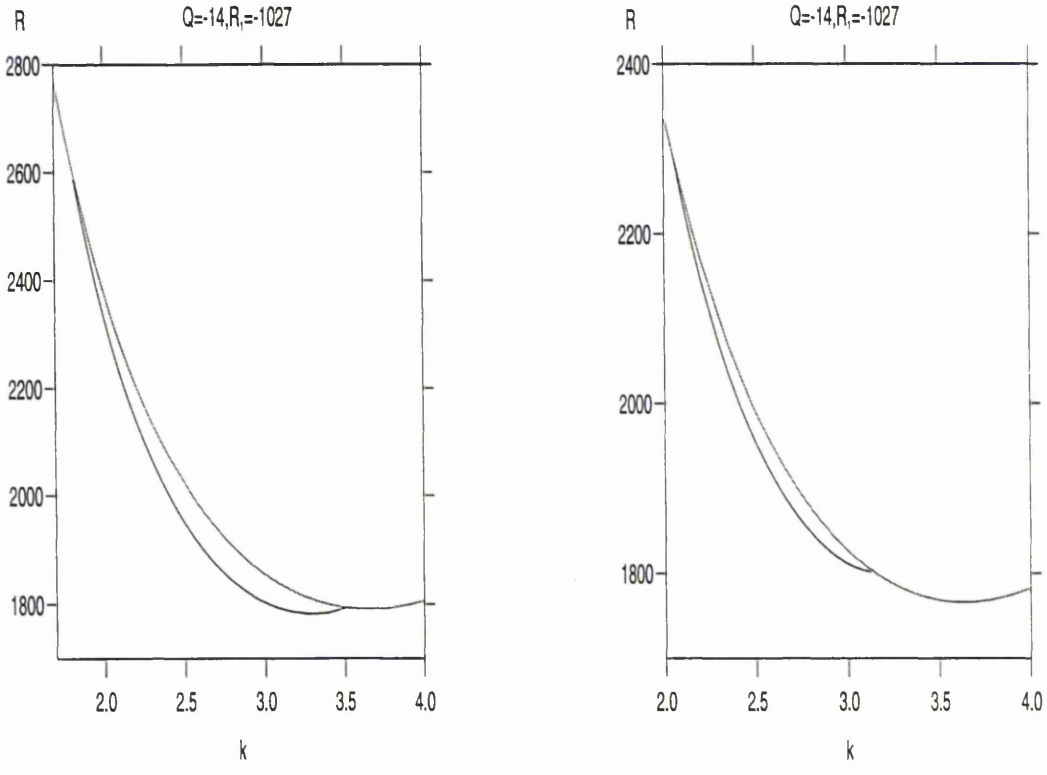

Figure 5.8: Some R-k neutral curves for fixed–free boundary conditions for the parameters $R_2 = 814.1119, \tau_1 = 0.22, \tau_2 = 0.21, Pr = 10.2$. The negative values of Q denote an internal heat *sink*.

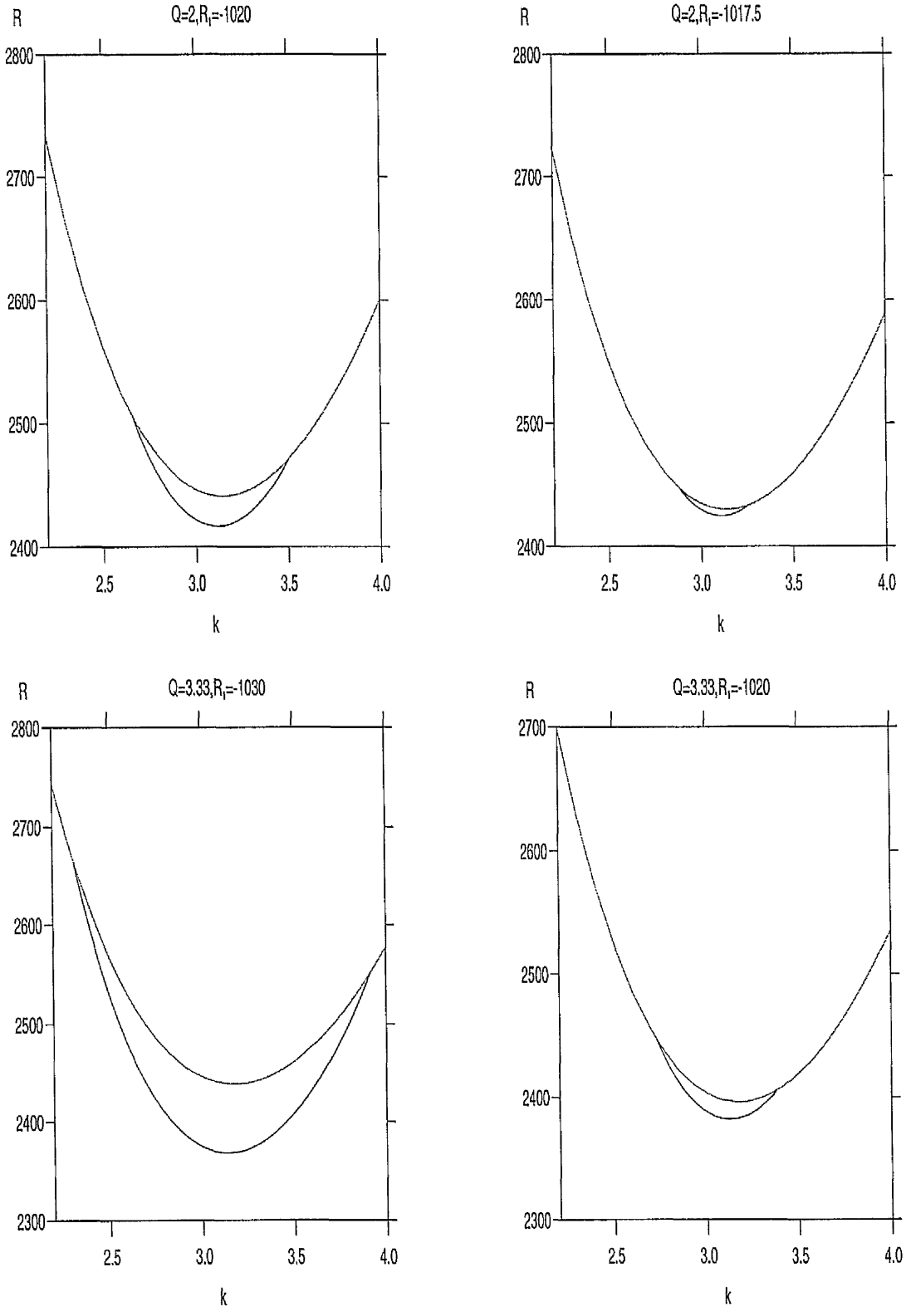

Figure 5.9: Some R-k neutral curves for fixed–fixed boundary conditions for the parameters $R_2 = 814.1119, \tau_1 = 0.22, \tau_2 = 0.21, Pr = 10.2$. The positive values of Q denote an internal heat *source*.

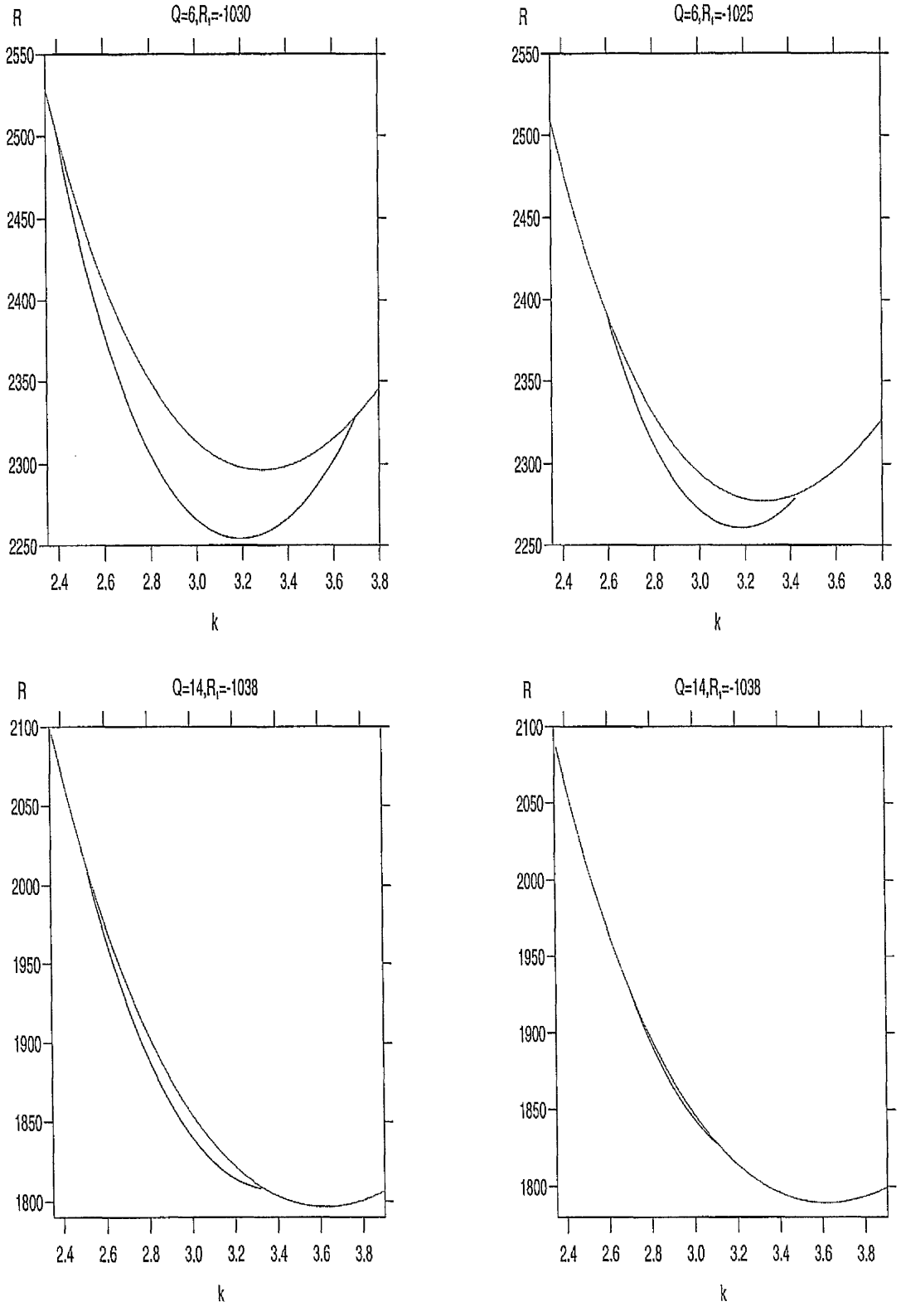

Figure 5.10: Some R-k neutral curves for fixed–fixed boundary conditions for the parameters $R_2 = 814.1119, \tau_1 = 0.22, \tau_2 = 0.21, Pr = 10.2$. The positive values of Q denote an internal heat *source*.

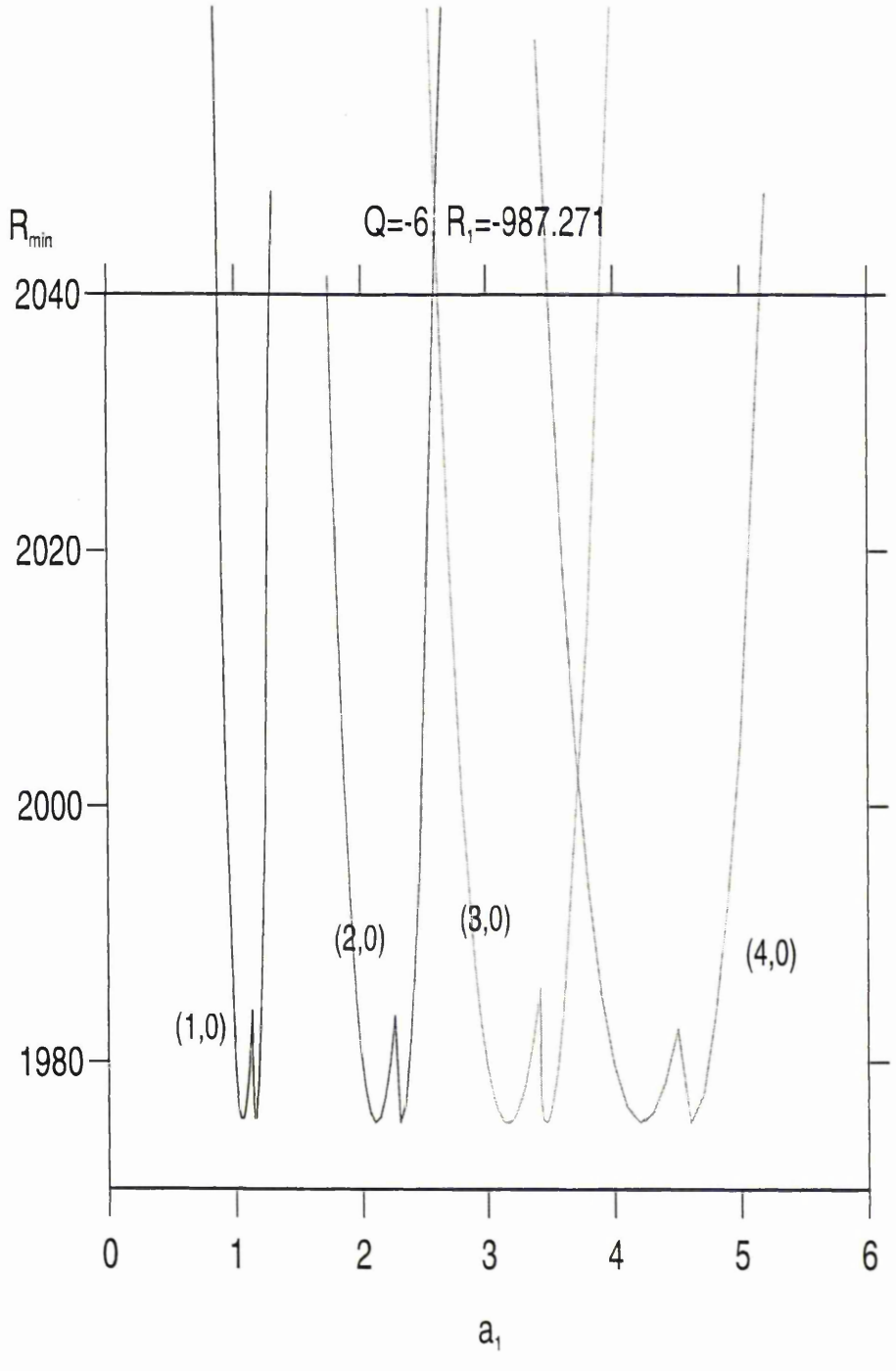

Figure 5.11: Plot of the critical Rayleigh number, minimised over the wavenumber λ against box dimension a_1 for fixed $a_2 = 1$ and $Q = -6, Pr = 10.2, R_1 = -987.271, R_2 = 814.1119, \tau_1 = 0.22, \tau_2 = 0.21$. The pairs (m_1, m_2) denote the integral number of cycles in (a_1, a_2).

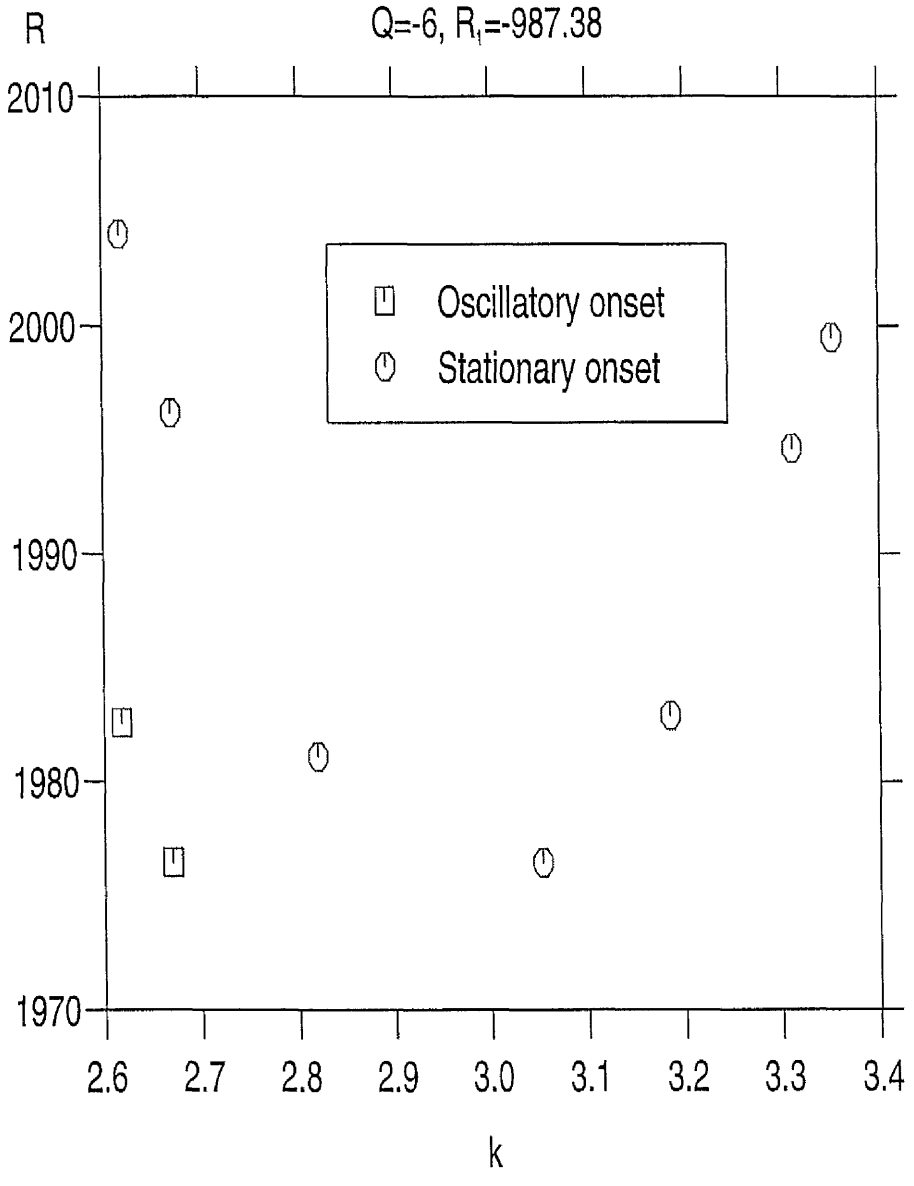

Figure 5.12: A section of the R–λ neutral curves for $a_1 = a_2 = 6$ and $Q = -6, Pr = 10.2, R_1 = -987.03, R_2 = 814.1119, \tau_1 = 0.22, \tau_2 = 0.21$.

Concluding remarks

In this thesis analytical and numerical techniques have been employed to investigate the stability of a variety of multi–component convection–diffusion problems. The most intriguing result is the effect seen in chapters 4 and 5 whereby the onset of linear instability occurs via stationary and oscillatory modes at two differing wavenumbers but the same thermal Rayleigh number. It is an interesting question whether this effect would be seen experimentally.

There is considerable scope for further extension of this work. The internal heat source problem of chapter 5, in particular, can be investigated in much more detail. One could include the effect of surface tension in the upper boundary. The number of parameters involved – three Rayleigh numbers, the Prandtl number, two diffusivity ratios, three Marangoni numbers and three radiation constants – clearly make a full investigation of this problem a time–consuming affair. Recently Chen and Su (1992) have considered this problem with one salt field. They find two distinct regimes, one where double diffusive effects dominate and another in which the effect of surface tension is more prevalent. The inclusion of surface tension and sidewalls would produce a physically realistic problem. If the numerical results again predicted the twin minima effect then this may merit experimental investigation.

One could also attempt to replicate the generalised energy stability analysis of chapter 3 for the penetrative convection problems in chapters 4 and 5. Indeed, the results of chapter 3 themselves may possibly be improved by alternative choices for the generalised variables.

Another avenue for future exploration is to include further salt fields. For the non–penetrative fluid problem Terrones and Pearlstein (1989) have considered the effect of four salt fields. Interestingly, they find *two* disconnected oscillatory neutral

curves as well as the stationary onset curve. This offers a variety of possibilities when extended to include penetrative convection. For instance, one could find instability occurring at three different wavenumbers, two via an oscillatory mechanism and one stationary.

As we have considered both porous and fluid problems one could find further research studying a fluid layer lying above a fluid–saturated porous layer. This would have applications in modelling the beds of seas and lakes. Would the twin minima effect still be found here?

Appendix A

The Chebyshev tau method

The Chebyshev tau method gained much prominence after the seminal paper of Orszag (1971), who obtained accurate solutions of the Orr–Sommerfeld equation. Since then the method has found widespread use in solving eigenvalue problems. One weakness of the Chebyshev tau method is the possible occurrence of spurious eigenvalues and several papers have attempted to resolve this problem, e.g. Gardner *et al.* (1989), McFadden *et al.* (1990), Lindsay and Ogden (1992) and Straughan and Walker (1996). In section A.1 the method of Straughan and Walker (1996) is applied to the eigenvalue problem (4.16)–(4.20). However, this method is restricted to free boundary conditions. Consequently, another method is required for chapter 5 where fixed boundaries are considered. This method is similar to that of Orszag (1971) and is described in section A.2.

A.1 A Chebyshev tau method for system (4.16)–(4.20)

The technique used to solve system (4.16)–(4.20) is described in detail in Straughan and Walker (1996).

Commence by defining the operators L_1, L_2, L_3 and L_4 by

$$\begin{aligned} L_1 u &= (D^2 - k^2)W - 2(\xi - z)k^2\Theta - k^2\Phi^1 - k^2\Phi^2, \\ L_2 u &= (D^2 - k^2)\Theta - RW - \sigma\Theta, \\ L_3 u &= (D^2 - k^2)\Phi^1 - R_1 W - P_1\sigma\Phi^1, \\ L_4 u &= (D^2 - k^2)\Phi^2 - R_2 W - P_2\sigma\Phi^2, \end{aligned} \tag{A1}$$

where u denotes the vector $(W, \Theta, \Phi^1, \Phi^2)^T$. The system is transformed to the interval (-1,1) and the problem to be solved is now

$$L_\alpha u = 0, \quad \alpha = 1, 2, 3, 4, \tag{A2}$$

with the boundary condition

$$W = \Theta = \Phi^1 = \Phi^2 = 0 \ \text{ at } \ z = -1, 1. \tag{A3}$$

Straughan and Walker (1996) advocate writing the equations as a system of second order equations. This lowering of order reduces the problem of round off error due to the growth of matrix terms. In the present work the individual equations in (A2) are already second order and so this problem does not arise.

Next, the variables $W, \Theta, \Phi^1, \Phi^2$ are represented as finite series of Chebyshev polynomials

$$\begin{aligned} W &= \sum_{l=0}^{N+2} W_l T_l(z), \\ \Theta &= \sum_{l=0}^{N+2} \Theta_l T_l(z), \\ \Phi^1 &= \sum_{l=0}^{N+2} \Phi_l^1 T_l(z), \\ \Phi^2 &= \sum_{l=0}^{N+2} \Phi_l^2 T_l(z), \end{aligned} \tag{A4}$$

where it is understood that (A4) are truncations of infinite series. Due to this truncation the problem to be solved is now

$$\begin{aligned} L_1 u &= \tau_1 T_{N+1} + \tau_2 T_{N+2}, \\ L_2 u &= \hat{\tau}_1 T_{N+1} + \hat{\tau}_2 T_{N+2}, \\ L_3 u &= \bar{\tau}_1 T_{N+1} + \bar{\tau}_2 T_{N+2}, \\ L_4 u &= \tilde{\tau}_1 T_{N+1} + \tilde{\tau}_2 T_{N+2}, \end{aligned} \tag{A5}$$

where the tau coefficients may be used to indicate the size of the error associated with the truncation in (A4) c.f. Gardner *et al.* (1989).

As a brief aside, it has been brought to my attention by Dr Kenneth Lindsay that equation $(A5)_1$ should perhaps contain another residual term, i.e.

$$L_1 u = \tau_1 T_{N+1} + \tau_2 T_{N+2} + \tau_3 T_{N+3}. \tag{A6}$$

His argument arises from the $z\Theta$ term in equation $(A1)_1$. With the approximation of $(A4)_2$ this is

$$z\Theta = \sum_{l=0}^{N+2} z\Theta_l T_l(z) = \Theta_0 T_0 T_1 + \Theta_1 T_1^2 + \frac{1}{2}\sum_{l=2}^{N+2} \Theta_l \left(T_{l-1} + T_{l+1}\right).$$

The problem arise from the very last term i.e.

$$z\Theta = \Theta_0 T_0 T_1 + \ldots + \frac{1}{2}\Theta_{N+2}\left(T_{N+1} + T_{N+3}\right)$$

In the absence of the extra residual term one can then form $(L_1 u, T_{N+3}) = \frac{1}{2}\Theta_{N+2}\|T_{N+3}\|^2 = 0$ and so $\Theta_{N+2} = 0$ which is not desirable. To overcome this one could indeed include another residual term as in (A6), however I have not seen this in other literature. Instead one can argue that since $(A4)_1$ is a truncation of an infinite series, i.e.

$$\Theta = \sum_{l=0}^{\infty} \Theta_l T_l(z)$$

which is then truncated at $N+2$, then one can apply the same logic to $z\Theta$, i.e.

$$z\Theta = \sum_{l=0}^{\infty} \Theta_l T_1(z) T_l(z),$$

and *this* is also truncated at $N+2$. With this argument no T_{N+3} term arises and I believe that equation $(A5)_1$ is now valid. This is the argument that I employ.

Returning again to equations $(A5)$ the next step in the procedure is to take the inner product of each of (A5) with T_i in the weighted $L^2(-1,1)$ space with the inner product defined by

$$(T_m, T_n) = \int_{-1}^{1} \frac{T_m(z) T_n(z)}{\sqrt{1-z^2}}\, dz. \tag{A7}$$

The Chebyshev polynomial are orthogonal in this space and so equation (A5) yields the $4(N+1)$ equations

$$(L_\alpha u, T_i) = 0, \quad \alpha = 1,2,3,4, \quad i = 0,1,\ldots,N, \tag{A8}$$

together with eight further equations,

$$\begin{aligned}
(L_1 u, T_{N+j}) &= \|T_{N+j}\|^2 \tau_j, \quad j = 1,2, \\
(L_2 u, T_{N+j}) &= \|T_{N+j}\|^2 \hat{\tau}_j, \quad j = 1,2, \\
(L_3 u, T_{N+j}) &= \|T_{N+j}\|^2 \bar{\tau}_j, \quad j = 1,2, \\
(L_4 u, T_{N+j}) &= \|T_{N+j}\|^2 \tilde{\tau}_j, \quad j = 1,2,
\end{aligned} \tag{A9}$$

where $\|\cdot\|$ represents the norm associated with the inner product (A7). Equations (A9) may be used to determine the tau coefficients and used in error analysis c.f. Gardner *et al.* (1989). However, normally one does not calculate these coefficients and instead eight further equations are obtained from the boundary equations (A3) which are (since $T_n(\pm 1) = (\pm 1)^n$, Orszag (1971)),

$$\begin{aligned}
&\sum_{l=0}^{N+2} (-1)^l W_l = 0, && \sum_{l=0}^{N+2} W_l = 0, \\
&\sum_{l=0}^{N+2} (-1)^l \Theta_l = 0, && \sum_{l=0}^{N+2} \Theta_l = 0, \\
&\sum_{l=0}^{N+2} (-1)^l \Phi_l^1 = 0, && \sum_{l=0}^{N+2} \Phi_l^1 = 0, \\
&\sum_{l=0}^{N+2} (-1)^l \Phi_l^2 = 0, && \sum_{l=0}^{N+2} \Phi_l^2 = 0.
\end{aligned} \tag{A10}$$

So, equations (A8) and (A10) yield a system of $4(N+3)$ equations for the $4(N+3)$ unknowns $W_i, \Theta_i, \Phi_i^1, \Phi_i^2$, $i = 0,1,\ldots,N+2$. Using the properties of Chebyshev polynomials (Orszag (1971)) one can show that

$$D^2 W = \sum_{l=0}^{N+2} W_l^{(2)} T_l(z), \tag{A11}$$

where

$$W_l^{(2)} = \frac{1}{c_l} \sum_{\substack{p=l+2 \\ p+l \text{ even}}}^{p=N+2} p(p^2 - l^2) W_p, \tag{A12}$$

with $c_0 = 2, c_i = 1, i = 1,2,\ldots$. Analogous expressions exist for $D^2\Theta, D^2\Phi^1$ and $D^2\Phi^2$. If the coefficients of the second differentiation matrix (the matrix that arises from the Chebyshev representation of D^2) are denoted by $D^2_{i,j}$, then equations (A11)

and (A12) may be used to show that

$$\begin{aligned} D^2_{0,2j} &= \frac{1}{2}(2j)^3, \qquad j \geq 1, \\ D^2_{i,i+2j} &= 4j(i+j)(i+2j), \qquad i \geq 1, j \geq 1. \end{aligned} \tag{A13}$$

This matrix is started at (0,0) and truncated at column $N+2$.

It follows then that equations (A8) and (A10) represent a matrix equation of form

$$A\mathbf{x} = \sigma B\mathbf{x}, \tag{A14}$$

with $\mathbf{x} = (W_0, \ldots, W_{N+2}, \Theta_0, \ldots, \Theta_{N+2}, \Phi^1_0, \ldots, \Phi^1_{N+2}, \Phi^2_0, \ldots, \Phi^2_{N+2})^T$.

As already described, one problem with previous applications of the Chebyshev tau method has been the existence of spurious eigenvalues. Gardner *et al.* (1989) attribute the existence of these spurious eigenvalues to the fact that the matrix B in (A14) will be singular as a result of the inclusion of the boundary conditions in A. The method of Straughan and Walker (1996) overcomes this problem by removing the $N+1, N+2$ rows from the $(N+3) \times (N+3)$ matrix D^2 and then eliminating the $N+1, N+2$ columns by making use of the boundary conditions, a device that seems to have been used first by Haidvogel and Zang (1979). This results in a $(N+1) \times (N+1)$ matrix D^2. Details are given in Straughan and Walker (1996). The removal of boundary condition rows in the matrix A above and consequently the removal of extraneous rows of zeros in the B matrix stabilises the numerical eigenvalue problem and eliminates the occurrence of spurious eigenvalues. In the present problem A and B are $4(N+1) \times 4(N+1)$ matrices of form

$$A = \begin{pmatrix} D^2 - k^2 I & Zk^2 + (1-2\xi)k^2 I & -k^2 I & -k^2 I \\ -RI & D^2 - k^2 I & 0 & 0 \\ -R_1 I & 0 & D^2 - k^2 I & 0 \\ -R_2 I & 0 & 0 & D^2 - k^2 I \end{pmatrix},$$

$$B = \begin{pmatrix} 0 & 0 & 0 & 0 \\ 0 & I & 0 & 0 \\ 0 & 0 & P_2 I & 0 \\ 0 & 0 & 0 & P_3 I \end{pmatrix},$$

where D^2 is the second differentiation matrix with the $N+1$ and $N+2$ columns removed using the boundary conditions and Z is the Chebyshev representation of z.

The eigenvalues σ in (A14) were found by using the QZ algorithm of Moler and Stewart (1973). The underlying idea of the QZ algorithm is that there exist unitary matrices Q and Z such that QAZ and QBZ are both upper triangular. The algorithm yields values α_i and β_i which are the diagonal elements of QAZ and QBZ. The eigenvalues can then be obtained from the relation $\sigma_i = \dfrac{\alpha_i}{\beta_i}$ for $\beta_i \neq 0$. When the matrix B is singular (as it is in the present problem) some of the β_i will be zero and these must be filtered out. A formulation of the QZ algorithm is available in the NAG library routine F02BJF.

A.2 A Chebyshev tau method for system (5.47)–(5.53)

As described in the previous section, Straughan and Walker (1996) advocate writing equations (5.47)–(5.50) as a system of second order equations in order to reduce the problem of round–off error. Here, this produces

$$(D^2 - k^2)W = A, \tag{A15}$$

$$(D^2 - k^2)A - k^2\Theta + k^2\Phi^1 + k^2\Phi^2 = Pr^{-1}\sigma A, \tag{A16}$$

$$(D^2 - k^2)\Theta + RW(1 - h(z)) = \sigma\Theta, \tag{A17}$$

$$(D^2 - k^2)\Phi^1 - \frac{R_1}{\tau_1}W = \frac{\sigma}{\tau_1}\Phi^1, \tag{A18}$$

$$(D^2 - k^2)\Phi^2 - \frac{R_1}{\tau_2}W = \frac{\sigma}{\tau_2}\Phi^2. \tag{A19}$$

For free–free boundaries one can use the method of removing the boundary condition columns as in the previous section. However, when fixed boundaries are considered this method cannot be used, as pointed out by McFadden *et al.* (1990) p. 232, since the boundary conditions are all on W and none are on A. Consequently an alternative method must be used and is described in this section.

The boundary conditions for fixed–free boundaries are

$$\begin{aligned} \Theta = \Phi_1 = \Phi_2 = 0 \text{ at } z = 0, 1, \\ W = DW = 0 \text{ at } z = 0, \\ W = A = 0 \text{ at } z = 1, \end{aligned} \tag{A20}$$

while for fixed–fixed boundary conditions,

$$W = DW = \Theta = \Phi^1 = \Phi^2 = 0 \text{ at } z = 0, 1 \tag{A21}$$

We transform to the interval (-1,1) and the above system reduces to the matrix system

$$A\mathbf{x} = \sigma B\mathbf{x}, \tag{A22}$$

where A and B are the following $5(N+1) \times 5(N+1)$ matrices

$$A = \begin{pmatrix} D^2 - k^2 I & -I & 0 & 0 & 0 \\ 0 & D^2 - k^2 I & -k^2 I & k^2 I & k^2 I \\ R(I - \frac{QZ}{2}) & 0 & D^2 - k^2 I & 0 & 0 \\ -\frac{R_1}{\tau_1} I & 0 & 0 & D^2 - k^2 I & 0 \\ -\frac{R_2}{\tau_2} I & 0 & 0 & 0 & D^2 - k^2 I \end{pmatrix},$$

$$B = \begin{pmatrix} 0 & 0 & 0 & 0 & 0 \\ 0 & \frac{I}{Pr} & 0 & 0 & 0 \\ 0 & 0 & I & 0 & 0 \\ 0 & 0 & 0 & \frac{I}{\tau_1} & 0 \\ 0 & 0 & 0 & 0 & \frac{I}{\tau_2} \end{pmatrix},$$

and $\mathbf{x} = (W_0, \ldots, W_N, A_0, \ldots, A_N, \Theta_0, \ldots, \Theta_N, \Phi_0^1, \ldots, \Phi_N^1, \Phi_0^2, \ldots, \Phi_N^2)^T$. Z is the Chebyshev representation of z. The problem remains to incorporate the boundary conditions. An alternative approach is to write in the boundary conditions as rows of the matrices A and B, a technique employed by Orszag (1971). Rows $N, N+1, 2N, 2N+1, \ldots, 5N, 5N+1$ are replaced with boundary information. The result is a generalised eigenvalue problem like (A22) where

$$A = \begin{pmatrix}
D^2 - k^2 I & -I & 0 & 0 & 0 \\
BC1 & BC1 & BC1 & BC1 & BC1 \\
BC2 & BC2 & BC2 & BC2 & BC2 \\
0 & D^2 - k^2 I & -k^2 I & k^2 I & k^2 I \\
BC3 & BC3 & BC3 & BC3 & BC3 \\
BC4 & BC4 & BC4 & BC4 & BC4 \\
R(I - \frac{QZ}{2}) & 0 & D^2 - k^2 I & 0 & 0 \\
BC5 & BC5 & BC5 & BC5 & BC5 \\
BC6 & BC6 & BC6 & BC6 & BC6 \\
-\frac{R_1}{\tau_1} I & 0 & 0 & D^2 - k^2 I & 0 \\
BC7 & BC7 & BC7 & BC7 & BC7 \\
BC8 & BC8 & BC8 & BC8 & BC8 \\
-\frac{R_2}{\tau_2} I & 0 & 0 & 0 & D^2 - k^2 I \\
BC9 & BC9 & BC9 & BC9 & BC9 \\
BC10 & BC10 & BC10 & BC10 & BC10
\end{pmatrix},$$

$$B = \begin{pmatrix}
0 & 0 & 0 & 0 & 0 \\
0 & \frac{I}{Pr} & 0 & 0 & 0 \\
 & 0\ldots0 & \cdot & & \\
 & 0\ldots0 & & & \\
0 & 0 & I & 0 & 0 \\
 & & 0\ldots0 & & \\
 & & 0\ldots0 & & \\
0 & 0 & 0 & \frac{I}{\tau_1} & 0 \\
 & & & 0\ldots0 & \\
 & & & 0\ldots0 & \\
0 & 0 & 0 & 0 & \frac{I}{\tau_2} \\
 & & & & 0\ldots0 \\
 & & & & 0\ldots0
\end{pmatrix}$$

and $\mathbf{x} = (W_0, \ldots, W_N, A_0, \ldots, A_N, \Theta_0, \ldots, \Theta_N, \Phi_0^1, \ldots, \Phi_N^1, \Phi_0^2, \ldots, \Phi_N^2)^T$. The rows of the matrix A labelled $BC1, \ldots, BC10$ refer to the discrete versions of the boundary conditions (A20) or (A21). These are written with the aid of the properties $T_n(\pm1) = (\pm1)^n$, $T_n'(\pm1) = (\pm1)^{n-1}n^2$ (see Orszag (1971)). As an explicit example consider the row $BC1$ which in both problems corresponds to the boundary condition $W(-1) = 0$. For definiteness assume N to be even. The row $BC1$ is then

$$1 - 1 \ldots - 11 \quad 00\ldots0 \quad 00\ldots0 \quad 00\ldots0 \quad 00\ldots0$$

where each block contains $N + 1$ terms.

To help describe more concisely the other boundary conditions we introduce the four $(N + 1)$–dimensional vectors $\mathbf{p}, \mathbf{q}, \mathbf{r}$ and $\mathbf{s}$ defined by

$$p_n = 1, \quad q_n = (-1)^n, \quad r_n = n^2, \quad s_n = (-1)^{n-1}n^2 \qquad n = 0, 1, \ldots, N.$$

The following tables show the exact nature of all the boundary condition rows. For the fixed–free problem,

Condition	Label	Row	Overwrites
$W(-1)=0$	$BC1$	N	$(\mathbf{q},0,0,0,0)$
$W(1)=0$	$BC2$	$N+1$	$(\mathbf{p},0,0,0,0)$
$DW(-1)=0$	$BC3$	$2N$	$(\mathbf{s},0,0,0,0)$
$D^2W(1)=A(1)=0$	$BC4$	$2N+1$	$(0,\mathbf{p},0,0,0)$
$\Theta(-1)=0$	$BC5$	$3N$	$(0,0,\mathbf{q},0,0)$
$\Theta(1)=0$	$BC6$	$3N+1$	$(0,0,\mathbf{p},0,0)$
$\Phi^1(-1)=0$	$BC7$	$4N$	$(0,0,0,\mathbf{q},0$
$\Phi^1(1)=0$	$BC8$	$4N+1$	$(0,0,0,\mathbf{p},0)$
$\Phi^2(-1)=0$	$BC9$	$5N$	$(0,0,0,0,\mathbf{q})$
$\Phi^2(1)=0$	$BC10$	$5N+1$	$(0,0,0,0,\mathbf{p})$

while for the fixed–fixed problem

Condition	Label	Row	Overwrites
$W(-1)=0$	$BC1$	N	$(\mathbf{q},0,0,0,0)$
$W(1)=0$	$BC2$	$N+1$	$(\mathbf{p},0,0,0,0)$
$DW(-1)=0$	$BC3$	$2N$	$(\mathbf{s},0,0,0,0)$
$DW(1)=0$	$BC4$	$2N+1$	$(\mathbf{r},0,0,0,0)$
$\Theta(-1)=0$	$BC5$	$3N$	$(0,0,\mathbf{q},0,0)$
$\Theta(1)=0$	$BC6$	$3N+1$	$(0,0,\mathbf{p},0,0)$
$\Phi^1(-1)=0$	$BC7$	$4N$	$(0,0,0,\mathbf{q},0$
$\Phi^1(1)=0$	$BC8$	$4N+1$	$(0,0,0,\mathbf{p},0)$
$\Phi^2(-1)=0$	$BC9$	$5N$	$(0,0,0,0,\mathbf{q})$
$\Phi^2(1)=0$	$BC10$	$5N+1$	$(0,0,0,0,\mathbf{p})$

As before, the eigenvalues σ in (A22) were found by using the QZ algorithm of Moler and Stewart (1973). Straughan and Walker (1996) find that this method may give rise to spurious eigenvalues. However, in this problem no spurious eigenvalues appear to occur.

References

Allen, M.B. and Curran, M.C. 1993. Parallelizable methods for modelling flow and transport in heterogeneous porous media. *International Series of Numerical Mathematics* **114**, 5–14.

Allen, M.B. and Khosravani, A. 1992. Solute transport via alternating direction collocation using the modified method of characteristics. Adv. Water Resources **15**, 125–132.

Celia, M.A., Kindred, J.S. and Herrera, I. 1989. Contaminant transport and biodegradation. 1. A numerical model for reactive transport in porous media. *Water Resources Res.* **25**, 1141–1148.

Chen, B., Cunningham, A., Ewing, R., Peralta, R. and Visser, E. 1994. Two–dimensional modelling of microscale transport and biotransformation in porous media. *Numer. Methods Partial Differential Equations* **10**, 65–83.

Chen, C.F. and Su, T. F. 1992. Effect of surface tension on the onset of convection in a double–diffusive layer. *Phys. Fluids* A **4**, 2360–2367.

Cheney, W. and Kincaid, D. 1985. *Numerical mathematics and computing.* Brooks–Cole Publishing Co., Monterey, California.

Cheng, P. 1978. Heat transfer in geothermal systems. *Adv. Heat Transfer* **14**, 1–105.

Coriell, S.R., McFadden, G.B., Voorhees, P.W. and Sekerka, R.F. 1987. Stability of a planar interface during solidification of a multicomponent system. *J. Crystal Growth* **82**, 300–313.

Curran, M.C. and Allen, M.B. 1990. Parallel computing for solute transport models

via alternating direction collocation. Adv Water Resources **13**, 70–75.

Degens, E.T., von Herzen, R.P., Wong, H.K., Deuser, W.G. and Jannasch, H.W. 1973. Lake Kivu: structure, chemistry and biology of an East African rift lake. *Geol. Rundschau* **62**, 245–277.

Drazin, P.G. & Reid, W.H. 1981. *Hydrodynamic stability.* Cambridge University Press.

Fischer, H. 1971. The dilution of an undersea sewage cloud by salt fingers. *Water Res.* **5**, 909–915.

Gardner, D.R., Trogdon S.A. and Douglas, R.W. 1989. A modified tau spectral method that eliminates spurious eigenvalues. *J. Computational Physics* **80**, 137–167.

George, J.H., Gunn, R.D. and Straughan, B. 1989. Patterned ground formation and penetrative convection in porous media. *Geophys. Astrophys. Fluid Dynamics* **46**, 135–158.

Griffiths, R.W. 1979. The influence of a third diffusing component upon the onset of convection. *J. Fluid Mech.* **92**, 659–670.

Griffiths, R.W. 1981. Layered double–diffusive convection in porous media. *J. Fluid Mech.* **102**, 221–248.

Guo, J.L. and Kaloni, P.N. 1995a. Nonlinear stability problem of a rotating double–diffusive porous layer. *J. Math. Anal. App.* **190**, 373–390.

Guo, J.L. and Kaloni, P.N. 1995b. Double–diffusive convection in a porous medium, nonlinear stability, and the Brinkman effect. *Studies in Applied Mathematics* **94**, 341–358.

Haidvogel, D.B. and Zang, T. 1979. The accurate solution of Poisson's equation by expansion in Chebyshev polynomials. *J. Computational Physics* **30**, 167–180.

Hansen, U. and Yuen, D.A. 1989. Subcritical double–diffusive convection at infinite Prandtl number. *Geophys. Astrophys. Fluid Dynamics* **47**, 199–224.

Huppert, H.E. and Turner, J.S. 1981. Double–diffusive convection. *J. Fluid Mech.*

106, 299–329.

Joseph, D.D. 1976. *Stability of fluid motions II* Springer–Verlag. Berlin, Heidelberg, New York.

Kaloni, P.N. and Guo, J.L. 1996. Steady nonlinear double–diffusive convection in a porous medium based upon the Brinkman–Forchheimer model. *J. Math. Anal. App.* **204**, 138–155.

Kaloni, P.N. and Qiao, Z.C. 1997. Non–linear stability of convection in a porous medium with inclined temperature gradients. *Int. J. Heat Mass Transfer* **40**, 1611–1615.

Kaye, J.A. and Rood, R.B. 1989. Chemistry and transport in a three–dimensional stratospheric model: chlorine species during a simulated stratospheric warming. *J. Geophys. Res. D* **94**, 1057–1083.

Krishnamurti, R. and Howard, L.N. 1983. Double–diffusive instability: Measurement of heat and salt fluxes. *Bull. Am. Phys. Soc.* **28**, 1398.

Lindsay, K.A. and Ogden, R.R. 1992. A practical implementation of spectral methods resistant to the generation of spurious eigenvalues. *Int. J. Numer. Methods. Fluids* **15**, 1277–1294.

Lopez, A.R., Romero, L.A. and Pearlstein, A.J. 1990. Effect of rigid boundaries on the onset of convective instability in a triply diffusive fluid layer. *Phys. Fluids A* **2**, 897–902.

McFadden, G.B., Murray, B.T. and Boisvert, R.F. 1990. Elimination of spurious eigenvalues in the Chebyshev tau spectral method. *J. Computational Physics* **91**, 228–239.

McKay, G. and Straughan, B. 1992. Nonlinear energy stability and convection near the density maximum. *Acta Mechanica* **5**, 9–28.

McKenzie, D.P., Roberts J.M. and Weiss, N.O. 1974. Convection in the Earth's mantle: towards a numerical solution. *J. Fluid Mech.* **62**, 465–538.

Moler, C.B. and Stewart, G.W. 1973. An algorithm for generalized matrix eigen-

problems, *SIAM. J. Numerical Anal.* **10**, 241–256.

Mulone, G. 1994. On the nonlinear stability of a fluid layer of a mixture heated and salted from below. *Continuum Mech. Thermodyn.* **6**, 161–184.

Murray, B.T. and Chen, C.F. 1989. Double–diffusive convection in a porous medium. *J. Fluid Mech.* **201**, 144–166.

Nield, D.A. 1968. Onset of thermohaline convection in a porous medium. *Water Resources Res.* **5**, 553–560.

Nield, D.A. and Bejan, A. 1992. *Convection in porous media.* Springer–Verlag. New York London

Noulty, R.A. and Leaist, D.G. 1987. Quarternary diffusion in aqueous $KCl - K_2PO_4 - H_3PO_4$ mixtures. *J. Phys. Chem.* **91**, 1655–1658.

Orszag, S.A. 1971. Accurate solution of the Orr–Sommerfeld stability equation. *J. Fluid Mech.* **50**, 689–703.

Patil, P.R. and Rudraiah, N. 1980. Linear convective stability and thermal diffusion of a horizontal quiescent layer of a two component fluid in a porous medium. *Int. J. Engng. Sci.* **18**, 1055–1059.

Payne, L.E., Song, J.C. and Straughan, B. 1988. Double diffusive porous penetrative convection — thawing subsea permafrost. *Int. J. Engng. Sci.* **26**, 797–809.

Payne, L.E. and Straughan, B. 1987. Unconditional nonlinear stability in penetrative convection. *Geophys. Astrophys. Fluid Dynamics* **39**, 57–63. (Also, Corrected and extended numerical results. *Geophys. Astrophys. Fluid Dynamics* 1988. **43**, 307–309.)

Pearlstein, A.J., Harris, R.M. and Terrones, G. 1989. The onset of convective instability in a triply diffusive fluid layer. *J. Fluid Mech.* **202**, 443–465.

Poulikakos,D. 1985. Effect of a third diffusing component on the onset of convection in a horizontal layer. *Phys. Fluids* **28**, 3172–3174.

Proctor, M.R.E. 1981. Steady subcritical thermohaline convection. *J. Fluid Mech.* **105**, 507–521.

Qin, Y., Guo, J.L. and Kaloni, P.N. 1995. Double–diffusive penetrative convection in porous media. *Int. J. Eng. Sci.* **33**, 303–312.

Ray, R.J., Krantz, W.B., Caine, T.N. and Gunn, R.D. 1983. A model for sorted patterned–ground regularity. *J. Glaciology* **29**, 317–337.

Rosenblat, S., Homsy, G.M. and Davis, S.H. 1982. Nonlinear Marangoni convection in bounded layers. Part 2. Rectangular cylindrical containers. *J. Fluid Mech.* **120**, 123–138.

Rubin, H. 1973. Effect of nonlinear stabilizing salinity profiles on thermal convection in a porous medium layer. *Water Resources Res.* **9**, 211–221.

Rudraiah, N., Shivakumara, I.S. and Friedrich, R. 1986. The effect of rotation on linear and nonlinear double–diffusive convection in a sparsely packed porous medium. *Int. J. Heat Mass Transfer* **29**, 1301–1317.

Rudraiah, N., Srimani, P.K. and Friedrich, R. 1982. Finite amplitude convection in a two component fluid saturated porous layer. *Int. J. Heat Mass Transfer* **25**, 715–722.

Rudraiah, N. and Vortmeyer, V.D. 1982. Influence of permeability and of a third diffusing component upon the onset of convection in a porous medium. *Int. J. Heat Mass Transfer* **25**, 457–464.

Straughan, B. 1992. *The energy method, stability and nonlinear convection.* Springer–Verlag Ser. in Appl. Math. Sci.

Straughan, B. and Walker, D.W. 1996. Two very accurate and efficient methods for computing eigenvalues and eigenfunctions in porous convection problems. *J. Computational Physics* **127**, 128–141.

Straughan, B. and Walker, D.W. 1997. Multi–component convection–diffusion and penetrative convection. *Fluid Dyn. Res.* **19**, 77–89.

Tabor, H. 1979. Non–convecting solar ponds. *Phil. Trans. Roy. Soc. A* **295**, 423–433.

Taunton, J.W., Lightfoot, E.N. and Green, T. 1972. Thermohaline instability and

salt fingers in a porous medium *Phys. Fluids* **15**, 748–759.

Terrones, G and Pearlstein, A.J. 1989. The onset of convection in a multi–component fluid layer. *Phys. Fluids A* **1**, 845-853.

Tracey 1996. Multi–component convection–diffusion in a porous medium. *Continuum Mech. Thermodyn.* **8**, 361–381.

Tracey 1997a. Penetrative convection and multi–component convection in a porous medium. To appear in *Adv. Water Resources*

Tracey 1997b. Nonlinear stability of multi–component convection–diffusion in a porous medium. To appear in *Math. Models Meth. Appl. Sci.*

Turner, J.S. 1979. *Buoyancy effects in fluids.* Cambridge University Press

Veronis, G. 1963. Penetrative convection. *Astrophys. J.* **137**, 641–663.